Article:
Cosgrove, G.I.E., Colombera, L., Mountney, N.P. orcid.org/0000-0002-8356-9889 et al. (3 more authors) (2023) Precambrian aeolian systems: A unique record? Precambrian Research, 392. 107075. ISSN 0301-9268

https://doi.org/10.1016/j.precamres.2023.107075

TITLE: Precambrian Aeolian Systems: A Unique Record?

AUTHORS: Grace I.E. Cosgrove*[1], Luca Colombera[2], Nigel P. Mountney[1], Giorgio Basilici[3,4], Áquila Ferreira Mesquita[3], Marcus Vinícius Theodoro Soares[3]

* Corresponding author (g.i.e.cosgrove@leeds.ac.uk)

[1] School of Earth and Environment, Institute of Applied Geoscience, University of Leeds, Woodhouse, Leeds, LS2 9JT

[2] Dipartimento di Scienze della Terra e dell'Ambiente, Università di Pavia, Via Ferrata 1, 27100, Pavia, Italy

[3] Department of Geology and Natural Resources, Institute of Geosciences, State University of Campinas, 13083-870 Campinas, SP, Brazil

[4] Centro Regional de Investigaciones Científicas y Transferencia Tecnológica, La Rioja / CONICET, Argentina

ABSTRACT

The Precambrian is associated with a set of geologically unique palaeoenvironmental conditions arising from differences in the Earth's atmosphere, biosphere and geosphere. The extent to which these conditions operated to generate an aeolian stratigraphic record that is geologically distinct from that of the Phanerozoic remains poorly understood. This study presents a quantitative comparison of the preserved sedimentary architectures of 87 globally distributed aeolian successions from the Precambrian and the Phanerozoic. Compared to those of the Phanerozoic, Precambrian aeolian successions are characterised by: (1) thinner aeolian dune sets, mostly documenting the accumulation of small, rapidly migrating barchan dunes; and (2) a greater occurrence of sandsheet, zibar, and damp and wet interdune deposits, many occurring interdigitated with non-aeolian strata. The nature of the Precambrian aeolian stratigraphic record reflects in part the absence of sediment-stabilizing terrestrial vegetation: compared to Phanerozoic systems developed since the evolution of land plants, aeolian processes (erosion, transport and deposition) were more active, even under markedly more humid

climates. Precambrian aeolian successions record greater evidence of fluvial and marine incursions into contiguous aeolian dune fields. Water tables were commonly elevated close to the level of the accumulation surface for protracted episodes; extensive damp and wet substrates restricted the availability of dry sand for aeolian dune construction, thereby limiting dune size. In some Precambrian aeolian systems, sediment supply was additionally restricted by the development of cryptobiotic films and crusts that preferentially developed on damp substrates in the absence of vegetation. Common fluvial and marine aqueous interactions promoted the reworking of aeolian dunes into sandsheet deposits; many such accumulations likely represent eroded remnants of larger aeolian dune fields. Given the absence of vegetation-induced sediment binding and baffling, and wind-buffering effects, coarser sand fractions were more readily transported by the wind in the Precambrian; this led to the preferential development of coarse-grained zibar deposits. This study demonstrates how the Precambrian aeolian sedimentary record is geologically distinct from that of the majority of the Phanerozoic, providing new insights into the controlling factors that governed aeolian sedimentation during the Precambrian through interactions between the geosphere, biosphere and atmosphere.

KEYWORDS:

Sandsheet, Zibar, Proterozoic, Dune, Palaeoenvironment, Architecture

1. INTRODUCTION

Many facets of modern geology are underpinned by the principle of modern uniformitarianism: '*the present is the key to the past'* (e.g., Hallam, 1990). This conviction predicates that modern sedimentary environments can suitably represent the processes and products of sedimentation that prevailed during earlier episodes of Earth history (e.g., Donaldson et al., 2002; Bose et al., 2012). Indeed, when comparisons are made between many modern sedimentary systems and comparable successions of Precambrian age, the similarities outweigh the differences (Eriksson et al., 1998; Eriksson et al., 2004; Altermann and Corcoran, 2002). Precambrian sedimentary architectures and their interpreted formative processes commonly have a close Phanerozoic counterpart (e.g., Eriksson

et al., 1998, 2004; Eriksson, 2005; Altermann and Corcoran, 2002; Bose et al., 2012). The similarities between the sedimentary successions of the Precambrian and Phanerozoic arise primarily as a consequence of the universal interactions between primary (i.e. plate tectonic and magmatic-thermal processes) and secondary (i.e. prevailing climatic conditions and eustasy) controls on patterns of sedimentation (e.g., Eriksson et al., 2001a,b; Bose et al., 2001; Eriksson et al., 2004, 2005).

Yet, despite the many commonalities between sedimentary successions of the Precambrian and the Phanerozoic, numerous important palaeoenvironmental conditions that influenced patterns of sedimentation were uniquely in operation during the Precambrian (e.g., Eriksson and Simpson, 1998; Eriksson et al., 2005; Bose et al., 2012). The Precambrian is associated with the following traits. (1) Absence of vegetation; the evolution of land plants commenced ca. 500 Ma (Morris et al., 2018). (2) High rates of continental weathering and erosion; this is associated with an absence of stabilizing vegetation, and the action of a hot and humid climate during much of the Archaean and Paleoproterozoic (Bose et al., 2012). (3) A general lack of widespread and abundant biogenic activity (and associated bioturbation) until ~600Ma (Eriksson et al., 2001b). (4) The presence of microbial mats in some terrestrial environments (Schieber, 1998; Noffke et al., 2001; Schieber, 2004; Eriksson et al., 2000; Basilici et al., 2020). The cumulative effect of these conditions has been suggested to have markedly influenced sedimentary processes, including rates of weathering, erosion, transport and deposition during the Precambrian (Donaldson et al., 2002; Eriksson et al., 2005; Bose et al., 2012), such that successions from this era might be expected to differ in several regards from their Phanerozoic counterparts. However, the extent to which a unique set of Precambrian palaeoenvironmental conditions may produce a global aeolian stratigraphic record that is geologically distinct from that of the Phanerozoic remains to be determined.

The aim of this study is to demonstrate and explain the similarities and differences between aeolian systems of Precambrian age and those of Phanerozoic age that post-date extensive land-plant evolution and colonization. Specific objectives of this research are as follows: (1) to undertake a comprehensive quantitative analysis of the geometry, spatial relationships and lithological heterogeneity of aeolian successions developed in the Precambrian; (2) to demonstrate the sedimentological variability seen in the studied aeolian successions; (3) to interpret the presented

results in terms of the prevailing environmental conditions at the time of deposition. To address this problem, and to facilitate the quantitative stratigraphic and sedimentological characterization of aeolian systems, this study employs a relational database: the Database of Aeolian Sedimentary Architecture (DASA) (Cosgrove et al., 2021a, b, 2022a, b).

2. BACKGROUND

With regard to the aeolian sedimentary record, there exist numerous noteworthy studies of Precambrian systems (e.g., Pulvertaft, 1985; Clemmensen, 1988; Chakraborty and Chaudhuri, 1993; Simplicio and Basilici, 2015; Bállico et al., 2017; Basilici et al., 2020; Mesquita et al., 2021a,b; Table 1). However, the great majority of publications on aeolian sedimentology and stratigraphy relate to examinations of Phanerozoic successions (see Rodríguez-López et al., 2014 for a review). The principal reasons for this are summarised as follows.

(1) Until the early 2000s, studies of Phanerozoic aeolian successions of Europe and North America had dominated the published scientific literature. For example, much attention has been paid to the aeolian sedimentology and stratigraphy of the Permian Rotliegend Group (e.g., Ellis, 1993; Minervini et al., 2011; Besly et al., 2018) and the Triassic Sherwood Sandstone Group ("Bunter" Sandstone) of northwest Europe (e.g., Cowan, 1993; Meadows and Beach, 1993; Wakefield, 2019). In North America, the Pennsylvanian to Jurassic aeolian sedimentary record of the Colorado Plateau region of the Western Interior of the United States has been the focus of considerable sedimentological research (e.g., Loope, 1985; Langford and Chan, 1988; Crabaugh and Kocurek, 1993; Mountney and Jagger, 2004; Newell et al., 2019; Priddy and Clarke, 2020). However, since the early 2000s, there has been a marked increase in the number of studies reporting aeolian successions from elsewhere in the world, including descriptions of hitherto scantly documented aeolian systems across Asia (e.g., Hasegawa et al., 2010; Xu et al., 2019; Cao et al., 2020) and South America (e.g., Scherer and Lavina, 2005; Abrantes et al., 2020; Mesquita et al., 2021a,b; Basilici et al., 2021). In particular, there now exists a valuable set of studies that describe Precambrian systems, and this has grown considerably since the 2000s (e.g., Simplicio and Basilici, 2015; Bállico et al., 2017; Basilici et al., 2020, 2021; Mesquita et al., 2021a,b; see Table 1).

(2) Phanerozoic aeolian successions that have been documented in detail are more widespread geographically. The majority of reported occurrences of Precambrian aeolian successions are restricted to the stable interiors of ancient cratons, and many are located in relatively inaccessible regions (e.g., Eriksson and Simpson, 1998; Bose et al., 1999; Rainbird and Hadlari, 2000; Rainbird et al., 2003).

(3) Aeolian deposits of Phanerozoic age are generally better preserved that their older Precambrian counterparts. This allows for more detailed analyses of the sedimentary features (textures and structures) of younger Phanerozoic aeolian deposits.

(4) Prior research directives have been partly driven by exploration for hydrocarbons and related resources that are primarily recovered from Phanerozoic basins.

Despite the current predominance of published studies of Phanerozoic aeolian successions, the Phanerozoic record might not necessarily be representative of the sedimentary record as a whole, given that the Precambrian spans 85% of Earth's geological history (Gradstein, 2020).

During the Precambrian, the absence of vegetation – and the associated absence of the sediment binding and baffling effects, and the wind dampening action that it determines – should have provided a plentiful source of loose and dry sediment for wind transport and aeolian system construction (Eriksson and Simpson, 1998; Rodríguez-López et al., 2014). Therefore, aeolian sand seas (ergs) might be expected to have been widespread in the Precambrian. However, although numerous aeolian systems are recorded from the late Paleoproterozoic to the Neoproterozoic (~ 1800 – 540 Ma), documented aeolian systems from the Archean and Paleoproterozoic are few (Eriksson and Simpson, 1998). The rarity of aeolian systems of >1800 Ma age remains unexplained, and has been argued to be unexpected given that deposits of this age that formed in closely associated continental palaeoenvironments, such as braided rivers, are relatively abundant and well preserved (Schumm, 1968; Cotter, 1978; Long, 1978). The lack of documented aeolian systems older than 1800 Ma, may be associated with (i) misidentification (i.e. aeolian successions remain unrecognised in the geological record, possibly having been misinterpreted as of fluvial or marine origin; e.g., Ross, 1983), or (ii) non-preservation (e.g., Eriksson and Simpson, 1998; Eriksson et al., 1998).

Alongside these uncertainties about the presence and preservation potential of Precambrian aeolian systems, differences in aeolian architecture between Precambrian systems and their Phanerozoic counterparts have also been noted. Preserved dune sets of Precambrian aeolian systems are, on average, relatively thin (Cosgrove et al., 2022b) and simple dune sets with only modest architectural complexity are the most commonly reported type (e.g., Simpson and Eriksson, 1993; Tirsgaard and Øxnevad, 1998; Simpson et al., 2002; Basilici et al., 2020). This raises an important question that remains to be addressed: why are the deposits of Precambrian aeolian systems characterised by relatively low architectural complexities (e.g., formative dune types that are simple in form, rather than compound and complex megadunes), despite likely abundant sand availability for their construction?

3. METHODS

3.1 Case Studies and Associated Metrics

This study employs a relational database: the Database of Aeolian Sedimentary Architecture (DASA; Cosgrove et al., 2021a; cf. Colombera et al., 2012, 2016). DASA stores data on the sedimentary architecture and organisation of aeolian systems and their preserved successions. Data have been synthesised from 30 Precambrian aeolian successions (Fig. 1; Table 1) and 57 Phanerozoic aeolian successions (Fig. S1; Table S1). Case studies that are suitable for inclusion in DASA are datasets described by graphic sedimentary logs, core descriptions, outcrop photos and architectural-element panels, or any other similar sedimentological data, from which quantitative metrics can be extracted. All case studies included in this investigation represent a significant part of an ancient aeolian system (e.g., the Mesoproterozoic Dala Sandstone; Pulvertaft, 1985; Fig.1, Table 1).

The case studies included herein represent all examples of Precambrian aeolian systems as summarised by Eriksson and Simpson (1998) and Rodríguez-López et al. (2014) that contain data suitable for inclusion in DASA (Fig. 1; Table 1). Alongside this, multiple Precambrian aeolian successions (mainly from South America) that have been documented since the publication of these aforementioned summaries have also been included (Table 1). Phanerozoic aeolian systems – studied

here for purposes of comparison – span geological time from the Middle Cambrian to the Neogene and have been chosen to provide a broad and representative global coverage of aeolian systems of different types, age and geographic distribution (Fig. S1; Table S1). The latest studies suggest that land-plant colonisation took place in the Middle Cambrian (ca. 500 Ma; Morris et al., 2018). No Cambrian aeolian successions that predate land-plant colonisation (i.e. 500 to 541 Ma) are considered in this study.

All of the case studies included in this investigation are accompanied by one or more sets of data (cf. 'subsets' of Colombera et al., 2012). A subset denotes an assortment of data (e.g., an architectural panel, or graphic sedimentary log) retrieved from an original source (e.g., a thesis, a publication). The kinds of data contained within individual subsets may vary significantly according to the manner by which the original data were gathered, and with regard to the hierarchical levels that the dataset covers (see Section 3.2). Upon data entry to DASA, a process of standardisation is completed in order to guarantee that the terminology used is consistent and to resolve any issues relating to the variability in data types that were utilised in the source literature to characterise each ancient aeolian succession. Included in DASA are quantitative and qualitative data on geological entities of different types (e.g., architectural elements and lithofacies), and on their depositional systems, themselves classified according to multiple attributes (e.g., geological age, basin setting). Further information on database structure, interrogation, output and interpretation is provided by Cosgrove et al. (2021a).

3.2 Architectural Elements and Lithofacies

DASA stores both quantitative and qualitative data on different types of geological entity (e.g., architectural elements and lithofacies), and on their depositional systems, which are in turn classified according to numerous attributes (e.g., geological age, basin setting, physiographic aeolian setting) and metadata (e.g., data sources and data types).

Geological entities considered in detail here are architectural elements and lithofacies. Architectural elements are defined as distinct sedimentary bodies with characteristic sedimentological properties (e.g., internal composition, geometry, bounding surfaces), and that are the products of deposition in a specific sub-environment (e.g., a dune, a sandsheet, a dry interdune). Many commonly occurring

188 architectural element types, such as dune elements, interdune elements and sandsheet elements, are
189 interpreted from aeolian successions (e.g., Kocurek, 1988; Karpeta, 1990); these bodies of strata
190 represent the accumulated and preserved products of deposition in specific sub-environments.
191 Architectural elements provide a record of both the lateral migration and vertical accumulation of
192 components of the sedimentary system through geological time (cf. Mountney, 2012; Cosgrove et al.,
193 2021a). As such, many architectural elements have preserved geometries that, inevitably, do not
194 resemble the form of the original components (e.g., a dune, a sandsheet, an interdune). The
195 environmental significance of an architectural element needs to be interpreted in the context of both
196 its spatial and temporal development (Kocurek and Havholm, 1993). Non-aeolian architectural
197 elements (e.g., elements of fluvial, marine, alluvial or lacustrine origins) are recorded in DASA in
198 cases where they interfinger with sedimentary bodies of aeolian origin.
199 Facies elements are defined as sedimentary bodies differentiated on the basis of sediment
200 composition, texture, structure, bedding geometry, fossil content, or by the nature of their bounding
201 surfaces (cf. Miall, 1985; Colombera et al., 2012, 2016). Key aeolian lithofacies, and the architectural
202 elements with which they are commonly associated are defined in Table 2.

203 ### 3.2.1 Aeolian Dune-Set Architectural Elements

204 Dune sets represent a fundamental accumulated unit of deposition of an aeolian sand dune; most dune
205 sets are characterised internally by packages of cross-strata (Sorby, 1859; Allen, 1963; Rubin and
206 Hunter 1982; Chrintz and Clemmensen, 1993); if dunes migrate over each other, cross-stratified
207 packages are truncated, delineating sets that are bounded by erosional surfaces (Brookfield, 1977).
208 Aeolian dune sets are recognised by the arrangement of (1) lithofacies, (2) cross-strata, and (3)
209 bounding surfaces. These are discussed below. Dune foreset deposits consist of inclined cross-strata
210 composed of various combinations of wind-ripple, grainfall and grainflow deposits (Hunter, 1977;
211 Kocurek and Dott, 1981; Table 2). The inclined strata may laterally grade into dune toeset deposits
212 (dune plinth), which occur at the lowermost part of a dune lee slope, and which are characterised
213 dominantly by horizontal to low-angle-inclined wind-ripple stratification (Kocurek, 1986).

Cross-strata are almost ubiquitous in dune-set deposits. The shape of cross-strata can vary in orientations both parallel and perpendicular to the dominant direction of bedform migration (Rubin and Hunter, 1982). Cross-strata can be planar, concave, convex and trough-shaped; a common diagnostic form of aeolian deposition are sets characterised internally by tangential concave cross-strata that downlap asymptotically onto to a lower set bounding surface (e.g., Pulvertaft, 1985). In the absence of other diagnostic features (i.e. lithofacies arrangements and bounding surfaces), it is essential to assess whether tidal or fluvial processes may have been responsible for the generation of said cross-bedding (Eriksson and Simpson, 1998). A hierarchy of aeolian bounding surfaces was proposed by Brookfield (1977): third-, second- and first-order, in increasing scale. Kocurek (1996) expanded this scheme to assign descriptive identifiers of surface type and defined bounding-surface types of approximately equal significance to those of Brookfield (1977): reactivation surfaces, superposition surfaces, and interdune migration surfaces, respectively.

3.2.2 Aeolian Sandsheet Architectural Elements

Sandsheet deposits are low-relief accumulations of aeolian sediment in areas where dunes are generally absent (Kocurek and Nielson, 1986). Sandsheets rarely exceed 20 m in thickness and are typically preserved as tabular and laterally continuous sheet-like bodies. Sandsheet deposits are characterised by horizontal to low-angle stratification, typically composed of wind-ripple strata, and to a lesser degree, plane-bed strata (Fryberger et al., 1979; Kocurek and Nielson, 1986). Sandsheets can also be associated with granule lags, also referred to as deflationary lags (e.g., Fryberger et al., 1979; Kocurek and Nielson, 1986). Aeolian sandsheets can also be associated with adhesion strata (Table 2) and subaqueous ripples in circumstances where the sandsheet environment is intermittently inundated by aqueous agents, including fluvial and marine incursions (e.g., Chakraborty, 1991; Chakraborty and Chakraborty, 2001; Bállico et al., 2017; Basilici et al., 2021).

3.2.3 Aeolian Zibar Architectural Elements

Zibars are low-relief, rounded, coarse-grained, sand dunes that lack slipfaces (Nielson and Kocurek, 1986; Biswas, 2005). Regularly spaced zibars produce an undulating surface on otherwise level ground. In the geological record, preserved zibar elements take the form of sheet-like bodies (Biswas,

2005). Internally, zibar elements are characterised by low-angle to horizontal laminations of wind-ripple and/or plane-bed strata (Table 2), which may be punctuated by small cross-bedded lenticular sandstones (proto-dune forms) and granule sand-lags. Zibars are primarily differentiated from sandsheets (Section 3.2.2) based on their grain-size: zibars are composed of coarse-grain (0.5 – 1 mm) to very coarse-grain (1 – 2 mm) sand and can contain granule lags (2 – 4 mm) (Biswas, 2005; Simplicio and Basilici, 2015). Conversely, true sandsheets are typically composed of fine-grain (0.125 – 0.25 mm) to medium-grain sand (0.25 – 0.5 mm).

3.2.4 Aeolian Interdune Architectural Elements

Interdune deposits are formed in the low-relief, flat, or gently sloping areas between dunes; neighbouring dunes are separated by interdunes; commonly referred to as the interdune corridors, interdune areas, or interdune hollows (Hummel and Kocurek, 1984). Interdune architectural elements are preserved in a variety of shapes and styles; see below for detail.

Wet interdunes are characterised by deposits that accumulate on a substrate where the water table is elevated above the ground surface such that the interdune is episodically or continuously flooded with water (Kocurek and Havholm, 1993; Loope et al., 1995; García-Hidalgo et al., 2002). In cases where interdune flooding is caused by fluvial incursion, the geometry of wet interdune architectural elements can reflect the immediate shape of the interdune pond or lake (Herries, 1993; Mountney and Jagger, 2004). Conversely, in cases where there is a sustained high water table but where dune migration is not curtailed, thick and laterally extensive wet interdune elements can accumulate over a protracted time episode to form laterally extensive and continuous bodies of strata.

Damp interdunes are characterised by deposits that accumulate on a substrate where the water table is at or close to the ground surface, such that sedimentation is influenced by the presence of moisture (Fryberger et al., 1988; Lancaster and Teller, 1988; Kocurek et al., 1992). The translation of isolated damp interdunes through space over time results in the preservation of elliptical and ribbon-shaped architectural elements. Conversely, the translation of laterally extensive interdune corridors through space over time, which develop and advance in front of migrating straight-crested transverse dunes, tend to generate laterally extensive, sheet-like architectural elements (Mountney, 2012).

Wet to damp interdunes are associated with a variety of aeolian and related non-aeolian lithofacies. Most notably, this includes subaqueous current and wave ripples (sometimes associated with mud drapes), wavy laminae (Kocurek, 1981), contorted bedding (Doe and Dott, 1980), desiccation cracks, raindrop impressions, hard-pan crusts, mud flakes and mud curls (Fryberger, 1990b). Additionally, chemical precipitates may accumulate in hypersaline wet interdune ponds. Salt deposits may be prone to later dissolution, in which case crinkly lamination or pseudomorphs (e.g., after halite or gypsum) may be evident. Additionally, efflorescent salts, characterised by a thin crust on the sedimentary surface, can develop in these environments (Smoot and Castens-Seidell, 1994; Goodall et al., 2000; (Basilici et al., 2021). Non-marine carbonate sediments or freshwater chert may also accumulate in long-lived wet interdune ponds (e.g., Driese, 1985). Damp interdunes are also intimately associated with adhesion structures, which result from deposition from sediment-laden wind blowing across a damp surface (Kocurek and Fielder, 1982). Damp and wet interdunes can also be associated with microbially induced sedimentary structures (MISS), in which cryptobiotic films and crusts develop on damp and wet sedimentary surfaces (e.g., Eriksson et al., 2000; Basilici et al., 2021).

Dry interdunes are characterised by deposits that accumulate on a substrate where the water table is substantially below the ground surface, such that sedimentation is neither controlled nor greatly influenced by the effects of moisture (Ahlbrandt and Fryberger, 1981). Resultant dry interdune architectural elements tend to be relatively thin and typically form only the lowermost metre or less of accumulated deposits above an interdune-migration bounding surface (*sensu* Kocurek, 1996). Dry interdunes are associated with wind-ripple strata, and – less extensively – plane-bed lamination.

3.3 Proportions and Geometries of Architectural Elements and Lithofacies

At the scale of architectural elements and facies elements, each sedimentary unit is assigned an interpretation derived from the original source work (e.g., a sandsheet at the architectural-element scale, or grainflow strata at the facies-element scale). For each architectural or lithofacies element, thicknesses are recorded. The maximum observable (or recorded) thickness of an architectural element is considered, as presented in an outcrop panel or sedimentary log, for example. The relative

proportion of types of architectural or lithofacies elements in successions, or in parts thereof, are considered as fractions of total recorded thicknesses.

In this investigation, output from DASA describes the following: (1) the relative proportion of architectural elements of different types preserved in aeolian systems of Precambrian and Phanerozoic age; (2) the thickness of architectural elements in Precambrian and Phanerozoic age systems; and (3) the proportions of lithofacies contained within aeolian architectural elements.

Output from DASA also describes metadata of the case studies included in this investigation, for example, the geological background of a case study and the boundary conditions present at the time of deposition. Considered in this investigation are contextual data describing (1) basin setting, (2) aeolian system type (i.e. whether the system is dry, wet, mixed, or stabilizing, *sensu* Kocurek and Havholm, 1993), and (3) dune type interpretations. Contextual data are derived from the original source work and additional published literature.

3.4 Statistical Analyses

Following similar methods to those employed in Cosgrove et al. (2021a, 2022a,b), data on element thicknesses have been analysed statistically. Two-tailed t-tests have been undertaken to determine if a significant difference exists between the means of Precambrian and Phanerozoic groups. The statistical significance of differences across groups are expressed as a p-value (p). In all statistical analyses, the p-value was considered significant for $\alpha < 0.05$, to determine if the null hypothesis was rejected.

3.5 Limitations

Potential limitations to this investigation are highlighted below.

1. Absolute dating of ancient aeolian successions can be problematic due to the general lack of material suitable for dating (Rodríguez-López et al., 2014). In some cases, extrusive volcanic deposits, else marine interbeds bearing macro- or micro-fossils, within otherwise aeolian-dominated aeolian successions, enable geochronometric dating or assignment to a biostratigraphic age (e.g., Jerram et al., 2000; Scherer, 2002; Petry et al., 2007). For numerous cases, no specific age has been determined. However, given that aeolian cases studies are

typically broadly assigned to geological periods (or parts thereof), this limitation is not a significant shortcoming.

2. The study relies on the accurate interpretation of the palaeoenvironmental significance of formative aeolian architectural elements by the authors in all original source works (i.e. the recognition of dune sets, interdunes and sandsheets). Diagnostic criteria for the identification of aeolian architectural elements of different types are discussed in Section 3.2. Both modern and ancient aeolian deposits typically comprise some combination of wind-ripple strata, grainflow strata, grainfall strata, and plane beds (Hunter, 1977, 1981; Kocurek and Dott, 1981; see Table 2). However, due to their very ancient age, many Precambrian aeolian deposits have been subject to intense diagenesis, deformation and metamorphism. These effects can destroy primary sedimentary structures that are diagnostic of processes of aeolian deposition (Eriksson and Simpson, 1998). To assign a measure of quality to interpretations, data included in DASA are classified in terms of perceived quality based on the type, quantity and resolution of the original source data (cf. Baas et al., 2005; Colombera et al., 2012, 2016). A tripartite data quality index ('A', highest quality, to 'C', lowest quality) has been applied on the basis of expert judgement and quality criteria. Of the subsets considered here, 92% fall under the highest data quality indexes (i.e. are ranked A or B; see Supplementary Information).
3. Due to the effects discussed in Limitation 2 – i.e. the destruction of primary sedimentary fabric and structures that can be used to identify Precambrian aeolian successions – there could potentially be multiple examples of Precambrian aeolian deposits that have been omitted from this investigation. It is possible that some exposed Precambrian aeolian successions remain unrecognised as such, and some might have been erroneously misidentified as the products of different sedimentary environments in the wider literature (see Stewart (2002), Ielpi et al. (2016) and Lebeau and Ielpi (2017).
4. This study predicates that, in all source works, the original dune type was accurately interpreted from preserved dune sets. However, interpretations of formative dune type from evidence in the rock record are not always straightforward. Original dune morphology is only

rarely preserved in the stratigraphic record; dune topography can be variably preserved where buried beneath extrusive lava flows (e.g., Clemmensen, 1989; Jerram et al., 2000; Scherer, 2002), or by sediment of marine or other origin (e.g., Eschner and Kocurek, 1986, 1988; Chan and Kocurek, 1988). Yet, in the great majority of instances, dunes are represented by sets that preserve only their basal-most portions; successive vertically stacked sets are typically deposited progressively or intermittently over relatively long time periods (Hunter, 1977; Kocurek, 1991; Kocurek and Havholm, 1993). A complicating factor when interpreting dune types from such preserved ancient deposits is that dunes of the same morphology can exhibit different migratory behaviours through time and thereby generate different styles of deposits; preserved aeolian dune-set deposits capture only a partial record of this temporal variation (Kocurek, 1991). As such, an aeolian dune set could potentially have more than one interpretation of formative dune type. For example, the preserved deposits of linear dunes can come to resemble those of crescentic dunes if the migrating bedforms undertook a component of lateral migration (Rubin and Hunter, 1985; Clemmensen, 1989; Besly et al., 2018; Scotti and Veiga, 2019). Notwithstanding, the challenges in confidently interpreting formative dune type, all dune-type interpretations are taken from published literature that has undergone peer review; as such, in most cases, it is reasonable to adopt (with a note of caution) dune-type interpretations made by the original authors.

5. This study records the presence of non-aeolian architectural elements (for example fluvial, marine and sabkha deposits) where they occur interdigitated with otherwise aeolian-dominated systems. In this context, it is acknowledged that interdigitating palaeosols of Precambrian age may be under-recognised due to their marked difference in texture and structure when compared to those of the Phanerozoic (see Retallack et al., 1984).
6. The number of recorded architectural and lithofacies elements associated with a particular case study depends on the original data source and is reflective of the type and scale of that data source. In the source literature, many Precambrian case studies are described only by 1D graphic sedimentary logs, which may not fully capture the lateral variability of aeolian architectures. To mitigate this effect, where possible, this study utilises a variety of data

sources (outcrop architectural panels drawn to scale, photo panels, photogrammetry panels, cores, and well logs) to provide comprehensive, although not exhaustive, coverage of Precambrian aeolian systems.

4. RESULTS

4.1 Architectural Assemblage

Aeolian and non-aeolian elements represent 56% and 44%, respectively, of the total recorded stratigraphy of the examined aeolian-dominated sedimentary successions of Precambrian age (Fig. 2A). In the studied Phanerozoic successions, instead, aeolian and non-aeolian elements represent 76% and 24% of the total recorded stratigraphy, respectively (Fig. 2B).

Considering Precambrian aeolian architectural elements in more detail, deposits of aeolian dune, interdune and sandsheet origin form 59%, 6% and 35% of the total recorded aeolian stratigraphy, respectively (Fig. 2C). In the studied Phanerozoic successions, the equivalent proportions are 84%, 3%, and 5%, respectively; the remaining 8% is composed of aeolian loess deposits (Fig. 2D).

Interdune elements are subdivided into wet, damp and dry types, based on the association of features (sedimentary structures) indicative of substrate conditions. Considering interdune type, in the Precambrian, deposits of dry, damp and wet interdune origin form 15%, 24%, and 61% of the total recorded interdune stratigraphy (Fig. 2E). In the Phanerozoic, deposits of dry, damp and wet interdune origin form 35%, 24%, and 44% of all interdune deposits (Fig. 2F).

Aeolian sandsheet elements are subdivided into (1) typical sandsheets (*sensu* Nielsen and Kocurek, 1986) and (2) zibar sheet-like deposits (*sensu* Biswas, 2005); refer to Section 3.2 for definitions of these element types. In the Precambrian, typical sandsheet deposits form 69% of the total recorded sandsheet stratigraphy; zibar sheet-like deposits make up the remaining 31% (Fig. 2G). In the Phanerozoic, sandsheet and zibar sheet-like deposits form 95% and 5%, respectively, of the total recorded sandsheet stratigraphy (Fig. 2H).

In Precambrian systems, the non-aeolian stratigraphy that occurs interdigitated in dominantly aeolian successions comprises of: 31% fluvial deposits, 28% igneous rocks, 20% marine deposits, and 18%

sabkha deposits (Fig. 2I). By comparison, Phanerozoic non-aeolian stratigraphies comprise 56% fluvial deposits, 14% igneous rocks, 10% alluvial deposits, 7% lacustrine deposits, 7% sabkha deposits, and 4% marine deposits (Fig. 2J).

4.2 Architectural-Element Thickness

For a full breakdown of the architectural element thicknesses and associated statistical analyses refer to Table 3. Aeolian dune elements (Fig. 3A) are, on average, significantly thinner in Precambrian successions (mean = 2.3 m; median = 1.5 m), compared to those in Phanerozoic successions (mean = 6.2 m; median = 2.0 m). On average, aeolian sandsheet elements (Fig. 3B) and zibar elements (Fig. 3C) are both significantly thicker in Precambrian successions (sandsheet mean = 2.4 m; sandsheet median = 0.5 m; zibar mean = 20.4 m; zibar median = 2.3 m), compared to those in Phanerozoic successions (sandsheet mean = 1.5 m; sandsheet median = 0.9 m; zibar mean = 1.7 m; zibar median = 1.6 m). There is no significant difference in the mean thickness of interdune elements between Precambrian and Phanerozoic aeolian successions (Fig. 3D); interdune elements of both Precambrian and Phanerozoic age have mean thicknesses of 1.2 m and median thicknesses of 0.5 m (Table 3). Non-aeolian elements (Fig. 3E) are significantly thicker in Precambrian successions (mean = 4.9 m; median = 0.8 m), compared to those in Phanerozoic successions (mean = 3.3 m; median = 1.1 m)

4.3 Dune Types

Classifications of aeolian dune type are informed by the authors' original interpretations in the publications from which data were sourced. Percentages are based on element counts, i.e., on the number of instances a particular aeolian dune type is recorded. Considering interpreted dune types, in the Precambrian, the most common dune types are barchan (49%), transverse (25%), and barchanoid (23%) dunes (Fig. 4A). In the Phanerozoic, the most common dune types are sinuous-crested dunes (48%) and transverse dunes (17%; Fig. 4B). It is important to reiterate the challenges of interpreting dune types from the ancient aeolian record (see Limitations; Section 3.5) and it is assumed that in all source works, the original dune type was accurately interpreted from preserved dune sets.

4.4 Aeolian Systems

Aeolian systems are classified as wet, dry, mixed or stabilizing, according to the scheme of Kocurek (1998). For Precambrian aeolian successions, 83%, 11% and 6% of architectural elements were deposited in wet, dry and mixed aeolian systems, respectively (Fig. 5A). For Phanerozoic successions, 64%, 23%, 12%, 1% of architectural elements were deposited in wet, dry, mixed and stabilizing aeolian systems, respectively (Fig. 5B).

4.5 Basin Setting

Each case study is associated with deposition in a specific tectonic basin setting. Precambrian aeolian successions are most commonly preserved in rift (41%) and intracratonic (41%) basins (Fig. 6A). Phanerozoic aeolian successions are commonly preserved in intracratonic (37%), rift (24 %) and foreland (18 %) basins (Fig. 6B).

4.6 Facies Assemblages

Precambrian aeolian elements tend to be simpler in terms of their internal facies makeup, i.e., they tend to be made of fewer facies types, compared to their Phanerozoic counterparts (Fig. 7). In Precambrian successions (Fig. 7A), dune sets are predominantly composed of interfingering packages of wind-ripple, grainfall and grainflow strata (87%); the remaining 13% is composed of wind-ripple strata. In Phanerozoic successions (Fig. 7B), interfingering packages of wind-ripple, grainfall and grainflow strata form 42% of recorded facies types; the remainder is made up of: interfingered grainfall and grainflow strata (42%), wind-ripple strata (8%), grainflow strata (5%), grainfall strata (3%) and plane-bed strata (<1%). Precambrian sandsheet elements are composed of wind-ripple (55%), adhesion (43%), and deflation-lag strata (2%; Fig. 8A). Phanerozoic sandsheet elements are composed of wind-ripple (47%), adhesion (22%), deflation-lag (15%), plane-bed (13%) and subaqueous-ripple (2%) strata (Fig. 8B); the remaining 1% is composed of undifferentiated laminated sandstone. Regarding interpretations of facies associations in Precambrian aeolian systems, it is important to reiterate that metamorphism or and intense diagenesis that is commonly associated with deposits of this age can make it challenging to distinguish between grainfall, grainflow and wind-ripple strata etc. (see Limitations; Section 3.5).

5. DISCUSSION

5.1 Aeolian Dune-Set Architecture, Dune Wavelength and Angle of Climb

Aeolian dune sets are significantly thinner in Precambrian successions, compared to their Phanerozoic counterparts (Fig. 3; Fig. 9). The relative thickness of dune-set elements is largely governed by the relationship between the size of the original dune forms (i.e., their wavelength) and their regional angle of climb. The wavelength of dunes reflects the availability of sediment of a suitable grade for dune construction, the capacity of the wind to transport such sediment, and the flow behaviour of the wind (Lancaster, 1985; Lancaster, 1992; Kocurek and Lancaster, 1999). Climbing dunes of a larger wavelength are likely to result in the accumulation of thicker dune sets, relative to dunes of a smaller wavelength that are climbing at the same angle. Meanwhile, for dunes of the same wavelength, a steeper angle-of-climb will, on average, result in the accumulation of thicker dune sets, as the upper parts of bedforms in a train would be truncated to a lesser degree (Kocurek and Havholm, 1993; George and Berry, 1997; Howell and Mountney, 1997; Cosgrove et al., 2022a). The angle of climb is determined by the ratio between the rate of rise of the accumulation surface and the rate of horizontal migration of the bedform (Kocurek and Havholm, 1993; George and Berry, 1997; Cosgrove et al., 2022a).

In the Precambrian, considering interpreted dune types, barchan dunes are the most common reconstructed bedform type (Fig. 4). Barchan dunes are spatially isolated, crescent-shaped dunes that open downwind and, in modern settings, migrate relatively rapidly (Fig. 10A); presently active barchan dunes measure from ca. <10-30 m in height and have widths of up to ca. 400 m (Wilson, 1973; Bourke, 2010; Elbelrhiti and Douady, 2011; Dong et al., 2019). Barchans commonly migrate as isolated dune forms across extensive flat surfaces but do not populate the entirety of those surfaces (Durán et al., 2009). True barchan dunes in modern systems tend to be sediment transporting bedforms, rather than sediment accumulating bedforms (e.g., Slattery, 1990; Jimenez et al., 2002; Yang et al., 2021). As such, barchan dunes have only a low potential to accumulate in dry aeolian systems and their long-term preservation potential in such systems is low. However, barchan dunes can accumulate and be preserved more readily in response to a relative water-table rise in wet systems

(Mountney and Russell, 2009). It is noteworthy that both wet and damp interdunes, and aeolian systems that are classified as wet systems (*sensu* Kocurek and Havholm, 1993) are more common in the Precambrian, relative to the Phanerozoic.

Of the case studies considered here, in the Phanerozoic, dunes are most likely to be sinuous-crested and transverse dune forms (Fig. 4). Sinuous-crested and transverse dunes have heights of up to ca. 400 m, widths of up to ca. 3000 m, and lengths of up to 50 km (Wilson, 1973; Fitzsimmons, 2015). Although these geometries represent maximum likely dune sizes, on average sinuous-crested and transverse dunes are typically larger than barchan dunes (Tsoar, 2001). It is important to note, however, that linear dunes – which are one of the most common bedform types in modern dune fields – remain under-recognized in the geological record and can be misidentified as transverse dunes (Rodríguez-López et al., 2014; see Limitations; Section 3.5). Linear dunes have heights of up to ca. 400 m, widths of up to ca. 2 km, and lengths of compound forms that can be larger than 100 km (Breed and Grow, 1979; El Baz et al., 1979).

In this context, the size of formative dunes was likely to have been a significant control on the resulting thickness of dune sets preserved in the geological record; i.e. the dominance of smaller dune types (barchan dunes) in the Precambrian is likely to equate to the accumulation of thinner dune sets in the geological record. The size of dune forms is also intrinsically linked to the regional angle-of-climb, such that smaller dune forms tend to experience more rapid rates of horizontal migration (Mountney and Thompson; Mountney, 2006; Mountney, 2012). In turn, rapid bedform migration can result in smaller angles-of-climb, as the ratio between the rate of vertical accumulation (potentially controlled by subsidence-driven accommodation generation) and rate of horizontal migration is low (Mountney and Thompson; Mountney, 2006; Mountney, 2012).

In the Precambrian, the prevalence of small bedforms undergoing rapid migration is supported by the organisation of facies within aeolian dune sets. Smaller formative dunes that migrate rapidly typically lack broad, low-angle inclined plinths, resulting in the preservation of relatively less wind-ripple strata and relatively more grainflow avalanche strata (Romain et al., 2014). In the Precambrian, the dominance of small, rapidly migrating aeolian dunes is supported by the facies organisation of dune sets, such that interfingered packages of grainfall and grainflow (dune foreset) form a greater

proportion of recorded facies types in dune-set elements of Precambrian aeolian systems, relative to those of Phanerozoic age (Fig. 7). It is common for a greater proportion of grainflow and grainfall strata to extend closer to the base of a dune set in small, rapidly migrating dunes (cf. Hunter, 1977; Romain and Mountney, 2014; Nield et al., 2017).

The angle-of-climb of aeolian systems may also be affected by the rate of accommodation generation. The remains of many Precambrian supercontinents selectively crop out in the ancient stable interiors of continents; these continental shields are typically associated with intracratonic basins (Shaw et al., 1991; Aspler and Chiarenzelli, 1997). Intracratonic basins are generally associated with slow rates of basin subsidence relative to other basin settings (Xie and Heller, 2009). The slow generation of accommodation is likely associated with low angles-of-climb, and sporadic aeolian accumulation between long episodes of sediment bypass (e.g., Basilici et al., 2020; Cosgrove et al., 2022a,b). Some Precambrian successions originally accumulated in other basin types are less likely to have survived in the long-term geological record due to the significant tectonic reworking that has taken place since the Precambrian.

However, some Precambrian aeolian successions are also documented in the fills of basins that experienced more rapid subsidence, for example the aeolian deposits of the rift-sag Espinhaço Basin, Brazil (Simplicio and Basilici, 2015; Abrantes et al., 2020; Mesquita et al., 2021a,b). Indeed, when Precambrian case studies are classified according to their tectonic basin setting, rift and intracratonic basins account for 41% each of recorded case studies (Fig. 6). This suggests that the rate of accommodation generation and its effect on regional angles-of-climb are unlikely to be the only factor governing accumulated dune-set thickness. Rather, the dominance of small barchan dunes, and their rapid migration, is likely to be the dominant control on the preserved thickness of dune-sets.

5.2 Precambrian Barchan Dunes

Open questions remain as to why small, isolated, barchan dunes are the dominant Precambrian dune type, and why larger more complex dune forms are relatively rarer, when compared to the Phanerozoic record (Fig. 4). Barchan dunes are documented in the Mesoarchean Lower Moodies Group (Simpson et al., 2012), the Paleoproterozoic Makgabeng Formation (Fig. 9; Heness et al.,

2014), the Paleoproterozoic Whitworth Formation (Simpson and Eriksson, 1993), the Paleoproterozoic Lower Quilalar Formation (Jackson et al., 1990), and the Neoproterozoic Venkatpur Sandstone (Fig. 9; Basilici et al., 2020), amongst others.

Throughout geological time, the notable variety of aeolian system types – associated with different tectonic basin settings, climates, rates of sediment supply – means that is it challenging to make generalisations about the preferential formation of various dune types; nonetheless, it is possible to make some noteworthy comments. The formation of dunes of a specific type (e.g., barchan, linear, star etc.) reflects the long-term adjustment of aeolian bedforms to wind regimes, sand supply, and topographic variations (Breed et al., 1979). Dune construction is a function of the rate of aeolian sediment supply, aeolian sediment availability and the sediment-carrying capacity of the wind (Loope, 1985; Langford and Chan, 1988; Kocurek, 1988, 1996; Fryberger, 1993).

Considering barchan dunes (the dominant dune type recorded in the Precambrian), modern day observations on Earth and on extra-terrestrial planetary bodies (e.g., Mars and Titan) indicate that such dunes are formed in response to the following conditions: (1) unidirectional winds (Bagnold, 1941; McKee, 1966); (2) where there is a restricted sediment supply (Bishop, 2010); (3) on stable, coherent substrates (Cooke et al. 1993); and (4) in non-vegetated areas (Fryberger 1979; Wasson and Hyde 1983). These factors are discussed below.

5.2.1 Unidirectional Winds

In the Precambrian, palaeogeographical changes and the growth of orogenic belts may have influenced mechanisms of aeolian transport and patterns of palaeowind flow. Given that barchan dunes typically develop under dominantly unidirectional winds (Wasson and Hyde, 1983), is it possible that unidirectional winds were more common in the Precambrian, relative to the Phanerozoic?

In part, unidirectional winds may be accounted for by Precambrian palaeo-landmass distributions. Although reconstructions of palaeo-landmass distributions are difficult to constrain in the Precambrian, the landmass of Pannotia (Fig. 11; 650-500 Ma) is widely accepted to have been centred on the South Pole during the Neoproterozoic (Valentine and Moores, 1970; Nance et al., 2022). This

564 situation would have made the development of bimodal winds – associated with a monsoonal climate
565 – less likely, as bimodal winds are typically associated with an equatorial landmass distribution.
566 However, this palaeogeographical distribution would only affect deposits of Neoproterozoic age,
567 which account for only 23% of recorded case studies (Table 1). As such, it seems unlikely that a
568 dominance of unidirectional winds during the Precambrian alone could account for the dominance of
569 barchan dunes during this time period. This suggests that other factors – discussed below – may play a
570 more significant role in determining the dominance of barchan dunes in the Precambrian. In the
571 Phanerozoic, the formation of more complex dune types is likely to reflect both locally complex wind
572 regimes and a more abundant sediment supply (Rodríguez-López et al., 2014).

573 ### 5.2.2 Restricted Sediment Supply

574 Was sand supply for dune construction more likely to have been restricted in the Precambrian relative
575 to the Phanerozoic? Aeolian sediment availability is determined by the susceptibility of grains to
576 entrainment of sediment grains at the surface by the wind. The availability of sediment for aeolian
577 transport is influenced by a variety of factors, including: (1) the level of the water table; (2) the
578 presence and type of vegetation and other biogenic stabilising agents; (3) the presence of coarse-
579 grained lags that act to retard sediment entrainment; (4) the presence of chemical crusts that cement
580 surface sediments (Kocurek and Havholm, 1993; Kocurek and Lancaster, 1999; Rodríguez-López et
581 al., 2014; Basilici et al., 2020).
582 Precambrian aeolian sediment availability may have been markedly influenced by the nature of the
583 substrate, such that damp and wet interdunes form a greater combined proportion of observed
584 interdune deposits, relative to the Phanerozoic (Fig. 2). Additionally, wet aeolian systems (*sensu*
585 Kocurek, 1998) form a higher percentage of aeolian system types relative to the Phanerozoic (Fig. 5).
586 These observations may indicate a relatively higher average level of the water-table in the
587 Precambrian case studies considered here, relative to the Phanerozoic examples. The implication of
588 water tables that were higher on average in Precambrian aeolian systems is that aeolian activity was
589 not restricted to dryland settings, and was perhaps relatively common under more humid climatic
590 conditions (Tirsgaard and Øxnevad, 1998). In the Precambrian, aeolian processes may have been

591 more likely to operate under humid conditions due to the absence of stabilising vegetation, which
592 might otherwise have acted to bind and baffle sediment (Tirsgaard, and Øxnevad, 1998; Went, 2005;
593 Lebeau and Lelpi, 2017; Santos et al., 2019). This contrasts with Phanerozoic examples in which
594 vegetation existed, and where aeolian environments were preferentially located in subtropical regions
595 that were arid and lacked significant vegetation (Rodríguez-López et al., 2014). This pattern of
596 aeolian activity is also observed under modern conditions (Wilson, 1973).
597 Under more humid paleoenvironmental conditions, the water table typically lies close to or at the
598 accumulation surface. Higher water tables and the associated presence of damp and wet substrates can
599 inhibit sediment availability, as greater substrate moistures can increase the adhesive and capillary
600 forces that bind sediment together (e.g., McKenna-Neuman and Nickling, 1989; Sherman, 1990;
601 Scheidt et al., 2010). As such, the greater likelihood of encountering damp and wet substrates in the
602 Precambrian may have limited the availability of sand for dune construction, leading to the
603 preferential formation of small barchan dunes (e.g., Simpson and Eriksson, 1993; Heness et al., 2014;
604 Basilici et al., 2020).
605 Furthermore, the prevalence of damp and wet substrates (Figs. 2 and 5) may have promoted the
606 development of stabilising agents. The absence of vascular land plants in the Precambrian excludes
607 vegetation as a potential stabilising agent. However, prior to the evolution of vegetation on land,
608 aeolian substrates may have been stabilised by other biogenic agents, such as cryptobiotic films and
609 crusts, which have persisted in the terrestrial realm since the early Precambrian. Cyanobacteria and
610 other members of the bacterial domain have existed since ca. 3500 Ma (Early Archean; Schopf, 2000;
611 Golubic and Seong-Joo, 2010) and the fossil record is widespread since ca. 2100 Ma
612 (Paleoproterozoic; Golubic and Knoll, 1993). Moreover, cryptobiotic films and crusts are suggested to
613 have been geographically widely distributed throughout the Precambrian and found in hot, temperate,
614 cool, cold-arid and semi-arid environments (Fig. 9; Horodyski and Knauth, 1994, Prave, 2002,
615 Belnap, 2003; Labandeira, 2005).
616 In arid conditions of the modern day, where vegetation is largely absent, cryptobiotic films and crusts
617 play an important role in stabilising surfaces (Belnap et al., 2001); ground-hugging films and crusts
618 have been shown to increase resistance to wind erosion by up to four times when compared to

surfaces that lack crusts (Belnap, 2001). Furthermore, as cryptobiotic films – such as microbial mats – stabilise the depositional surface, they protect underlying (i.e., previously accumulated) aeolian deposits from post-depositional wind erosion. This effect further restricts sediment supply by reducing the opportunity that stored aeolian sands could be recycled as a time-lagged sediment source for a future downwind aeolian system (Basilici et al., 2020).

Biogenic stabilising agents, indicated by the presence of MISS are found, for example, in the Paleoproterozoic Makgabeng Formation (Fig. 9; Eriksson et al., 2000), the Mesoproterozoic Mangabeira Formation (Bállico et al., 2017), the Mesoproterozoic Galho do Miguel Formation (Basilici et al., 2021; Mesquita et al., 2021a,b), the Mesoproterozoic Stoer Group (Upfold, 1984), and the Neoproterozoic Venkatpur Sandstone Formation (Fig. 9; Basilici et al., 2020).

5.2.3 Stable Coherent Substrates

The preferential formation of stable coherent substrates in the Precambrian may, at first, seem counterintuitive given the lack of stabilizing vegetation during this time period (see Section 4.2.4) and the consequent absence of stabilising roots (Schumm, 1968; Gibling and Davies, 2012). However, in the absence of vegetation, the development of stabilising ground-hugging crusts in the Precambrian may have been more likely (see Section 4.2.3; Bállico et al., 2017; Basilici et al., 2020, 2021; Mesquita et al., 2021b). Such cryptobiotic films and crusts may have provided stable and coherent substrates upon which barchan dunes could preferentially form.

In the modern record, stable coherent substrates for barchan dune development are commonly provided by gravel-bed fluvial braidplains that lack vegetation (Fig. 10A; Krapf et al., 2003; Liu et al., 2012). In these environments sand for dune construction is provided by the winnowing of fluvial deposits, and barchan dunes can even develop under relatively humid climatic conditions (Mountney and Russell, 2004, 2006; Zhou et al., 2014). Of the Precambrian case studies considered here, 40% (12 of 30 case studies; see Table 1) are associated with coeval neighbouring fluvial systems. Additionally, Precambrian fluvial systems are associated with a predominance of interpreted braided channel patterns (e.g., Eriksson et al., 1998, 2006; Long, 2006, 2011; Bose et al., 2012); as such,

gravel-bed fluvial braidplains may have also provided stable coherent bases upon which barchan dunes could develop during the Precambrian.

5.2.4 Absence of Vegetation

Terrestrial vegetation was entirely absent in the Precambrian. Land-plant colonisation took place in the Middle Cambrian (ca. 500 Ma; Morris et al., 2018) and vascular land plants became widespread in the Early Silurian (ca. 425 Ma; Morris et al., 2012). During the Precambrian, the absence of vegetation allowed aeolian processes (i.e. the entrainment, transport and deposition of sediment) to operate in relatively humid settings (e.g., Dalrymple et al., 1985; Marzo, 1986; Kocurek et al., 1992; Simpson and Eriksson, 1993; Trewin, 1993).

The evolution of vegetation in the Phanerozoic may have affected the construction and stabilisation of formative dunes, because vegetation can disturb near-surface airflow and cause the deceleration of winds, resulting in the deposition of sand grains as they fall-out of airborne suspension (Nielson and Kocurek, 1986). Furthermore, vegetation can retard the re-suspension of sand once it has been deposited, thereby protecting dunes from further erosion (Byrne and McCann, 1990; Ruz and Allard, 1994). In part, the effects of vegetation may contribute to the larger variety and greater complexity of dune forms inferred for the Phanerozoic, relative to those interpreted for the Precambrian (Fig. 4). Conversely, the absence of vegetation – and the lack of its effects on sediment deposition and re-mobilisation – may have contributed to the development of simpler and smaller dune forms in the Precambrian. It is notable that barchan dunes are also the most documented dune type on Mars where vegetation is also lacking (Breed et al., 1979).

5.2.5 Dune Complexity

The dominance of simple barchan dune forms in the Precambrian emphasises that the preservation of larger more complex dune forms was relatively rare in the Precambrian, when compared to the Phanerozoic (Fig. 4). Under modern conditions, and during the Phanerozoic, complex aeolian systems are preferentially developed in arid environments (Wilson, 1973; Rodríguez-López et al., 2014); in part, this is due to the abundant availability and supply of dry sand for dune construction in arid environments, which can form sediment-accumulating bedforms.

In the Precambrian, it is likely that an abundant supply of dry sand may have been readily available due to the relatively higher rates of continental erosion, associated with the action of a hot and humid climate during much of the Archaean and Paleoproterozoic (Bose et al., 2012). However, the absence of sand-stabilising agents – most notably terrestrial vegetation – is likely to have resulted in only temporary accumulation of sand and preferential dune bypass (Kocurek and Ewing, 2012). As such, dry aeolian systems that developed (1) in basins with low rates of accommodation generation, (2) outside the influence of the water table, and/or (3) without cyanobacterial films or crusts, were more vulnerable to post depositional reworking by exogenous agents (e.g., wind, waves, rivers; Fig. 2; Chakraborty and Chakraborty, 2001; Gibling and Davies, 2012; Simplicio and Basilici, 2015). As such, complex dry aeolian systems *may* have accumulated in the Precambrian but without becoming preserved in the long-term geological record, due to progressive erosion over time in the absence of stabilising vegetation (Mesquita et al., 2021a). Consequently, dry aeolian systems with complex dune forms *could* have been present, or even predominant, over Precambrian continental surfaces; however, their preservation potential may have been low. The dominance of simple dune forms (such as barchan dunes) rather than more complex types (such as megadunes – draas) in the Precambrian may be closely associated with the greater frequency of recorded damp and wet paleoenvironmental conditions (Figs. 2E and 5), which are not conducive to the formation of complex dune systems (Mesquita et al., 2021a).

Compound and complex dune forms are, however, documented in the Mesoproterozoic Galho do Miguel Formation, Brazil (Abrantes et al., 2020; Basilici et al., 2021; Mesquita et al., 2021a). This system was deposited under both wet and dry paleoenvironmental conditions in rapidly subsiding rift-sag basin – the Espinhaço Basin. In this basin, a number of conditions facilitated the accumulation and preservation of compound dunes and complex draas. Under dry paleoenvironmental conditions – i.e. when the water table was not influencing sediment accumulation – draas where constructed under a high rate of sediment supply. The level of the water table was intermittently raised during shifts to more humid climatic conditions. Rapid subsidence placed the previously accumulated compound and complex dunes beneath the erosional baseline (defined by the level of the water table). Once placed beneath this baseline, these compound dunes and complex draas were protected from post-

depositional reworking by exogeneous agents, resulting in their long-term preservation in the geological record (Mesquita et al., 2021a).

5.3 Sandsheets

Of the case studies considered here, sandsheets form a greater proportion of the total recorded lithology and are thicker, relative to those documented in the Phanerozoic (Figs. 2, 3, 9). Sandsheets are documented, for example, in the Mesoproterozoic Mangabeira Formation (Fig. 10; Bállico et al., 2017), the Mesoproterozoic Stoer Group (Ielpi et al., 2016), the Mesoproterozoic Galho do Miguel Formation (Basilici et al., 2021; Mesquita et al., 2021a,b), the Neoproterozoic Mancheral Quartzite (Chakraborty and Chaudhuri, 1993), and the Neoproterozoic Venkatpur Sandstone (Basilici et al., 2020) (Fig. 1; Table 1).

Circumstances favourable for sandsheet development include: (1) a sediment budget that is limited by sediment supply or availability; (2) the presence of stabilising agents (vegetation, microbial mats or chemical crusts), which can inhibit the movement of sand; (3) shallow water tables, or episodic flooding, whereby the presence of damp and wet substrates inhibit the movement of sand (Kocurek and Nielson, 1986; Nielson and Kocurek, 1986; Breed et al., 1987; Khalaf, 1989; Pye and Tsoar, 1990; Basilici and Dal Bó, 2014; Dal' Bó and Basilici, 2015). These three factors overlap with the causal mechanisms that are suggested to promote the formation of barchan dunes; this strongly suggests that these palaeoenvironmental conditions were widespread during the Precambrian in aeolian environments. For a discussion of the impact of these overlapping factors refer to Section 5.2.

Alongside these aforementioned factors, the erosion of higher-relief bedforms is also a factor that contributes to the formation of sandsheets (Kocurek and Nielson, 1986). For example, this could be the erosion and reworking of a dune into a lower-relief sandsheet (Cosgrove et al., 2021b). In this context, it is noticeable that interdigitating non-aeolian elements form a far greater proportion of the total recorded lithology in the Precambrian (Fig. 2A), relative to the aeolian systems considered in the Phanerozoic (Fig. 2B). Non-aeolian physical agents have the capability to interact with and rework existing aeolian dunes into lower-relief sandsheets (Cosgrove et al., 2022b). One possible explanation for the increased presence of interdigitating non-aeolian elements in the Precambrian is the lack of

727 vegetation (Schumm, 1968; Gibling and Davies, 2012). In the absence of riparian roots that could
728 bind, baffle and trap sediment, Precambrian fluvial systems likely had relatively more erodible
729 channel banks, higher surface runoff, more flashy hydrographs, and more rapid rates of channel
730 migration, compared to vegetated Phanerozoic systems (Schumm, 1968; Cotter, 1978; Long, 1978;
731 Fuller, 1985; Els, 1990; Long, 2004). These factors allow fluvial systems to frequently interact with
732 aeolian systems (Gibling and Davies, 2012).
733 More frequent flooding events – associated with more frequent fluvial incursions into aeolian systems
734 – may also recharge groundwater beneath the aeolian dune field and potentially raise the level of the
735 water table. In turn, this may limit the availability of dry sand for sediment transport and stabilise the
736 ground surface. Surface stabilisation through fluvial flooding events is likely to occur due to the
737 deposition of cohesive muddy coverings (mud drapes), which settle from suspension following fluvial
738 incursions into aeolian dunefields (Kocurek and Nielson 1986; Purvis, 1991; Clemmensen and Dam
739 1993; Chakraborty and Chakraborty 2001; Basilici and Dal Bó, 2014). Both of these factors would act
740 to restrict the availability of dry sand.
741 The facies organisations of sandsheets found in the Precambrian versus Phanerozoic also differ (Fig.
742 8). Most notably, adhesion strata are more likely to be documented in Precambrian sandsheets,
743 relative to their Phanerozoic counterparts (Figs. 8-10; Eriksson et al., 1998; Simpson and Eriksson,
744 1991; Simpson and Eriksson, 1993; Chakraborty and Chaudhuri, 1993; Tirsgaard and Oxnevad, 1998;
745 Chakraborty and Chakraborty, 2001; Basilici et al., 2020, 2021). The greater occurrence of adhesion
746 strata in the Precambrian may reflect: (1) relatively shallow water tables (as indicated by the relatively
747 greater occurrence of damp and wet interdunes; Fig 2); (2) the frequency of fluvial incursions
748 (associated with a lack of stabilising vegetation).
749 In addition, in the Precambrian case studies considered here, a higher proportion of non-aeolian
750 architectural elements are represented by marine deposits, indicating a coastal erg location (Fig. 2;
751 Fig. 10F). Repeated flooding of sandsheets, by marine or fluvial inundation, is likely to have produced
752 interlayered aeolian and subaqueous deposits (Chakraborty and Sensarma, 2008). Transgression
753 associated with marine incursion may have acted to destroy any incipient dunes and, inland from the
754 shoreline, may have catalysed the generation of widespread damp substrates, which are preserved as

adhesion strata (Eriksson et al., 1998; Chakraborty and Chaudhuri, 1993; Tirsgaard and Oxnevad, 1998). The presence of damp substrates may have reduced the supply of dry sand available for possible aeolian dune development (Chakraborty and Sensarma, 2008), thus leading to the preferential formation of further sandsheet deposits (Kocurek and Nielson, 1986; Nielson and Kocurek, 1986; Breed et al., 1987; Khalaf, 1989; Pye and Tsoar, 1990; Dal' Bó and Basilici, 2015).

5.4 Zibars

In the Precambrian, zibar deposits are thicker, and form a greater proportion of the total recorded stratigraphy, relative to the Phanerozoic (Figs. 2 and 3; Fig. 9). Zibar deposits are documented, for example, in the Paleoproterozoic Gulcheru Quartzite (Basu et al., 2014), the Paleoproterozoic Bandeirinha Formation (Simplicio and Basilici, 2015), the Mesoproterozoic Egalapenta Member (Biswas, 2005; Dasgupta et al., 2005), and the Neoproterozoic Venkatpur Sandstone (Chakraborty, 1991). In the modern record, zibars commonly occur as coarse-grained bedforms situated on sandsheets; zibars are low-relief aeolian dunes that lack a properly developed slip-face (Figs 10; Biswas, 2005). The formation of zibars – as opposed to true dune forms – is typically associated with a limited supply of sediment available for aeolian transport (Lea and Waythomas, 1990; Nielson and Kocurek, 1986). It is noticeable that a restricted sediment supply is also causally associated with the formation of barchan dunes (Section 4.2) and sandsheets (Section 4.3); this suggests that restricted sediment supply may have been a common palaeoenvironmental condition during the Precambrian. Alongside a restricted sediment supply, zibars are associated with a coarse-grained sediment source (Biswas, 2005). A readily available early Precambrian (>2 Ga) coarse-grained sand supply may have been limited due to enhanced chemical weathering during this time period, as a result of high temperatures, humidity and greenhouse gases (Fig. 11; Corcoran et al., 1998; Kasting and Siefert, 2002). However, during the Neoproterozoic, rates of weathering likely were reduced as the greenhouse atmosphere waned (Fig. 11) and physical, rather than chemical, weathering became dominant in pre-vegetation environments (Went, 2005; Davies et al., 2011); this favoured the production of sand and gravel, rather than mud (Santos and Owen, 2016). In the absence of vegetation, and its sediment binding and baffling effects, Precambrian aeolian processes were able to

782 more readily transport such coarser sand fractions, leading to the preferential development of coarse-
783 grained zibar deposits.
784 Additionally, more frequent fluvial and marine incursions into coeval aeolian systems during the
785 Precambrian, associated with the lack of stabilising vegetation, may have promoted the destruction of
786 developing dunes and reduced the availability of dry sand for aeolian transport, by both wetting the
787 ground surface and raising the water table. These conditions may have been more favourable for the
788 formation of zibar bedforms (proto-dunes) rather than true dune forms (Simplicio and Basilici, 2015).
789 In addition, differences in the composition of the atmosphere during the Precambrian may have
790 influenced the grain-size of resulting aeolian deposits. During the Precambrian, the atmosphere is
791 thought to have been less dense, compared to present (Fig. 11; Som et al., 2012, 2016). The
792 movement of aeolian sediment has been observed in low-pressure wind tunnel observations (Iversen,
793 1982; Greeley and Iversen, 1985; Runyon et al., 2017). For example, it is demonstrated that for a
794 given wind speed, lower air pressure and density reduce the ability of airflow to transport sand, but
795 increase saltation height and length – the so-called long-hop saltation (Runyon et al., 2017). These
796 observations, alongside traditional force-balance theory, indicate that under low-pressure and low-
797 density atmospheric conditions, larger mean grain-sizes can be suspended and saltate during high-
798 speed wind gusts (Edgett and Christensen, 1991). As such, air density variations can affect the texture
799 of aeolian deposits by governing the trajectories of grains through the air and their deposition on
800 different parts of dunes that subsequently accumulate and are preserved.
801 However, atmospheric conditions during the Precambrian remain contended (Fig. 11; Johnson and
802 Goldblatt, 2015; Kavanagh and Goldblatt, 2015). The lack of proxies for atmospheric pressure and
803 density makes reliable inferences of these conditions challenging. Moreover, the way in which grains
804 are entrained and transported by lower-density atmosphere conditions remains controversial, even in
805 modelling and wind-tunnel experiments (Parteli and Herrmann, 2007; Almeida et al., 2008; Sullivan
806 and Kok, 2017; Sullivan et al., 2020). As such, even if the prevailing atmosphere was less dense, it is
807 debated whether these conditions could actually induce the aeolian transport of coarser-grained sand
808 fractions (Goosman et al., 2018). On Mars, for example, even though the atmospheric density at the
809 planetary surface is 60 to 100 times lower than that of the Earth, sand dunes are mostly composed of

very fine- to fine-grained sand, which does not differ significantly to that observed on Earth (Edgett and Christensen, 1991). As such, it is more likely that the lack of vegetation and its associated physical weathering led to the preferential formation of coarse-grained zibars during the Precambrian.

5.5 Precambrian Case Studies

Five selected Precambrian case studies are discussed in detail below; these examples highlight the variability in architecture and facies characteristics discussed above. Most notably this includes: (1) the presence of thin dune sets; (2) the presence of damp and wet interdunes; (3) the presence of MISS; (4) the presence of thick sandsheets; and (5) the presence of thick zibar deposits.

5.5.1 The Paleoproterozoic Makgabeng Formation (South Africa)

A variety of MISS have been documented in Precambrian aeolian systems. For example, in the Paleoproterozoic Makgabeng Formation (Fig. 9A), roll-up structures are seen that are interpreted to form via the desiccation-facilitated curling of cohesive surface layer into a sub-cylindrical cigar-shape (Fig. 10B, Eriksson et al., 2000). Roll-ups are typically formed in association with filamentous cyanobacteria, which secrete exo-polymeric substances that increase the cohesiveness of fine sediment (Beraldi-Campesi and Garcia-Pichel, 2010). This makes biotic roll-up structures more resistant to erosion and increases their preservation potential. In the Makgabeng, muddy roll-up structures are found within ephemeral wet interdune deposits that separate thin dune-sets (<1m), which are interpreted to be formed by barchan dunes. Periodically wet conditions within interdunes are inferred from a variety of sedimentary structures, including subaqueous ripples, adhesion strata and desiccation cracks (Eriksson et al., 2000). These muddy roll-up structures, alongside frequent tufted cyanobacterial mats suggest that microbial communities thrived in the wet and damp interdune deposits of the Makgabeng Formation (Eriksson et al., 2000, 2007; Porada and Eriksson, 2009; Simpson et al., 2013; Heness et al., 2014). Modern analogues for the muddy roll-ups of the Makgabeng have been documented in variety of desert settings, including the Sonoran Desert, Chihuahuan Desert, and Mojave Desert, USA (Beraldi-Campesi and Garcia-Pichel, 2010).

5.5.2 The Paleoproterozoic Bandeirinha Formation (Brazil)

The Bandeirinha Formation (Fig. 9B) is composed of very thick (> 50 m) dry zibar sheet-like deposits that are composed of planar to sub-planar parallel laminations that are 2 to 12 mm in thickness and are occasionally inversely graded. These deposits are interpreted to be subcritically climbing translatent wind-ripple strata (Hunter 1977; Hunter 1981). The grain size of these deposits is variable but reaches up to coarse-grained sand size (0.5 – 1 mm). Zibar deposits are punctuated by isolated, thin (<1m) cross-stratified beds that are interpreted to be formed by small, isolated slip-faced dunes (Simplicio and Basilici, 2015); the thin dune sets are composed of very fine to fine-grain sand (62.5 – 250 μm). Aeolian deposits of the Bandeirinha Formation are episodically punctuated by conglomerates, which are interpreted to be formed by the incursion of ephemeral fluvial channels (Fig. 9B). The great thickness of these zibar deposits is interpreted to the result of early cementation in combination with rapid accommodation generation that allowed the succession to be sequestered beneath the erosional baseline. Rapid accommodation generation is attributed to early rifting in the Espinhaço Basin (Chemale et al. 2012). The Upper Tulum (Argentina) aeolian sandsheet provides a modern analogue for the Bandeirinha Formation, in which surface cementation and periodic flooding prevents the formation of fully developed slip-faced dunes (Dal' Bó and Basilici, 2015). The extensive development of zibars in the Ténéré Desert (South-East Niger) also provide a modern analogue (Warren, 1971); zibars form gently undulating morphologies upon an extensive sandsheet (Fig. 10C).

5.5.3 The Mesoproterozoic Mangabeira Formation (Brazil)

The Mangabeira Formation (Fig. 9C) is formed of aeolian dune, interdune and sandsheet deposits and minor fluvial deposits (Bállico et al., 2017). Dune sets are composed of trough-tangential cross-beds with variable dip azimuths; these deposits are interpreted to be formed by three-dimensional crescentic bedforms (Rubin and Hunter, 1982). Interdune deposits are predominantly composed of crinkly laminations that are interpreted to be adhesion strata, indicating a damp depositional setting where the water table was in contact with the depositional surface (Kocurek and Fielder, 1982). Adhesion strata have also alternatively been interpreted as having microbial origin, i.e., as MISS (Souza, 2012). The thick sandsheet deposits of the Mangabeira Formation show two dominant

lamination types: (1) planar to sub-planar, inversely graded translatent laminations and (2) interlayered sandstone and mudstone with crinkly lamination (Fig. 10D). The formed are interpreted to be wind-ripple strata climbing over a dry depositional surface. The latter are interpreted to be adhesion strata, indicating a damp depositional surface. The repeated stacking of wind-ripple and adhesion strata within sandsheet deposits indicated frequent fluctuations in the level of the water table, resulting in temporal changes in the availability of dry sand for transport (Chakraborty and Chaudhuri, 1993; Scherer and Lavina, 2005) Bállico et al. (2017) interpret the Mangabeira Formation to be composed of a series of drying-upwards trends.

5.5.4 The Neoproterozoic Venkatpur Sandstone (India)

The Venkatpur Sandstone (Figs. 9D, 10E) is largely composed of water-table influenced sandsheet deposits, which separate thin (<1.5 m) dune sets. MISS are documented in biolaminites, which record interactions between aeolian processes and microbial mats (Basilici et al., 2020). The biolaminites of the Venkatpur Sadnstone are planar to disturbed planar beds that arise from the expansion, contraction, and destruction of microbial mats, which are interpreted as related to the expulsion of gases following organic matter decay, or to changes in humidity at the depositional surface (Eriksson et al., 2007). In the Venkatpur Sandstone, MISS are predominantly composed of petee (cf. Gavish et al., 1985; Reineck et al., 1990; Gerdes et al., 1994), sand stromatolites (cf. domal sand build-ups; Bottjer and Hagadorn, 2007) and palimpsest ripples (cf. Bottjer and Hagadorn, 2007). Petees form where a sand is overlain by a relatively impermeable microbial mat layer, which is disturbed to form small domes as gas escapes from decaying microbial matter (Gavish et al., 1985, Reineck et al., 1990; Gerdes et al., 1994). Sand stromatolites form where cryptobiotic films on sandy surfaces facilitate the binding of quartz sand grains and their vertical accretion (Bottjer and Hagadorn, 2007). Palimpsest ripples from where sequential sets of sandy ripples are preserved intact due to the presence of a microbial mat, which separates successive sandy ripple beds and protects underling ripple beds from reworking (Bottjer and Hagadorn, 2007).

5.5.5 The Neoproterozoic Shikaoda Formation (India)

The aeolian portion of the Shikaoda Formation (Fig. 9E) is characterised by ca. 40 m-thick sandsheet deposits, which overlie marine shoreface deposits (Chakraborty and Chakraborty, 2001). The sedimentary structures associated with the Shikaoda sandsheet reflect conditions at the time of deposition; these conditions describe the relative wetness of the depositional surface and can be classified as dry, damp and wet conditions. Dry sandsheet conditions are indicated by translatent wind-ripple strata (cf. Hunter, 1977); damp sandsheet conditions are indicated by a variety of adhesion strata (including adhesion plane-beds and ripples; cf. Olsen et al., 1989); wet conditions are indicated by subaqueous cross-stratification (c.f. Hunter, 1985). The sedimentological features reflect the periodic wetting and drying of the sandsheet, associated with episodic marine incursions; these aqueous interactions form sub-horizontal bounding surfaces that subdivide the sandsheet deposits of the Shikaoda Formation (Chakraborty and Chakraborty, 2001). The conditions that formed the Shikaoda sandsheet are comparable to the modern-day coastal aeolian system of Padre Island, Texas (Fig. 10F; Hummel and Kocurek, 1984; Kocurek and Nielson, 1986).

6. CONCLUSIONS

This study has compared the preserved deposits of Precambrian (Archean and Proterozoic) aeolian systems with those of the Phanerozoic. Deposits of Precambrian age record notable differences in aeolian architecture, when compared with their Phanerozoic counterparts. (1) Precambrian aeolian systems are associated with more limited architectural complexity, defined by thin aeolian dune sets, which are interpreted as predominantly produced by small, simple barchan dunes. (2) Interdune deposits are predominantly damp and wet, indicating that Precambrian aeolian systems were prevalent in wetter paleoenvironmental conditions. (3) Relative to the Phanerozoic, Precambrian aeolian systems are associated with a greater occurrence of (i) sandsheets, (ii) zibars, and (iii) interdigitating non-aeolian elements.

The above attributes of Precambrian aeolian systems can, in part, be related to the absence of stabilising vegetation. The lack of vegetation that would otherwise act to bind and baffle sediment allowed aeolian processes to operate under relatively humid climate regimes. This contrasts with

914 vegetated Phanerozoic systems, for which aeolian processes were largely restricted to arid subtropical
915 regions that lacked significant vegetation cover, as occurs at present. Furthermore, the absence of
916 stabilising vascular land plants allowed aeolian systems to experience more common interactions with
917 non-aeolian environments; for example, marine and fluvial incursions commonly occurred into coeval
918 aeolian systems during the Precambrian. Common aqueous interactions recharged groundwater levels
919 and raised the water table beneath aeolian systems.
920 Both of the above factors – i.e. the operation of aeolian systems in relatively humid climatic
921 conditions, and frequent incursions of aqueous agents into aeolian dunefields – led to the widespread
922 development of damp and wet substrates. Greater substrate moistures (1) increased the adhesive and
923 capillary forces that bound sediments together, and (2) in the absence of vegetation, allowed
924 substrate-stabilising crusts and films to develop. These factors increased the resistance of the substrate
925 to wind erosion restricting the availability of dry sand for dune construction. Low rates of sediment
926 supply, in combination with the lack of vegetation and relatively high water tables, led to the
927 preferential formation of simple barchan dunes, sandsheets and zibars during the Precambrian.
928 Within dry aeolian systems, complex aeolian bedforms (i.e. those containing larger, complex and
929 compound dunes and draas) could have developed in the Precambrian; however, their preservation
930 potential may have been low. The absence of sand-stabilising terrestrial vegetation is likely to have
931 resulted in only temporary accumulation of sand, making such complex bedforms more vulnerable to
932 post-depositional reworking by exogenous agents (e.g., wind, waves, rivers).

933 ## 7. ACKNOWLEDGEMENTS

934 We thank the sponsors and partners of FRG-ERG-SMRG for financial support for this research:
935 AkerBP, Areva (now Orano), BHP, Cairn India (Vedanta), Chevron, ConocoPhillips, CNOOC,
936 Equinor, Murphy Oil, Occidental, Petrotechnical Data Systems, Aramco, Shell, Tullow Oil, Woodside
937 and YPF.

8. REFERENCES

Abrantes, F.R., Basilici, G., Soares, M.V.T., 2020. Mesoproterozoic erg and sand sheet system: Architecture and controlling factors (Galho do Miguel Formation, SE Brazil). Precam. Res., 338, 105592. https://doi.org/10.1016/j.precamres.2019.105592.

Ahlbrandt, T.S., Fryberger, S.G., 1981. Sedimentary Features and Significance of Interdune Deposits, in: Recent and Ancient Nonmarine Depositional Environments: Models for Exploration, Ethridge, F.G., Flores, R.M., SEPM Spec. Pub. 31, 293 – 314. https://doi.org/10.2110/pec.81.31

Allen, J.R.L., 1963. The classification of cross-stratified units. With notes on their formation. Sedimentology. 2, 93-114. https://doi.org/10.1111/j.1365-3091.1963.tb01204.x

Allen, P., Hoffman, P., 2005. Extreme winds and waves in the aftermath of a Neoproterozoic glaciation. Nature. 433, 123–127. https://doi.org/10.1038/nature03176.

Almeida, M. P., Parteli E. J., Andrade J. S., Herrmann H. J., 2008. Giant saltation on Mars. Proc. Natl. Acad. Sci. U.S.A. 105, 6222–6226. https://doi.org/10.1073/pnas.0800202105

Altermann, W., Corcoran, P.L., 2002. Precambrian Sedimentary Environments: A Modern Approach to Ancient Depositional Systems, Blackwell, Oxford, pp. 450.

Aspler, L.B., Chiarenzelli, J.R., 1997. Initiation of ca 2.45-2.1 Ga intracratonic basin sedimentation of the Hurwitz Group, Keewatin Hinterland, Northwest Territories. Canada. Precam. Res. 81, 265-297. https://doi.org/10.1016/S0301-9268(96)00038-1

Bagnold, R.A., 1941. The Physics of Blown sand and Desert Dunes. Methuen, London.

Bállico, M.B., Scherer, C.M.S., Mountney, N.P., Souza, E.G., Chemale, F., Pisarevsky, S.A., Reis A.D., 2017. Wind-pattern circulation as a palaeogeographic indicator: Case study of the 1.5-1.6 Ga Mangabeira Formation, Sao Francisco Craton, Northeast Brazil. Precambrian Res., 298, 1-15. https://doi.org/10.1016/j.precamres.2017.05.005

Basilici and Dal Bó, 2014. Influence of subaqueous processes on the construction and accumulation of an aeolian sand sheet. Earth Surface Processes and Landforms, 39, 1014-1029. https://doi.10.1002/esp.3498

964 Basilici, G., Soares, M.V.T., Mountney, N.P., Colombera, L., 2020. Microbial influence on the
965 accumulation of Neoproterozoic aeolian-dominated depositional systems: Venkatpur Sandstone
966 Formation, Telangana State, southern India. Precam. Res. 347, 105854.
967 https://doi.org/10.1016/j.precamres.2020.105854
968 Basilici, G, Mesquita, A, F., Soares, A.V.T., Janočko, J., Mountney, N.P., Colombera, L., 2021. A
969 Mesoproterozoic hybrid dry-wet aeolian system: Galho do Miguel Formation, SE Brazil. Precam.
970 Res. 359, 106216. https://doi.org/10.1016/j.precamres.2021.106216
971 Basu,H., Sastry, R.S., Achara, K.K., Umamaheswara, K., Parihara, P.S., 2014. Palaeoproterozoic
972 fluvio-aeolian deposits from the lower GulcheruFormation, Cuddapah Basin, India. Precam. Res. 246,
973 321-333. http://dx.doi.org/10.1016/j.precamres.2014.03.011
974 Belnap, J. 2001. Biological soil crusts and wind erosion, in: Belnap, J., Lange, O. L.(Eds.), Biological
975 soil crusts: structure, function, and management. Springer-Verlag, Berlin, pp. 339–348.
976 Belnap, J., 2003. The World at Your Feet: Desert Biological Soil Crusts. Ecol. Soc. Am. 1, 181-189.
977 https://doi.org/10.2307/3868062
978 Belnap, J., Budel, B., Lange, O.L., 2001. Biological soil crusts: characteristics and distribution. In: J.
979 Belnap, J., Lange, O.L. (Eds.), Biological Soil Crusts: Structure, Function, and Management.Springer-
980 Verlag, Berlin, pp. 3-30.
981 Beraldi-Campesi, H., Garcia-Pichel, F., 2010. The biogenicity of modern terrestrial roll-up structures
982 and its significance for ancient life on land. Geobio. 9, 10-23. https://doi.org/10.1111/j.1472-
983 4669.2010.00258.x
984 Besly, B., Romain, H.G., Mountney, N.P., 2018. Reconstruction of linear dunes from ancient aeolian
985 successions using subsurface data: Permian Auk Formation, Central North Sea, UK. Mar. Pet. Geol.
986 91, 1 -18. https://doi.org/10.1016/j.marpetgeo.2017.12.021
987 Bishop, M.A., 2010. Nearest neighbor analysis of mega-barchanoid dunes, Ar Rub' al Khali, sand sea:
988 The application of geographical indices to the understanding of dune field self-organization, maturity
989 and environmental change. Geomorphology, 120, 186-194.
990 https://doi.org/10.1016/j.geomorph.2010.03.029

991 Biswas, A., 2005. Coarse aeolianites: sand sheets and zibar-interzibar facies from the
992 Mesoproterozoic Cuddapah Basin, India. Sed. Geol., 174, 149-160.
993 https://doi.org/10.1016/j.sedgeo.2004.11.005
994 Bleeker, W., 2003. The late Archean record: a puzzle in ca. 35 pieces. Lithos. 71, 99-134.
995 https://doi.org/10.1016/j.lithos.2003.07.003
996 Bleeker, W., 2004. Taking the pulse of planet Earth: a proposal for a new multi-disciplinary flagship
997 project in Canadian solid Earth sciences. Geosci. Canada. 31, 179-190.
998 Blount G., Lancaster N., 1990. Development of the Gran Desierto sand sea. Geology, 18, 724-728.
999 https://doi.org/10.1130/0091-7613(1990)018<0724:DOTGDS>2.3.CO;2
1000 Bose, P.K., Chakrabarty, S., Sarkar, S., 1999. Recognition of ancient eolian longitudinal dunes: a case
1001 study in upper Bhander Sandstone, Son Valley. India. J. Sed. Res. 69, 74-83.
1002 https://doi.org/10.2110/jsr.69.74
1003 Bose, P.K., Sarkar, S., Chakrabarty, S., Banerjee, S., 2001. Overview of the Meso- to Neoproterozoic
1004 evolution of the Vindhyan basin, central India. Sed. Geol. 141–142, 395 – 419.
1005 https://doi.org/10.1016/S0037-0738(01)00084-7
1006 Bose, P.K., Eriksson, P.G., Sarkar, S., Wright, D.T., Samanta, P., Mukhopadhyay, S., Mandal, S.,
1007 Banerjee, S., Altermann, W., 2012. Sedimentation patterns during the Precambrian: a unique record?
1008 Mar. Pet. Geol. 33, 34–68. https://doi.org/10.1016/j.marpetgeo.2010.11.002
1009 Bottjer, D., Hagadorn, J.W., 2007. Mat Growth Features, in: Schieber, J., Bose, P.K., Eriksson, P.G.,
1010 Banerjee, S., Sarkar, S., Altermann, W., Catuneanu, O., (Eds.), Atlas of Microbial Mat Features
1011 Preserved within the Clastic Rock Record. pp. 53-71. Elsevier, Amsterdam.
1012 Bourke, M.C., 2010. Barchan dune asymmetry: observations from Mars and Earth. Icarus, 205, 183–
1013 197. https://doi.org/10.1016/j.icarus.2009.08.023
1014 Breed, C.S., Grow, T., 1979. Morphology and distribution of dunes in sand seas observed by remote
1015 sensing. In: McKee, E.D., (Ed.), A study of global sand seas. United States Government Printing
1016 Office, Washington, DC, pp 253–304

1017 Breed, C.S., Grolier, M.J., McCauley, J.F., 1979. Morphology and distribution of common 'sand'
1018 dunes on Mars: Comparison with the Earth. JGR Solid Earth. 84, 8183-8204.
1019 https://doi.org/10.1029/JB084iB14p08183
1020 Brookfield, M.E., 1977. The origin of bounding surfaces in ancient aeolian sandstones.
1021 Sedimentology. 24, 303-332. https://doi.org/10.1111/j.1365-3091.1977.tb00126.x
1022 Cao, S., Zhang, L., Wang, C., Ma, J., Tan, J., Zhang, Z., 2020. Sedimentological characteristics and
1023 aeolian architecture of a plausible intermountain erg system in Southeast China during the Late
1024 Cretaceous. GSA Bull., 132, 2475-2488. https://doi.org/10.1130/B35494.1
1025 Cather, S.M., Connell, S.D., Chamberlin, R.M., McIntosh, W.C., Jones, G.E., Potochnik, A.R., Lucas,
1026 S.G., Johnson, P.S., 2008. The Chuska erg: Paleogeomorphic and paleoclimatic implications of an
1027 Oligocene sand sea on the Colorado Plateau. Geol. Soc. Am. Bull. 120, 13-33.
1028 https://doi.org/10.1130/B26081.1
1029 Chan, M.A., Kocurek, G., 1988. Complexities in eolian and marine interactions: processes and
1030 eustatic controls on erg development. Sed. Geol. 56, 283-300. https://doi.org/10.1016/0037-
1031 0738(88)90057-7
1032 Chakraborty, T., 1991. Sedimentology of a Proterozoic erg: the Venkatpur Sandstone, Pranhita-
1033 Godavari Valley, South-India. Sedimentology, 38, 301-322. https://doi.org/10.1111/j.1365-
1034 3091.1991.tb01262.x
1035 Chakraborty, T., Chakraborty, C., 2001. Eolian-aqueous interactions in the development of a
1036 Proterozoic sand sheet: Shikaoda Formation, Hosangabad, India. J. Sed. Res., 71, 107-117.
1037 https://doi.org/10.1306/031700710107
1038 Chakraborty, T., Chaudhuri, A.K., 1993. Fluvial-aeolian interactions in a Proterozoic alluvial plain:
1039 example from the Mancheral Quartzite, Sullavai Group, Pranhita-Godavari Valley, India, in: Pye, K.
1040 (Ed.), The Dynamics and Environmental Context of Aeolian Sedimentary Systems. Geol. Soc. Spec.
1041 Pub. 72, 127-141. https://doi.org/10.1144/GSL.SP.1993.072.01.12
1042 Chakraborty, T., Sensarma, S., 2008. Shallow marine and coastal eolian quartz arenites in the
1043 Neoarchean-Palaeoproterozoic Karutola Formation, Dongargarh volcano-sedimentary succession,
1044 central India. Precam. Res., 162, 284-301. https://doi.org/10.1016/j.precamres.2007.07.024

Chemale F., Dussin I.A., Alkmim F.F., Martins M.S., Queiroga G., Armstrong R., Santos M.N. 2012. Unravelling a Proterozoic basin history through detrital zircon geochronology: The case of the Espinhaço Supergroup, Minas Gerais, Brazil. Gondwana Res. 22, 200-206. https://doi.org/10.1016/j.gr.2011.08.016

Chrintz, T., Clemmensen, L.B., 1993. Draa reconstruction, the Permian Yellow Sands, northeast England, in: Pye, K., Lancaster, N., (Eds.), Aeolian sediments. Ancient and modern, IAS Spec. Publ. 16, 151-161. https://doi.org/10.1002/9781444303971.ch10

Clemmensen, L.B., 1985. Desert sand plain and sabkha deposits from the Bunter Sandstone formation (L.Triassic) at the northern margin of the German Basin. Geol. Rundsch., 74, 519-536. https://doi.org/10.1007/bf01821209

Clemmensen, L.B., 1988. Aeolian morphology preserved by lava cover, the Precambrian Mussartût Member, Eriksfjord Formation, South Greenland. Bull. Geol. Soc. Denmark. 37, 105-116. https://doi.org/10.1.1.529.8278

Clemmensen, L.B., 1989. Preservation of interdraa and plinth deposits by the lateral migration of large linear draas (Lower Permian Yellow Sands, northeast England). Sed. Geol. 65, 139-151. https://doi.org/10.1016/0037-0738(89)90011-0

Clemmensen, L.B., Abrahamsen, K., 1983. Aeolian stratification and facies association in desert sediments, Arran Basin (Permian), Scotland. Sedimentology. 30, 311-339. https://doi.org/10.1111/j.1365-3091.1983.tb00676.x

Cooke, R.U., Warren, A., Goudie, A.S., 1993. Desert geomorphology. UCL Press, London.

Colombera, L., Mountney, N.P., McCaffrey, W.D., 2012. A relational database for the digitization of fluvial architecture concepts and example applications. Pet. Geo., 18, 129-140. https://doi.org/10.1144/1354-079311-021

Colombera, L., Mountney, N.P., Hodgson, D.M., McCaffrey, W.D., 2016. The Shallow-Marine Architecture Knowledge Store: A database for the characterization of shallow-marine and paralic depositional systems. Mar. Pet. Geol. 75, 83-99. https://doi.org/10.1016/j.marpetgeo.2016.03.027

Cosgrove, G.I.E., Colombera, L., Mountney, N.P, 2021a. A database of Eolian Sedimentary Architecture for the characterization of modern and ancient sedimentary systems. Mar. Pet. Geol., 127, 104983. https://doi.org/10.1016/j.marpetgeo.2021.104983.

Cosgrove, G.I.E., Colombera, L., Mountney, N.P, 2021b. Quantitative analysis of the sedimentary architecture of eolian successions developed under icehouse and greenhouse climatic conditions. GSA Bull. 133, 2625–2644. https://doi.org/10.1130/B35918.1

Cosgrove, G.I.E., Colombera, L., Mountney, N.P, 2022a. The role of subsidence and accommodation generation in controlling the nature of the aeolian stratigraphic record. J. Geol. Soc. 179, jgs2021–042. https://doi.org/10.1144/jgs2021-042

Cosgrove, G.I.E., Colombera, L., Mountney, N.P, 2022b. Eolian stratigraphic record of environmental change through geological time. Geology. 50, 289-294. https://doi.org/10.1130/G49474.1

Cotter, E., 1978. The evolution of fluvial style, with special reference to the central Appalachian Palaeozoic, in: Miall, A.D. (Ed.), Fluvial Sedimentology. Bull. Can. Pet. Geol., 5, 361-383.

Cowan, G., 1993. Identification and significance of aeolian deposits within the dominantly fluvial Sherwood Sandstone Group of the East Irish Sea Basin UK, in: North, C.P., Prosser, D.J. (Eds.), Characterization of Fluvial and Aeolian Reservoirs.Geol. Soc. Spec. Pub., 73, 231-245. https://doi.org/10.1144/GSL.SP.1993.073.01.14

Crabaugh, M., Kocurek, G., 1993.Entrada Sandstone: An example of a wet aeolian system, in: Pye, K. (Ed.), The dynamics and environmental context of aeolian sedimentary systems. Geol. Soc. London Spec. Publ., 72, 103-126. https://doi.org/10.1144/GSL.SP.1993.072.01.1

Dal' Bó, P.F.F., Basilici, G., 2015.Intermontane eolian sand sheet development, Upper Tulum Valley, central-western Argentina. Braz. J. Geol., 45. https://doi.org/10.1590/2317-4889201530140

Dalrymple, R.W., Narbonne, G.M., Smith, L., 1985. Eolian action and the distribution of Cambrian shales in North America. Geology. 13, 608-610. https://doi.org/10.1130/0091-7613(1985)13<607:EAATDO>2.0.CO;2

Dasgupta, P.K., Biswas, A., Mukherjee, R., 2005. Cyclicity in Palaeoproterozoic to Neoproterozoic Cuddapah Supergroup and its significance in basinal evolution, in: Mabesoone, J.M., Neumann, V.H.,

(Eds.), Cyclic Development of Sedimentary Basins. Dev. Sediment. 57, 313-354. https://doi.org/10.1016/S0070-4571(05)80013-5

Davies, N.S., Gibling, M.R., Rygel, M.C., 2011. Alluvial facies during the Palaeozoic greening of the land: case studies, conceptual models and modern analogues. Sedimentology. 58, 220-258. https://doi.org/10.1111/j.1365-3091.2010.01215.x

Deynoux, M., Kocurek, G., Proust, J.N., 1989. Late Proterozoic periglacial aeolian deposits on the West African Platform, Taoudeni Basin, western Mali. Sedimentology. 36, 531-550. https://doi.org/10.1111/j.1365-3091.1989.tb02084.x

de Oliveira Chaves, A., Rezende, C., 2019. Fragments of 1.79-1.75 Ga Large Igneous Provinces in reconstructing Columbia (Nuna): A Statherian supercontinent-superplume coupling? Episodes. 42. 55-67. https://doi.org/10.18814/epiiugs/2019/019006.

Donaldson, J.A., Eriksson, P.G., W. Altermann, W., 2002. Actualistic versus non-actualistic conditions in the Precambrian: a reappraisal of an enduring discussion, in: Altermann, W., Corcoran, P.L. (Eds.), A Modern Approach to Ancient Depositional Systems. Precambrian Sedimentary Environments. IAS Spec. Pub. 33, Blackwell, Oxford, pp. 3-13. https://doi.org/10.1002/9781444304312.ch1

Dong, Z., Qian, G., Luo, W., Zhang, Z., Lv, P., 2012. Dune types and their distribution in the Kumtagh Sand Sea,northwestern China. Zeitschrift für Geomorphologie, 57, 207–224.

Durán, O., Schwämmle, V., Lind, P.G., Herrmann, H.J., 2009. The dune size distribution and scaling relations of barchan dune fields. Granular Matter, 11, 7–11. https://10.1007/s10035-008-0120-4

Edgett, K. S., Christensen, P. R., 1991. The particle-size of Martian aeolian dunes. J. Geophys. Res., 96, 765–776. https://doi.org/10.1029/91JE02412

El-Baz, F., Breed, C.S., Grolier, M.J., McCauley, J.F., 1979. Eolian features in the western desert of Egypt and some applications to Mars. J. Geophys. Res., 84, 8205–8221. https://doi.org/10.1029/JB084iB14p08205

El Belrhiti, H., Douady, S., 2011. Equilibrium versus disequilibrium of barchan dunes. Geomorphology. 125, 558–568. https://doi.org/10.1016/j.geomorph.2010.10.025

1126 Ellis, D., 1993. The Rough Gas Field: distribution of Permian aeolian and non-aeolian reservoir facies
1127 and their impact on field development. Geol. Soc. Spec. Pub., 73, 265-277.
1128 https://doi.org/10.1144/GSL.SP.1993.073.01.16
1129 Els, B.G., 1990. Determination of some palaeohydraulic parameters for a fluvial Witwatersrand
1130 succession. S. Afr. J. Geol. 93, 531–537. 10.10 https://doi.org/02/9781444304213.ch27
1131 Eriksson, E.A., 1995. Crustal growth, surface processes, and atmospheric evolution on the early Earth,
1132 in: Coward, M.P., Ries, A.C. (Eds.), Early Precambrian Processes. Geol. Soc. Spec. Publ. 95, 11–25.
1133 https://doi.org/10.1144/GSL.SP.1995.095.01.02
1134 Eriksson, P.G., Simpson, E.L., 1998. Controls on spatial and temporal distribution of Precambrian
1135 eolianites. Sed. Geol. 120, 275–294. https://doi.org/10.1016/S0037-0738(98)00036-0
1136 Eriksson, P.G., Condie, K.C., Tirsgaard, H., Mueller, W.U., Altermann, W., Miall, A.D., LAspler,
1137 L.B., Catuneanu, O., Chiarenzelli, J.R., 1998. Precambrian clastic sedimentation systems. Sed.
1138 Geol. 120, 5-53. https://doi.org/10.1016/S0037-0738(98)00026-8
1139 Eriksson, P.G., Simpson, E.L., Eriksson, K.A., Bumby, A.J., Steyn, G.L., Sarkar, S., 2000. Muddy
1140 roll-up structures in siliciclastic interdune beds of the c 1.8 Ga Waterberg Group, South
1141 Africa.Palaios, 15, 177 – 183. https://doi.org/10.2307/3515640
1142 Eriksson, P.G., Catuneanu, O., Aspler, L.B., Chiarenzelli, J.R., Martins-Neto, M.A., 2001a.Preface,
1143 special issue: the influence of magmatism, tectonics, sea level change and palaeo-climate on
1144 Precambrian basin evolution: change over time. Sed. Geol., 141–142, vii – xi.
1145 https://doi.org/10.1016/S0037-0738(01)00089-6
1146 Eriksson, P.G., Martins-Neto, M.A., Nelson, D.R., Aspler, L.B., Chiarenzelli, J.R. and Catuneanu O.,
1147 2001b. An introduction to Precambrian basins: their characteristics and genesis. Sed. Geol., 141–142,
1148 1 – 35. https://doi.org/10.1016/S0037-0738(01)00066-5
1149 Eriksson, P.G., Bumby, A.J., Popa, M.,2004. Sedimentation through time, in: Eriksson, P.G.,
1150 Altermann, W., Nelson, D.R., Mueller, W.U., Catuneanu, O. (Eds.), The Precambrian Earth: Tempos
1151 and Events. Elsevier, Amsterdam, pp. 593-602.
1152 Eriksson, P.G., Catuneanu, O., Sarkar, S., Tirsgaard, H., 2005. Patterns of sedimentation in the
1153 Precambrian. Sed. Geol. 176, 17-42. https://doi.org/10.1016/j.sedgeo.2005.01.003

1154 Eriksson, P.G., Bumby, A.J., Brümer, J.J., van der Neut, M., 2006. Precambrian fluvial deposits:
1155 enigmatic palaeohydrological data from the c. 2–1.9 Ga Waterberg Group, South Africa. Sed. Geol.
1156 190, 25-46.https://doi.org/10.1016/j.sedgeo.2006.05.003
1157 Eriksson, P.G., Porada, H., Banerjee, S., Bouougri, E., Sarkar, S., Bumby, A.J., 2007. Mat-destruction
1158 features, in: Schieber, J., Bose, P.K., Eriksson, P.G., Banerjee, S., Sarkar, A., Altermann, W.,
1159 Catuneanu, O. (Eds.), Atlas of microbial mat features preserved within the siliciclastic rock record.
1160 Atlases in Geosciences, 2. Elsevier, New York, pp. 76–105
1161 Eschner, T.B., Kocurek, G., 1986.Marine destruction of eolian sand seas: Origin of mass flows. J.
1162 Sed. Res. 56, 401-411. https://doi.org/10.1306/212F892C-2B24-11D7-8648000102C1865D
1163 Eschner, T.B., Kocurek, G., 1988. Origins of relief along contacts between eolian sandstones and
1164 overlying marine strata. AAPG Bull. 72, 923-949. https://doi.org/10.1306/703C9118-1707-11D7-
1165 8645000102C1865D
1166 Evans, G., Kendall, C.G.St.C., Skipwith, P., 1964. Origin of coastal flats, the sabkha of the Trucial
1167 Coast, Persian Gulf. Nature. 202, 759-761. https://doi.org/10.1038/202759a0
1168 Fitzsimmons, K.E., 2015. Transverse Dunes, in: Hargitai, H., Kereszturi, Á., (Eds.), Encyclopedia of
1169 Planetary Landforms. Springer, New York, NY. https://doi.org/10.1007/978-1-4614-3134-3_381
1170 Fryberger, S.G.,1979. Dune forms and wind regime, in: McKee, E.D. (Ed.), A study of global sand
1171 Seas. Geological Survey Professional Paper N 1052. U.S. Govt. Printing Office, Washington, DC, pp
1172 137–169.
1173 Fryberger, S.G., Schenk, C.J., Krystinik, L.F., 1988. Stokes surfaces and the effects of near-surface
1174 groundwater-table on Aeolian deposition. Sedimentology. 35, 21-41. https://doi.org/10.1111/j.1365-
1175 3091.1988.tb00903.x
1176 Fuller, A.O., 1985. A contribution to the conceptual modelling of pre-Devonian fluvial systems.
1177 Trans. Geol. Soc. S. Afr. 88, 189–194.
1178 García-Hidalgo, J.F., Temiño, J., Segura, M., 2002. Holocene eolian sediments on the southern border
1179 of the Duero Basin (Spain): origin and development of an eolian system in a temperate zone. J. Sed.
1180 Res. 72, 30-39. https://doi.org/10.1306/040501720030

1181 Garzanti E., Andó S., Vezzoli G, Dell´era D., 2003. From rifted margins to foreland basin:
1182 investigating provenance and sediment dispersal across desert Arabia (Oman, U.A.E.). J. Sed. Res.
1183 73, 572-588. https://doi.org/10.1306/101702730572
1184 Gavish, E., Krumbein, W.E., Halevy, J., 1985. Geomorphology mineralogy and groundwater
1185 geochemistry as factors of the hydrodynamic system of the Gavish Sabkha. In: Hypersaline
1186 Ecosystems - The Gavish Sabkha (Eds. G.M. Friedman, and W.E. Krumbein) Ecological Studies, 53,
1187 186–217.
1188 Gerdes, G., Krumbein, W.E., Reineck, H.E., 1994. Microbial mats as architects of sedimentary
1189 surface structures. In: Biostabilization of Sediments (Eds. W.E. Krumbein, D. M. Paterson, L.J. Stal),
1190 pp. 165–182. Bibliotheks und Informationssystem der Universität ldenburg, Oldenburg.
1191 Goldberg, A.S., 2010. Dyke swarms as indicators of major extensional events in the 1.9–1.2 Ga
1192 Columbia supercontinent. J. Geodynamics. 50, 176–190. https://doi.org/10.1016/j.jog.2010.01.017
1193 Goldblatt, C., 2018. Atmospheric Evolution, in: White, W.M. (Eds.), Encyclopaedia of Geochemistry.
1194 Encyclopaedia of Earth Sciences Series. Springer, Cham. https://doi.org/10.1007/978-3-319-39312-
1195 4_107
1196 Golubic, S., Knoll, A.H., 1993. Fossil prokaryotes. In: Lipps, J.H., (Eds.), Fossil Prokaryotes and
1197 Protists, 51–76. Blackwell Scientific, Oxford.
1198 Golubic, S., Seong-Joo, L., 2010. Early cyanobacterial fossil record: preservation,
1199 palaeoenvironments and identification. Eur. J. Phycol. 34, 339 – 348.
1200 https://doi.org/10.1080/09670269910001736402
1201 Goodall, T.M., North, C.P., Glennie, K.W., 2000. Surface and subsurface sedimentary structures
1202 produced by salt crusts. Sedimentology, 47, 99-118. https://doi.org/10.1046/j.1365-
1203 3091.2000.00279.x
1204 Goosman, E.A., Catling, D.C., Som, S.M., Altermann, W., Buick, R., 2018. Eolianite Grain Size
1205 Distributions as a Proxy for Large Changes in Planetary Atmospheric Density. JGR Plan. 123, 2506-
1206 2526. https://doi.org/10.1029/2018JE005723
1207 Gibling, M.R., Davies, N.S., 2012. Palaeozoic landscapes shaped by plant evolution. Nature
1208 Geoscience. 5, 99–105. https://doi .org/10.1038/ngeo1376.

Gradstein, F.M., 2020. Chapter 1 – Introduction, in: Gradstein, F.M., Ogg, J.G., Schmitz, M.D., Ogg, G.M. (Eds.), Geologic Time Scale, Elsevier. https://doi .org/10.1016/B978-0-12-824360-2.00001-2

Greeley, R., Iversen, J. D., 1985. Wind as a geological process: on Earth, Mars, Venus, and Titan, Cambridge Cambridgeshire, New York, Cambridge University Press, pp. 348.

Hadlari, T., Rainbird, R.H. and Donaldson, J.A., 2006. Alluvial, eolian and lacustrine sedimentology of a Paleoproterozoic half-graben, Baker Lake Basin, Nunavut, Canada. Sed. Geol. 190, 47-70. https://doi.org/10.1016/j.sedgeo.2006.05.005

Haines, P.W., Mory, A.J., Stevens, M.K., Ghori, K.A.R., 2004. GSWA Lancer 1 well completion report (basic data), Officer and Gunbarrel Basins, Western Australia. Geol. Surv. W. Australia. P. 46.

Hallam, A., 1990. Great Geological Controversies (Second Edition), Oxford University Press, Oxford, p. 256

Halverston, G.P., Hoffman, P.F., Schrag, D.P., Maloof, A.C., Rice, A.H.N., 2005. Toward a Neoproterozoic Composite Carbon Isotope Record. Bull. Geol. Soc. Am. 117, 1181–1207. https://doi.org/10.1130/B25630.1

Hasegawa, H., Imsamut, S., Charusiri, P., Tada, R., Horiuchi, Y., Hisada, K-I., 2010. Thailand was a desert during the mid-Cretaceous: Equatorward shift of the subtropical high-pressure belt indicated by eolian deposits (Phu Thok Formation) in the Khorat Basin, northeastern Thailand. Island Arc. 19,605-621. https://doi.org/10.1111/j.1440-1738.2010.00728.x

Heness, E.A., Simpson, E.L., Bumby, A.J., Eriksson, P.G., Eriksson, K.A., Hilbert-Wolf, H.L., Okafor, O.J., Linnevelt, S., Malenda, H.F., Modungwa, T., 2014. Evidence for climate shifts in the ~2.0 Ga upper Makgabeng Formation erg, South Africa. Palaeogeogr. Palaeoclimatol. Palaeoecol. 409, 265-279. http://dx.doi.org/10.1016/j.palaeo.2014.05.016

Herries, R.D., 1993. Contrasting styles of fluvio-aeolian interaction at a downwind erg margin: Jurassic Kayenta-Navajo transition, northern Arizona, USA, in: North, C.P., Prosser, D.J., (Eds.), Characterization of fluvial and aeolian reservoirs. Geol. Soc. London Spec. Publ. 73, 199-218. https://doi.org/ 10.1144/GSL.SP.1993.073.01.12

1235 Hoffman, P.F., Grotzinger, J.P. 1993. Orographic precipitation, erosional unloading, and tectonic
1236 style. Geology, 21, 195–198. https://doi .org/10.1130/0091-
1237 7613(1993)021<0195:OPEUAT>2.3.CO;2.
1238 Honda M., Yabuki S., Shimizu H., 2004. Geochemical and isotopic studies of aeolian sediments in
1239 China. Sedimentology. 51, 211-230. https://doi.org/10.1111/j.1365-3091.2004.00618.x
1240 Horodyski, R.J., Knauth, L.P., 1994. Life on land in the Precambrian. Science, 263, 494-498.
1241 https://www.jstor.org/stable/2883025
1242 Hummel, G., Kocurek, G., 1984. Interdune areas of the Back-Island dune field, North Padre-Island,
1243 Texas. Sed. Geol. 39, 1-26. https://doi.org/10.1016/0037-0738(84)90022-8
1244 Hunter, R.E., 1977. Basic types of stratification in small eolian dunes. Sedimentology. 24, 361–387.
1245 https://doi.org/10.1111/j.1365-3091.1977.tb00128.x
1246 Hunter, R.E., 1981.Stratification styles in eolian sandstones: Some Pennsylvanian to Jurassic
1247 examples from the western interior USA. In: Recent and Ancient Non-Marine Depositional
1248 Environments, Models for Exploration (Eds F.G. Ethridge and R.M. Flore) SEPM Spec. Publ., 31,
1249 315-329. https://doi.org/10.2110/pec.81.31.0315
1250 Hunter, R.E., 1985. Subaqueous sand-flow cross strata. J. Sediment. Petrol. 55, 886 – 894.
1251 https://doi.org/10.1306/212F8832-2B24-11D7-8648000102C1865D
1252 Ielpi, A., Ventra, D., Ghinassi, M., 2016. Deeply channelled Precambrian rivers: Remote sensing and
1253 outcrop evidence from the 1.2 Ga Stoer Group of NW Scotland. Precam. Res. 281, 291-311.
1254 http://dx.doi.org/10.1016/j.precamres.2016.06.004
1255 Iversen, J. D., White, B. R., 1982. Saltation threshold on Earth, Mars and Venus. Sedimentology. 29,
1256 111–119. https://doi.org/10.1111/j.1365-3091.1982.tb01713.x
1257 Jackson, M.J., Pianosi, J.G. and Donaldson, J.A., 1984. Aeolian dunes in Early Proterozoic Thelon
1258 Formation near Shultz Lake, central Keewatin. Current Res. B, Geol. Surv. Can. Pap. 84-1B, 53–63.
1259 Jackson, M.J., Simpson, E.L. and Eriksson, K.A., 1990. Facies and sequence stratigraphic analysis in
1260 an intracratonic, thermal relaxation basin; the early Proterozoic, lower Quilalar Formation and Ballara
1261 Quartzite, Mount Isa Inlier, Australia. Sedimentology. 37, 1053-1078. https://doi.org/10.1111/j.1365-
1262 3091.1990.tb01846.x

Jerram, D.A., Mountney, N.P., Howell, J.A., Long, D., Stollhofen, H., 2000. Death of a sand sea: an active aeolian erg systematically buried by the Etendeka flood basalts of NW Namibia. J. Geol. Soc. London, 157, 513-516. https://doi.org/10.1144/jgs.157.3.513

Jimenez, J.A., Maia, L.P., Serra, J., Morais, J., 2002. Aeolian dune migration along the Ceará coast, north-eastern Brazil. Sedimentology, 46, 689-701. https://doi.org/10.1046/j.1365-3091.1999.00240.x

Johnson, B., Goldblatt, C., 2015. The nitrogen budget of earth. Ear. Sci. Rev. 148, 150–173. https://doi.org/10.1016/j.earscirev.2015.05.006

Jordan, O.D., Mountney, N.P., 2012. Sequence stratigraphic evolution and cyclicity of an ancient coastal desert system: the Pennsylvanian-Permian lower Cutler beds, Paradox Basin, Utah, USA. J. Sed. Res. 82, 755-780. https://doi.org/10.2110/jsr.2012.54

Karpeta, W.P., 1990. The morphology of Permian palaeodunes - a reinterpretation of the Bridgnorth Sandstone around Bridgnorth, England, in the light of modern dune studies. Sed. Geol., 69, 59-75. https://doi.org/10.1016/0037-0738(90)90101-X

Kasper-Zubillaga, J.J., Carranza Edwards, A., 2005. Grain size discrimination between sands of desert and coastal dunes from northwestern Mexico.Rev. Mex. Cienc. Geol., 22, 383- 390. https://doi.org/10.4236/me.2014.51005

Kasting, J.F., Siefert, J.L., 2002. Life and the evolution of earth's atmosphere. Science. 296, 1066-1068. https://doi.org/10.1126/science.1071184

Kavanagh, L., Goldblatt, C., 2015. Using raindrops to constrain past atmospheric density. EPS. 413, 51–58. https://doi.org/10.1016/j.epsl.2014.12.032

Kirschvink, J.L., 1992. Late Proterozoic Low-Latitude Global Glaciation: The Snowball Earth, in: Schopf, J., Klein, C., (Eds.), In the Proterozoic Biosphere: A Multidisciplinary Study: New York, Cambridge University Press, Cambridge University Press, p. 51–52.

Kocurek, G., 1998. Aeolian system response to externalforcing factors–a sequence stratigraphic view of the Saharan Region, in: Alsharan, A.S., Glennie, K.W., Whittleand, G.L., Kendall, G.C.S.C.,Quaternary Deserts and ClimaticChange, pp. 327–338. Balkema, Rotterdam/Brookfield

Kocurek, G., Day, M., 2018. What is preserved in the aeolian rock record? A Jurassic Entrada Sandstone case study at the Utah-Arizona border. Sedimentology, 65, 1301-1321. https://doi.org/10.1111/sed.12422

Kocurek, G., Dott, R.H., 1981.Distinctions and uses of stratification types in the interpretation of eolian sand. J. Sed. Petrol. 51, 579-595. https://doi.org/10.1306/212F7CE3-2B24-11D7-8648000102C1865D

Kocurek, G., Ewing, R.C., 2012. Source-to-Sink: An Earth/Mars Comparison of Boundary Conditions for Eolian Dune Systems. In: Grotzinger, J.P., Milliken, R.E., (Eds.), Sedimentary Geology of Mars. SEPM Spec. Pub., 102. https://doi.org/10.2110/pec.12.102

Kocurek, G., Fielder, G., 1982. Adhesion structures. J. Sed. Petrol., 52, 1229-1241.https://doi.org/10.1306/212F8102-2B24-11D7-8648000102C1865D

Kocurek, G., Havholm, K.G., 1993. Eolian sequence stratigraphy-a conceptual framework, in: Weimer, P., Posamentier, H., (Eds.), Siliciclastic Sequence Stratigraphy, AAPG Mem. 58, 393-409. https://doi.org/10.1306/M58581C16

Kocurek, G., Nielson, J., 1986. Conditions favourable for the formation of warm-climate aeolian sand sheets. Sedimentology. 33, 795-816. https://doi.org/10.1111/j.1365-3091.1986.tb00983.x

Kocurek, G., Townsley, M., Yeh, E., Havholm, K., Sweet, M.L., 1992. Dune and dune-field development on Padre Island, Texas, with implications for interdune deposition and water-table controlled accumulation. J. Sed. Petrol. 62, 622-635. https://doi.org/10.1306/D4267974-2B26-11D7-8648000102C1865D

Kok, J. F., Parteli, E.J.R., Michaels, T.I., Bou Karam, D., 2012. The physics of wind-blown sand and dust. Rep. Prog. Phys., 75, 106901.

Krapf, C.B.E., Stollhofen, H., Stanistreet, I.G., 2003. Contrasting styles of ephemeral river systems and their interaction with dunes of the Skeleton Coast erg (Namibia). Quaternary International, 104, 41-52. https://doi.org/10.1016/S1040-6182(02)00134-9

Labandeira, C.C., 2005. Invasion of the continents: cyanobacterial crusts to tree-inhabiting arthropods.Trends Ecol. Evol. 20, 253-262. https://doi.org/10.1016/j.tree.2005.03.002

Lancaster, N., Teller, J.T., 1988. Interdune deposits of Namib Sand Sea. Sed. Geol. 55, 91-107. https://doi.org/10.1016/0037-0738(88)90091-7

Langford, R.P., Chan, M.A., 1988. Flood surfaces and deflation surfaces within the Cutler Formation and Cedar Mesa Sandstone (Permian), southeastern Utah. Geol Soc. Am. Bull., 100, 1541-1549. https://doi.org/10.1130/0016-7606(1988)100<1541:FSADSW>2.3.CO;2

Lebeau, L.E., Ielpi, A., 2017. Fluvial channel belts, floodbasins, and aeolian ergs in the Precambrian Meall Dearg Formation (Torridonian of Scotland): Inferring climate regimes from pre-vegetation clastic rock records. Sed. Geol. 357, 53-71. https://doi.org/10.1016/j.sedgeo.2017.06.003

Liu, B., Coulthard, T.J., McLelland, S.J., 2012. Interaction between sand dunes and rivers, and the impact on geomorphology. EGU General Assembly, Vienna, Austria. Geophys. Res. Abstr., 14. EGU2012-13165-3

Long, D.G.F., 1978. Proterozoic stream deposits: some problems of recognition and interpretation of ancient sandy fluvial systems, in: Miall, A.D. (Ed.), Fluvial Sedimentology. Can. Soc. Petrol. Geol., Calgary, Mem., 5, 313–342.

Long, D.G.F., 2004. Precambrian rivers, in: Eriksson, P.G., Altermann, W., Nelson, D.R., Mueller, W.U., Catuneanu, O. (Eds.), The Precambrian Earth: Tempos and Events. pp. 660–663, Elsevier, Amsterdam.

Long, D.F.G., 2006. Architecture of pre-vegetation sandy-braided perennial and ephemeral river deposits in the Paleoproterozoic Athabasca Group, northern Saskatchewan, Canada as indicators of Precambrian fluvial style. Sed. Geol. 190, 71-95. https://doi.org/10.1016/j.sedgeo.2006.05.006.

Long, D.G.F., 2011. Architecture and Depositional Style of Fluvial Systems Before Land Plants: A Comparison of Precambrian, Early Paleozoic, and Modern River Deposits. In: Davidson, S.K., Leleu, S., North, C.P., From River to Rock Record: The preservation of fluvial sediments and their subsequent interpretation. SEPM Spec. Pub. 97. https://doi.org/10.2110/sepmsp.097.037

Loope, D.B., 1984. Eolian origin of Upper Palaeozoic sandstones, southeastern Utah. J Sed. Petrol. 54, 563-580. https://doi.org/10.1306/212F846D-2B24-11D7-8648000102C1865D

1342 Loope, D.B., 1985. Episodic deposition and preservation of eolian sands: a Late Palaeozoic example
1343 from southeastern Utah. Geology, 13, 73-76. https://doi.org/10.1130/0091-
1344 7613(1985)13<73:EDAPOE>2.0.CO;2
1345 Loope, D.B., Swinehart, J.B., Mason, J.P., 1995. Dune-dammed paleovalleys of the Nebraska Sand
1346 Hills- intrinsic versus climatic controls on the accumulation of lake and marsh sediments. Geol. Soc.
1347 Am. Bull. 107, 396-406. DOI: 10.1130/0016-7606(1995)107<0396:DDPOTN>2.3.CO;2
1348 Long, D.G.F., 1978. Precambrian stream deposits: some problems of recognition and interpretation of
1349 ancient sandy fluvial systems, in: Miall, A.D., (Ed.), Fluvial Sedimentology, Can. Soc. Petrol. Geol.,
1350 Calgary, Mem., 5, 313-342.
1351 Marty, B., Zimmermann, L., Pujol, M., Burgess, R., Philippot, P., 2013. Nitrogen isotopic
1352 composition and density of the Archean atmosphere. Science. 342, 101–104.
1353 https://doi.org/10.1126/science.1240971
1354 Marzo, M., 1986. Sequencias fluvio–eolicas en el Buntsandstein del Macizo de Garraf (Provincia de
1355 Barcelona). Cuad. Geol. Iber., 10, 207-233.
1356 Master, S., Bekker, A., Hofmann, A., 2010. A review of the stratigraphy and geological setting of the
1357 Palaeoproterozoic Magondi Supergroup, Zimbabwe – Type locality for the Lomagundi carbon isotope
1358 excursion. Precam. Res. 182, 254-273. https://doi.org/10.1016/j.precamres.2010.08.013
1359 McKee, E.D., 1966. Structures of dunes at White Sands National Monument, New Mexico (and a
1360 comparison with structures of dunes from other selected areas). Sedimentology, 7, 1-69.
1361 https://doi.org/10.1111/j.1365-3091.1966.tb01579.x
1362 McKenna-Neuman, C., Nickling, W.G., 1989. A theoretical and wind tunnel investigation of the
1363 effect of capillarity water on the entrainment of sediment by wind. Can. J. Soil Sci., 69, 79–96.
1364 https://doi.org/10.4141/cjss89-008
1365 McLennan, S.M., Taylor, S.R., 1982. Geochemical constraints on the growth of continental crust. J.
1366 Geol. 90, 342–361.
1367 Meadows, N.S., Beach, A., 1993. Structural and climatic controls on facies distribution in a mixed
1368 fluvial and aeolian reservoir: the Triassic Sherwood Sandstone in the Irish Sea. Geol. Soc. London.
1369 Spec. Pub. 73, 247-264. https://doi.org/10.1144/GSL.SP.1993.073.01.15

Melton M.A., 1965. The geomorphic and paleoclimatic significance of alluvial deposits in southern Arizona. J. Geol., 73, 1–38. http://www.jstor.org/stable/30066379.

Mesquita, A.F., Basilici, G., Soares, M.V.T., Garcia, R.G.V., 2021a. Morphology, accumulation and preservation of draa systems in a Precambrian erg (Galho do Miguel Formation, SE Brazil). Sed. Geol., 412, 105807. https://doi.org/10.1016/j.sedgeo.2020.105807

Mesquita, A.F., Basilici, G., Soares, M.V.T., Janočko, J., Mountney, N.P., Colombera, L., de Souza, Filho, C.R., 2021b. Hybrid dry-wet interdune deposition in Precambrian aeolian systems: Galho do Miguel Formation, Southeast Brazil. Sed. Geol., 425, 106007. https://doi.org/10.1016/j.sedgeo.2021.106007

Miall, A.D., 1985. Architectural-Element Analysis: A New Method of Facies Analysis Applied to Fluvial Deposits. Ear. Sci. Re., 22, 261-308. https://doi.org/10.1016/0012-8252(85)90001-7

Minervini, M., Massimo Rossi, M., Mellere, D., 2011. Cyclicity and Facies Relationships at the Interaction Between Aeolian, Fluvial, and Playa Depositional Environments in the Upper Rotliegend: Regional Correlation Across Uk (Sole Pit Basin), the Netherlands, and Germany, in: Grötsch, J., Gaupp, R. The Permian Rotliegend of the Netherlands. SEPM Spec. Pub. 98, 106-119. https://doi.org/10.2110/pec.11.98

Morris, J.L., Wright, V.P., Edwards, D., 2012. Siluro-Devonian landscapes of southern Britain: the stability and nature of early vascular plant habitats. J. Geol. Soc., 169, 173-190. https://doi.org/10.1144/0016-76492011-07

Morris, J.L., Puttick, M.N., Clark, J.W., Edwards, D., Pressel, S., Wellman, C.H., Yang, Z., Schneider, H., Donoghue, P.C.J., 2018. The timescale of early land plant evolution. PNAS Biol. Sci. 115, E2274-E2283. https://doi.org/10.1073/pnas.1719588115

Mountney, N.P., 2006. Periodic accumulation and destruction of aeolian erg sequences: The Cedar Mesa Sandstone, White Canyon, southern Utah. Sedimentology. 53, 789-823. https://doi.org/10.1111/j.1365-3091.2006.00793.x

Mountney, N.P., 2012. A stratigraphic model to account for complexity in aeolian dune and interdune successions. Sedimentology. 59, 964-989. https://doi.org/10.1111/j.1365-3091.2011.01287.x

Mountney, N.P., Jagger, A., 2004.Stratigraphic evolution of an aeolian erg margin system: the Permian Cedar Mesa Sandstone, SE Utah, USA. Sedimentology. 51, 713-743. https://doi.org/10.1111/j.1365-3091.2004.00646.x

Mountney, N.P., Russell, A.J., 2004. Sedimentology of aeolian sandsheet deposits in the Askja region of northeast Iceland. Sedimentary Geology, 166, 223-244. https://doi: 10.1016/j.sedgeo.2003.12.007

Mountney, N.P., Russell, A.J., 2006. Coastal aeolian dune-field development and response to periodic fluvial inundation, Sólheimasandur, southern Iceland. Sedimentary Geology, 192, 167-181. https://doi: 10.1016/j.sedgeo.2006.04.004

Mountney, N.P., Russell, A.J., 2009. Aeolian dune-field development in a water table-controlled system: Skeidarársandur, Southern Iceland. Sedimentology, 56,2107–2131. https://10.1111/j.1365-3091.2009.01072.x

Mountney, N.P., Thompson, D.B., 2002. Stratigraphic evolution and preservation of aeolian dune and damp/ wet interdune strata: an example from the Triassic Helsby Sandstone Formation, Cheshire Basin, UK. Sedimentology. 49, 805-833. https://doi.org/10.1046/j.1365-3091.2002.00472.x

Nance, R. Damian; Evans, David A.D., Murphy, J. Brendan, 2022. Pannotia: To be or not to be? Ear. Sci. Rev., 232, 104128. https://doi.org/10.1016/j.earscirev.2022.104128

Nance R. D., Murphy J. B., 2013. Origins of the supercontinent cycle. Geosci. Front. 4, 439–448. https://doi.org/10.1016/j.gsf.2012.12.007

Nelson, B.K., DePaolo, D.J., 1985. Rapid production of continental crust 1.7 to 1.9 b.y. ago: Nd isotopic evidence from basement of the North America mid-continent. Bull. Geol. Soc. Am. 96, 746–754. https://doi.org/10.1130/0016-7606(1985)96<746:RPOCCT>2.0.CO;2

Newell, A.J., Pourmalek, A., Butcher, A.S., Shariatipour, S.M., 2019. The importance of lithofacies control on fluid migration in heterogeneous aeolian formations for geological CO2 storage: Lessons from observational evidence and modelling of bleached palaeoreservoirs at Salt Wash Graben, Utah. Int. J. Greenh. Gas Control. 91, 102841. https://doi.org/10.1016/j.ijggc.2019.102841

Nield, J.M., Wiggs, G.F.S., Baddock, M.C., Hipondoka, M.H.T., 2017. Coupling leeside grainfall to avalanche characteristics in aeolian dune dynamics. Geology. 45, 271–274. https://doi.org/10.1130/G38800.1

Nielson J., Kocurek G., 1986. Climbing zibars of the Algodones. Sed. Geol., 48, 1-15. https://doi.org/10.1016/0037-0738(86)90078-3

Noffke, N., Gerdes, G., Klenke, T., Krumbein, W.E., 2001. Microbially Induced Sedimentary Structures: A New Category within the Classification of Primary Sedimentary Structures. J. Sed. Res. 71, 649-656. https://doi.org/10.1306/2DC4095D-0E47-11D7-8643000102C1865D

Olsen, H., Due, P., Clemmensen, L., 1989. Morphology and genesis of asymmetrical warts – a new adhesion surface structure. Sed. Geol. 61. 277–285. https://doi.org/10.1016/0037-0738(89)90062-6.

Parrish, J. T., 1993. Climate of the Supercontinent Pangea. J. Geol., 10, 215-233.

Parrish, J.T., Soreghan, G., 2013. Sedimentary Geology and the Future of Paleoclimate Studies. The Sed. Rec. 11. 4-10. https://doi.org/10.2110/sedred.2013.2.4.

Parteli E. J., Herrmann H. J., 2007.Saltation transport on Mars. Phys. Rev. Lett. 98, 198001. https://doi.org/10.48550/arXiv.0705.1776

Petit, J.R., Jouzel, J., Raynaud, D., Barkov, N.I., Barnola, J.-M., Basile, I., Bender, M., Chappellaz, J., Davis, M., Delaygue, G., Delmotte, M., Kotlyakov, V.M., Le-grand, M., Lipenkov, V.Y., Lorius, C., Pépin, L., Ritz, C., Saltzman, E., Stievenard, M., 1999. Climate and atmospheric history of the past 420,000 years from the Vostok ice core, Antarctica. Nature, 399, 429–436. https://doi.org/10.1038/20859

Porada, H., Eriksson, P.G., 2009. Cyanobacterial mat features preserved in the siliciclastic sedimentary record: paleodeserts and modern supratidal flats, in: Seckbach, J., Walsh, M. (Eds.), From Fossils to Astrobiology: Records of Life on Earth and Search for Extraterrestrial Biosignatures. Cellular Origin, Life in Extreme Habitats and Astrobiology, 12, pp. 181–210.

Prave, A.R., 2002. Life on land in the Precambrian: evidence from the Torridonian rocks of northwest Scotland. Geology. 30, 811-814. https://doi.org/10.1130/0091-613(2002)030<0811:LOLITP>2.0.CO;2

Priddy, C.L., Clarke, S.M., 2020. The sedimentology of an ephemeral fluvial–aeolian succession. Sedimentology. 67, 2392-2425. https://doi.org/10.1111/sed.12706

1451 Prokoph, A., Shields, G.A., Vetzer, J., 2008. Compilation and Timeseries Analysis of a Marine
1452 Carbonate δ18O, δ13C, 87Sr/86Sr and δ34S Database through Earth History. Earth Sci. Rev. 87, 113–
1453 133. https://doi.org/10.1016/j.earscirev.2007.12.003
1454 Pulvertaft, T.C.R., 1985. Eolian dune and wet interdune sedimentation in the Middle Proterozoic Dala
1455 Sandstone, Sweden. Sed. Geol., 44, 93-111. https://doi.org/10.1016/0037-0738(85)90034-X
1456 Purser, B.H., Evans, G., 1973. Regional sedimentation along the Trucial Coast, Persian Gulf, in:
1457 Purser, B.H., (Ed.), The Persian Gulf, Berlin, Springer, pp. 211-231. https://doi.org/10.1007/978-3-
1458 642-65545-6_13
1459 Pye, K., Mazullo, J., 1994. Effects of tropical weathering on quartz shape: an example from
1460 northeastern Australia. J. Sed. Res., 64, 500-507. https://doi.org/10.1306/D4267DE8-2B26-11D7-
1461 8648000102C1865D
1462 Pye, K., Tsoar, H., 1990. Aeolian Sand and Sand Dunes.396 pp, London, Unwin Hyman.
1463 Rainbird, R.H., Hadlari, T., 2000. Revised stratigraphy and sedimentology of the Paleoproterozoic
1464 Dubawnt Supergroup at the northern margin of Baker Lake basin, Nunavut Territory. Geological
1465 Survey of Canada, Current Research 2000-C8, pp. 9.
1466 Rainbird, R.H., Hadlari, T., Aspler, L.B., Donaldson, J.A., LeCheminant, A.N., Peterson, T.D., 2003.
1467 Sequence stratigraphy and evolution of the Paleoproterozoic intracontinental Baker Lake and Thelon
1468 basins, western Churchill Province, Nunavut, Canada. Precam. Res. 125, 21-53.
1469 https://doi.org/10.1016/S0301-9268(03)00076-7
1470 Rea, D.K., Janecek, T.R., 1981. Mass-accumulation rates of the non-authigenic inorganic crystalline
1471 (Eolian) component of deep-sea sediments from the western Mid-Pacific Mountains, Deep Sea
1472 Drilling Project Site 463, in: Thiede, J., Vallier, T.L., et al., (Eds.), Initial Reports of the Deep Sea
1473 Drilling Project, Volume 62: Washington, D.C., U.S. Government Printing Office, p. 653–659.
1474 Reineck, H.E., Gerdes, G., Claes, M., Dunajtschik, K., Riege, H., Krumbein, W.E., 1990. Microbial
1475 modification of sedi-mentary structures. In: Sediments and Environmental Geochemistry (Eds. D.
1476 Helrig, P. Rothe, U. Förstner, P. Stoffers), pp. 254–276.
1477 Retallack, G., Grandstaff, D., Kimberley, M., 1984. The Promise and Problems of Precambrian
1478 Paleosols. Episodes, 7, 8-12. https://doi.org/10.18814/epiiugs/1984/v7i2/003

Ridgley, J.L., 1977. Stratigraphy and depositional environments of Jurassic-Cretaceous sedimentary rocks in the southwest part of the Chama Basin, New Mexico. New Mexico Geol. Soc., Guidebook, 28, 153-158.

Rodríguez-López, J.P., Clemmensen, L.B., Lancaster, N., Mountney, N.P., Veiga, G.D. 2014, Archean to Recent aeolian sand systems and their sedimentary record: Current understanding and future prospects. Sedimentology. 61, 1487–1534. https://doi.org/10.1111/sed.12123.

Romain, H.G., Mountney, N.P., 2014. Reconstruction of 3D eolian-dune architecture from 1D core data through adoption of analogue data from outcrop. AAPG Bull., 98, 1- 22. https://doi.org/10.1306/05201312109

Ross, G.M., 1981. Bedforms, facies association, and tectono-stratigraphic setting of Precambrian eolianites, Hornby Bay Group, Northwest Territories, Canada. AAPG. Bull., 65, 981-982.

Ross, G.M., 1984. Geological and depositional history of the Hornby Bay Group, Proterozoic, Northwest Territories, Canada. PhD Thesis. pp. 445. Carleton University, Ottawa, Ontario.

Ross, G.M., 1984. Proterozoic aeolian quartz arenites from the Hornby Bay Group, Northwest Territories, Canada: Implications for Precambrian aeolian processes. Precam. Res., 20, 149-160. https://doi.org/10.1016/0301-9268(83)90070-0

Rubin, D.M., Hunter, R.E., 1982. Migration directions of primary and superimposed dunes inferred from compound crossbedding in the Navajo Sandstone, in: Nriagu, J.O., Troost, R., (Eds.), 11th International Congress on Sedimentology, Hamilton, Ontario, August 1982. IAS. pp. 69-70.

Rubin, D.M., Hunter, R.E., 1985. Why deposits of longitudinal dunes are rarely recognized in the geologic record. Sedimentology. 32, 147-157. https://doi.org/10.1111/j.1365-3091.1985.tb00498.x

Runyon, K.D., Bridges, N.T., Newman, C.E., 2017. Martian sand sheet characterization and implications for formation: A case study. Aeolian Res., 29, 1-11.https://doi.org/10.1016/j.aeolia.2017.09.001

Santos, M.G.M., Owen, G., 2016. Heterolithic meandering-channel deposits from the Neoproterozoic of NW Scotland: Implications for palaeogeographic reconstructions of Precambrian sedimentary environments. Precam. Res. 272, 226-243. https://doi.org/10.1016/j.precamres.2015.11.003

1506 Santos, M.G.M., Mountney, N.P., Peakall, J., 2017. Tectonic and environmental controls on
1507 Palaeozoic fluvial environments: Reassessing the impacts of early land plants on sedimentation. J.
1508 Geol. Soc. 174, 393–404. https://doi .org/10.1144/jgs2016-063.
1509 Santos, M.G.M., Hartley, A.J., Mountney, N.P., Peakall, J., Owen, A., Merino, E.R., Assine, M.L.,
1510 2019. Meandering rivers in modern desert basins: Implications for channel planform controls and
1511 prevegetation rivers. Sed. Geol. 385, 1–14. https://doi .org/10.1016/ j.sedgeo.2019.03.011
1512 Scherer, C.M.S., 2002. Preservation of aeolian genetic units by lava flows in the Lower Cretaceous of
1513 the Parana Basin, southern Brazil. Sedimentology. 49, 97-116. https://doi.org/10.1046/j.1365-
1514 3091.2002.00434.x
1515 Scherer, C.M.S., Lavina, E.L.C., 2005. Sedimentary cycles and facies architecture of aeolian-fluvial
1516 strata of the Upper Jurassic Guara Formation, southern Brazil. Sedimentology. 52, 1323-1341.
1517 https://doi.org/10.1111/j.1365-3091.2005.00746.x
1518 Scheidt, S., Ramsey, M., Lancaster, N., 2010. Determining soil moisture and sediment availability at
1519 White Sands Dune Field, New Mexico, from apparent thermal inertia data. J. Geophys. Res. 112,
1520 F02019. https://doi .org/10.1029/2009JF001378
1521 Schieber J., 1998. Possible indicators of microbial mat deposits in shales and sandstones: examples
1522 from the mid-Precambrian Belt Supergroup, Montana, USA. Sed. Geol. 120, 105 – 24.
1523 https://doi.org/10.1016/S0037-0738(98)00029-3
1524 Schieber J., 2004. Microbial mats in the siliciclastic rock record: a summary of diagnostic features, in:
1525 Eriksson, P.G., Altermann, W., Nelson, D.R., Mueller, W.U., Catuneanu, O., (Eds.), The Precambrian
1526 Earth: Tempos and Events. pp. 663 – 73, Elsevier, Amsterdam.
1527 Schopf, J.W., 2000. The Fossil Record: Tracing the Roots of the Cyanobacterial Lineage. In: Whitton,
1528 B.A., Potts, M., (Eds.), The Ecology of Cyanobacteria. Springer, Dordrecht. https://doi.org/10.1007/0-
1529 306-46855-7_2
1530 Schumm, S.A., 1968. Speculations concerning palaeohydrologic controls of terrestrial sedimentation.
1531 GSA Bull. 79, 1573-1588. https://doi.org/10.1130/0016-7606(1968)79[1573:SCPCOT]2.0.CO;2

Scotti, A.A., Veiga, G.D., 2019. Sedimentary architecture of an ancient linear megadune (Barremian, Neuquén Basin): Insights into the long-term development and evolution of aeolian linear bedforms. Sedimentology. 66, 2191-2213. https://doi.org/10.1111/sed.12597

Sherman, D. J., 1990. Evaluation of aeolian sediment sand transport equations using intertidal-zone measurements, Saunton Sands, England. Sedimentology. 37, 385–392. https://doi.org/10.1111/j.1365-3091.1990.tb00967.x.

Shozaki, H., Hasegawa, H., 2022. Development of longitudinal dunes under Pangaean atmospheric circulation. Clim. Past. 18, 1529–1539. https://doi.org/10.5194/cp-18-1529-2022

Simplicio, F., Basilici, G., 2015. Unusual thick eolian sand sheet sedimentary succession: Paleoproterozoic Bandeirinha Formation, Minas Gerais, Brazil. J. Geol., 45, 3-11. https://doi.org/10.1590/2317-4889201530133

Simpson, E.L., Eriksson, K.A., 1993. Thin eolianites interbedded within a fluvial and marine succession: Early Precambrian Whitworth Formation, Mount Isa Inlier, Australia. Sed. Geol., 87, 39–62. https://doi.org/10.1016/0037-0738(93)90035-4

Simpson, E.L., Eriksson, K., Eriksson, P.A., Bumby, A.J., 2002. Eolian Dune Degradation and Generation of Massive Sandstone Bodies in the Paleoproterozoic Makgabeng Formation, Waterberg Group, South Africa. J. Sed. Res. 72, 40-45. https://doi.org/10.1306/050701720040

Simpson, E.L., Eriksson, K.A., Muller, W.U., 2012. 3.2 Ga eolian deposits from the Moodies Group, Barberton Greenstone Belt, South Africa: Implications for the origin of first-cycle quartz sandstones. Precambrian Res. 214-215, 185-191. https://doi.org/10.1016/j.precamres.2012.01.019

Simpson, E.L., Heness, E.A., Bumby, A.J., Eriksson, P.G., Eriksson, K.A., Hilbert-Wolf, H.L., Linnevelt, S., Fitzgerald Malenda, H., Modungwa, T., Okafor, O.J., 2013. Evidence for 2.0 Ga continental microbial mats in a paleodesert setting. Precambrian Res. 237, 36–50. https://doi.org/10.1016/j.precamres.2013.08.001

Soegaard, K., Callahan, D.M., 1994. Late middle Proterozoic Hazel Formation near Van Horn, Trans-Pecos Texas: evidence for transpressive deformation in Grenville basement. Bull. Geol. Soc. Am. 106, 413–423. https://doi.org/10.1130/0016-7606(1994)106<0413:LMPHFN>2.3.CO;2

1559 Slattery, M.C., 1990. Barchan migration on the Kuiseb River Delta, Namibia. South. Afr. Geogr. J.,
1560 72, 5-10. https://doi.org/10.1080/03736245.1990.9713540
1561 Smoot, J.P., Castens-Seidell, B., 1994. Sedimentary features produced by efflorescent crusts, Saline
1562 Valley and Death Valley, California. In: Renaut, R.W., Last, W.M. (Eds.) Sedimentology and
1563 Geochemistry of Modern Ancient Saline Lakes. Spec. Publ. Soc. Econ. Paleont. Miner., Tulsa 50, 73-
1564 90.
1565 Som, S. M., Buick, R., Hagadorn, J.W., Blake, T.S., Perreault, J.M., Harnmeijer, J.P., Catling, D.C.,
1566 2016. Earth's air pressure 2.7 billion years ago constrained to less than half of modern levels: Nat.
1567 Geo., 9, 448–451. https://doi.org/10.1038/ngeo2713
1568 Som, S. M., Catling, D.C., Harnmeijer, J.P., Polivka, P.M., Buick, R., 2012. Air density 2.7 billion
1569 years ago limited to less than twice modern levels by fossil raindrop imprints. Nature, 484, 359–362.
1570 https://doi.org/10.1038/nature10890
1571 Sorby, H.C., 1859. On the structures produced by the currents present during the deposition of
1572 stratified rocks. The Geol., 2, 137-147. https://doi.org/10.1017/S1359465600021122
1573 Souza, E.G., 2012. Arquitetura de fácies e evolução estratigráfica dos depósitos eólicos da Formação
1574 Mangabeira, Supergrupo Espinhaço - BA. (Monography Thesis). Universidade Federal do Rio Grande
1575 do Sul, Brasil.
1576 Stewart, A.D., 2002. The later Proterozoic Torridonian rocks of Scotland: their sedimentology,
1577 geochemistry, and origin. Geol. Soc. London Mem. 24, 5 - 21.
1578 https://doi.org/10.1144/GSL.MEM.2002.024.01.02
1579 Stewart, J.H., 2005. Eolian deposits in the Neoproterozoic Big Bear Group, San Bernardino
1580 Mountains, California, USA. Earth-Sci. Rev., 73, 47-62.
1581 https://doi.org/10.1016/j.earscirev.2005.07.012
1582 Sullivan R., Kok J., 2017. Aeolian saltation on Mars at low wind speeds. J. Geophys. Res. Plan. 122,
1583 2111–2143. https://doi.org/10.1002/2017JE005275
1584 Sullivan R., Kok J., Katra I., Yizhaq H., 2020. A broad continuum of aeolian impact ripple
1585 morphologies on Mars is enabled by low wind dynamic pressures. J. Geophys. Res. 125,
1586 e2020JE006485. https://doi.org/10.1029/2020JE006485

1587 Taylor, I.E., Middleton, G.V., 1990. Aeolian sandstones of the Copper Harbor Formation, Late
1588 Proterozoic, Lake Superior basin. Can. J. Earth Sci., 27, 1339-1347. https://doi.org/10.1139/e90-144
1589 Thompson, D.B., 1970a. Sedimentation of the Triassic (Scythian) red pebbly sandstones in the
1590 Cheshire Basin and its margins. Geol. J., 7, 183-216. https://doi.org/10.1002/gj.3350070111
1591 Thompson, D.B., 1970b.The stratigraphy of the so-called Keuper Sandstone Formation (Scythian-
1592 ?Anisian) in the Permo-Triassic Cheshire Basin. Quart. J. Geol. Soc. London. 126, 151-181.
1593 https://doi.org/10.1144/gsjgs.126.1.0151
1594 Tirsgaard, H., Øxnevad, I.E.I., 1998. Preservation of pre-vegetational mixed fluvio-aeolian deposits in
1595 a humid climatic setting: an example from the Middle Precambrian Eriksfjord Formation, Southwest
1596 Greenland. Sed. Geol. 120, 295-317. https://doi.org/10.1016/S0037-0738(98)00037-2
1597 Trewin, N.H., 1993. Controls on fluvial deposition in mixed fluvial and aeolian facies within the
1598 Tumblagooda Sandstone (Late Silurian) of Western Australia. Sediment. Geol. 85, 387-400.
1599 https://doi.org/10.1016/0037-0738(93)90094-L
1600 Tsoar, H., 2001. Types of Aeolian Sand Dunes and Their Formation, in: Balmforth, N.J., Provenzale,
1601 A., (Eds.), Geomorphological Fluid Mechanics. Lecture Notes in Physics. 582. Springer, Berlin,
1602 Heidelberg. https://doi.org/10.1007/3-540-45670-8_17
1603 Upfold, R., 1984. Tufted microbial (cyanobacterial) mats from the Proterozoic Stoer Group, Scotland.
1604 Geol. Magazine. 121, 351-355. https://doi.org/10.1017/S0016756800029253
1605 Valentine, J.W., Moores, E.M., 1970. Plate-tectonic regulation of animal diversity and sea level: a
1606 model. Nature. 228, 657-659. https://doi.org/ 10.1038/228657a0
1607 Veizer, J., Jansen, S.L., 1979. Basement and sedimentary recycling and continental evolution. J. Geol.
1608 87, 341–370.
1609 Wakefield, O., 2019. The importance of water in aeolian systems: an example from the Sherwood
1610 Sandstone of the West Midlands. Proc. Open Uni. Geol. Soc. 5. 81-84.
1611 https://nora.nerc.ac.uk/id/eprint/523075
1612 Wang, X., Dong, Z., Zhang, J., Qu, J. Zhao, A., 2003. Grain size characteristics of dune sands in the
1613 central Taklimakan Sand Sea. Sed. Geol. 161, 1-14. https://doi.org/10.1016/S0037-0738(02)00380-9

Warren, A., 1971. Dunes in the Tenere Desert. Geog. J. 137, 458-461.
https://doi.org/10.2307/1797141
Wasson, R.J., Hyde, R.,1983. Factors determining desert dunes type. Nature. 304, 337–339.
https://doi.org/10.1038/304337a0
Went, D.J., 2005. Pre-vegetation alluvial fan facies and processes: an examplefrom the Cambro-
Ordovician Rozel Conglomerate Formation, Jersey, Channel Islands. Sedimentology. 52,693–713.
https://doi.org/10.1111/j.1365-3091.2005.00716.xÓ2005
Wilson, I.G., 1973. Ergs. Sed. Geol. 10, 77-106. https://doi.org/10.1016/0037-0738(73)90001-8
Woodard, S.C., Thomas, D.J., Hovan, S., Röhl, U., Westerhold, T., 2011. Evidence for orbital forcing
of dust accumulation during the early Paleogene greenhouse.Geochem. Geophys. Geosystems. 12,
Q02007. https://doi.org/10.1029/2010GC003394.
Xu, H., Liu, Y., Kuang, H., Peng, N., 2019. Late Jurassic fluvial-eolian deposits from the Tianchihe
Formation, Ningwu-Jingle Basin, Shanxi Province, China.J. Asian Earth Sci., 174, 245-262.
https://doi.org/10.1016/j.jseaes.2018.12.012
Yang, J., Dong, Z., Liu, Z., Shi, W., Chen, G., Shao, T., Zeng, H., 2019. Migration of barchan dunes
in the western Quruq Desert, northwestern China. Earth Surface Processes and Landforms, 44, 2016-
2029. https://doi.org/10.1002/esp.4629C
Yang, Z., Qian, G., Dong, Z., Tian, M., Lu, J., 2021. Migration of barchan dunes and factors that
influence migration in the Sanlongsha dune field of the northern Kumtagh Sand Sea, China.
Geomorphology, 378, 107615. https://doi.org/10.1016/j.geomorph.2021.107615.
Yoshida, M., Santosh, M., 2011. Supercontinents, mantle dynamics and plate tectonics: a perspective
based on conceptual vs. numerical models. Earth Sci. Rev. 105, 1–24.
https://doi.org/10.1016/j.earscirev.2010.12.002
Zang, W.L., 1995. Early Neoproterozoic sequence stratigraphy and acritarch biostratigraphy, eastern
Officer Basin, South Australia. Precambrian Res., 74, 119-175. https://doi.org/10.1016/0301-
9268(95)00007-R
Zhou, N., Zhang, C-L., Wu, X-X., Wang, X-M., Kang, L-Q., 2014. The geomorphology and evolution
of aeolian landforms within a river valley in a semi-humid environment: A case study from Mainling

Valley, Qinghai–Tibet Plateau. Geomorphology,224,27-38.
https://doi.org/10.1016/j.geomorph.2014.07.012.

FIGURE CAPTIONS

Figure 1: A) World map showing the geographic distribution of 30 Precambrian case studies analysed in this investigation. The estimated extent of Precambrian cratonic regions are shaded in brown (modified after Bleeker, 2003). The numbers associated with the case studies correspond Table 1 and Part B. B) Geological timescale (modified after Gradstein, 2020) showing the distribution of the case studies shown in Part A through geological time.

Figure 2: Percentages of various architectural element types found in Precambrian and Phanerozoic aeolian systems.

Figure 3: Thicknesses of various architectural elements in the Precambrian and Phanerozoic.

Figure 4: percentages of recorded dune types in the Precambrian and the Phanerozoic.

Figure 5: percentages of architectural elements deposited in dry, wet, mixed and stabilizing aeolian systems during the Precambrian and the Phanerozoic.

Figure 6: percentages of case studies included in this investigation deposited in different tectonic basin settings in Precambrian and the Phanerozoic.

Figure 7: percentages of facies types found within Precambrian and Phanerozoic dune sets.

Figure 8: percentages of facies types found within Precambrian and Phanerozoic sandsheets.

Figure 9: Examples of Precambrian sedimentary logs that illustrate characteristic features of Precambrian aeolian systems. A) Damp and wet interdunes housing microbially induced sedimentary structures; modified after Eriksson et al. (2000). B) Thick zibar sandsheets associated with thin aeolian dune sets and interdigitating fluvial channels; modified after Simplicio and Basilici (2015). C) Thick sandsheet deposits associated with the extensive development of adhesion facies; modified after Bállico et al. (2017). D) Microbially induced sedimentary structures associated with the development of microbial mats in a damp sandsheet environment; modified after Basilici et al. (2021). E) Sandsheet deposits in close association with marine deposits. Facies within sandsheets, including

subaqueous ripples and adhesion strata indicate the frequent incursion of aqueous agents into aeolian sandsheet environments; modified after Chakraborty and Chakraborty (2001).

Figure 10. A) Modern example of a muddy roll-up structure from the Sonoron Desert. The cigar-shaped structures are analogous to those found in the Paleoproterozoic Makgabeng Formation. Modified from Beraldi-Campesi and Garcia-Pichel (2010). B) Modern example of extensive zibar deposits from the Tenéré Desert, SE Niger. The zibars are rounded arcuate ridges smaller linear dunes are oriented at right angles to the zibar dunes and are a younger feature of the landscape. Image courtesy of the International Space Station Earth Observations experiment (Image ISS022-E-5258). C) Sandsheet deposits of the Mangabeira Formation; sandsheets contain planar laminations and crinkly adhesion strata. Modified from Bállico et al., 2016. D) Biolaminated sandstone from the Neoproterozoic Venkatpur Sandstone. Planar laminations are interbedded with irregular laminations that are associated with disturbed planar beds that arise from the expansion, contraction, and destruction of microbial mat. Modified from Basilici et al. (2020). E) Modern example of coastal aeolian sandsheet, Padre Island, Texas, USA. Image courtesy of Google Earth.

Figure 11: Schematic representation of the distribution of aeolian systems, alongside major changes in the Earth's geosphere, atmosphere and biosphere during the Precambrian. A) Geologic timescale after Gradstein et al. (2020). B) Distribution of case studies through geological time; the numbers of the case studies correspond with Figure 1 and Table 1. C) Schematic representation of recorded aeolian systems throughout Precambrian Earth history. D) Crustal growth models; modified after Simpson and Eriksson (1998). E) Schematic representation of supercontinents throughout Precambrian Earth history; modified after Bleeker (2004). F) Precambrian carbon isotope composition; modified after Prokoph et al. (2008) and Halverston et al. (2005). G) Schematic representation of glacioeras throughout Precambrian Earth history; modified after Parrish and Soreghan (2013) H) Precambrian atmospheric evolution; modified after Goldblatt (2018). I) Possible reconstructions of Precambrian atmospheric density based on Marty et al. (2013), Som et al. (2012) Som et al. (2016). J) Major events in the evolution of the Precambrian biosphere.

Figure S1: World map showing the geographic distribution of 57 Phanerozoic case studies analysed in this investigation. The numbers associated with the case studies correspond Table S1.

TABLE CAPTIONS

Table 1: List of the case studies used in this investigation. The geographic location of each case study is outlined in Figure 1 (identified via the case number).

Table 2: Definitions of aeolian lithofacies discussed in the text.

Table 3: Results of statistical analysis for architectural element thickness

Table S1: List of the Phanerozoic case studies used in this investigation. The geographic location of each case study is outlined in Figure S1 (identified via the case number).

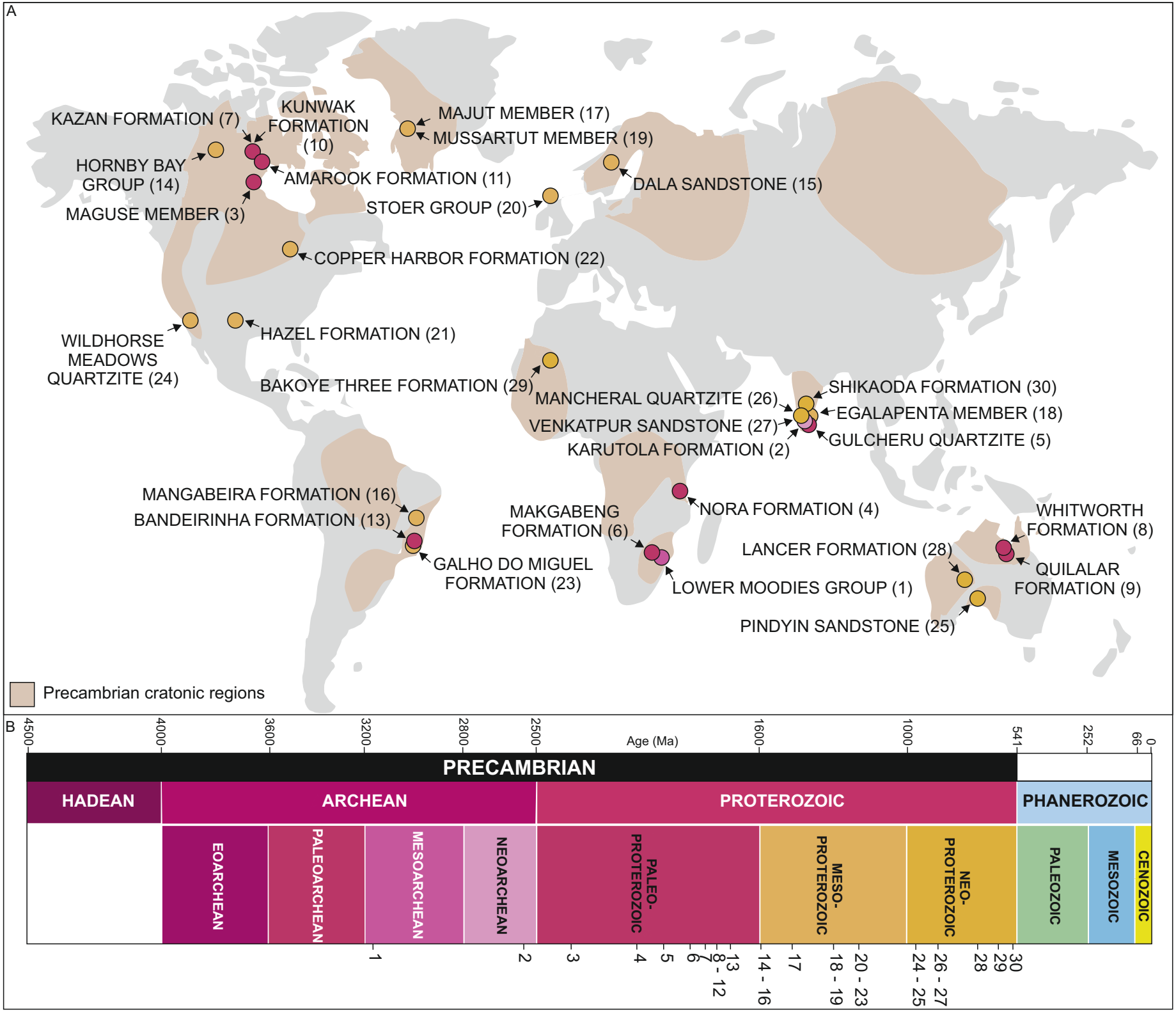

Figure 1: A) World map showing the geographic distribution of 30 Precambrian case studies analysed in this investigation. The estimated extent of Precambrian cratonic regions are shaded in brown (modified after Bleeker, 2003). The numbers associated with the case studies correspond Table 1 and Part B. B) Geological timescale (modified after Gradstein, 2020) showing the distribution of the case studies shown in Part A through geological time.

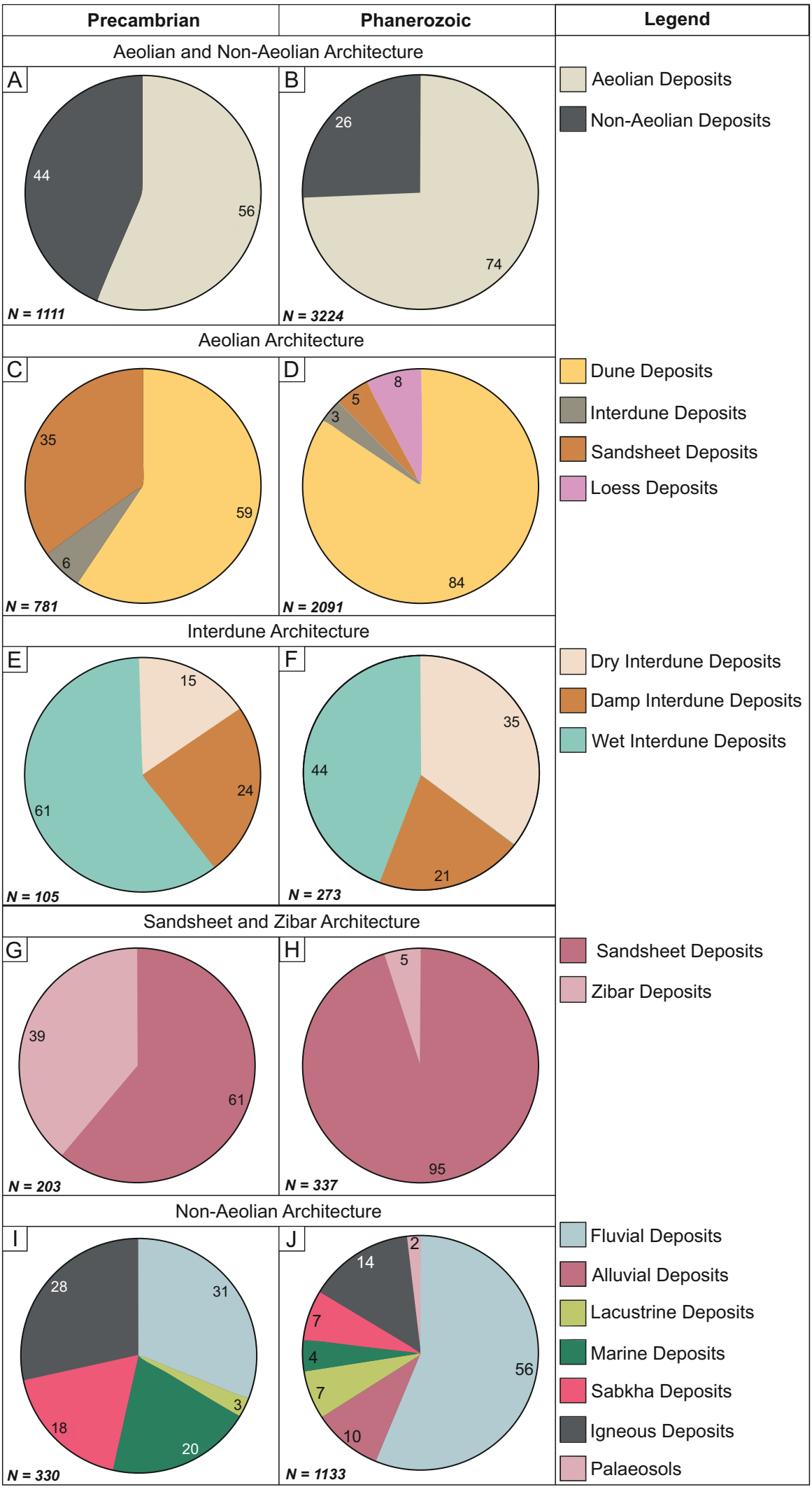

Figure 2: Percentages of various architectural element types found in Precambrian and Phanerozoic aeolian systems.

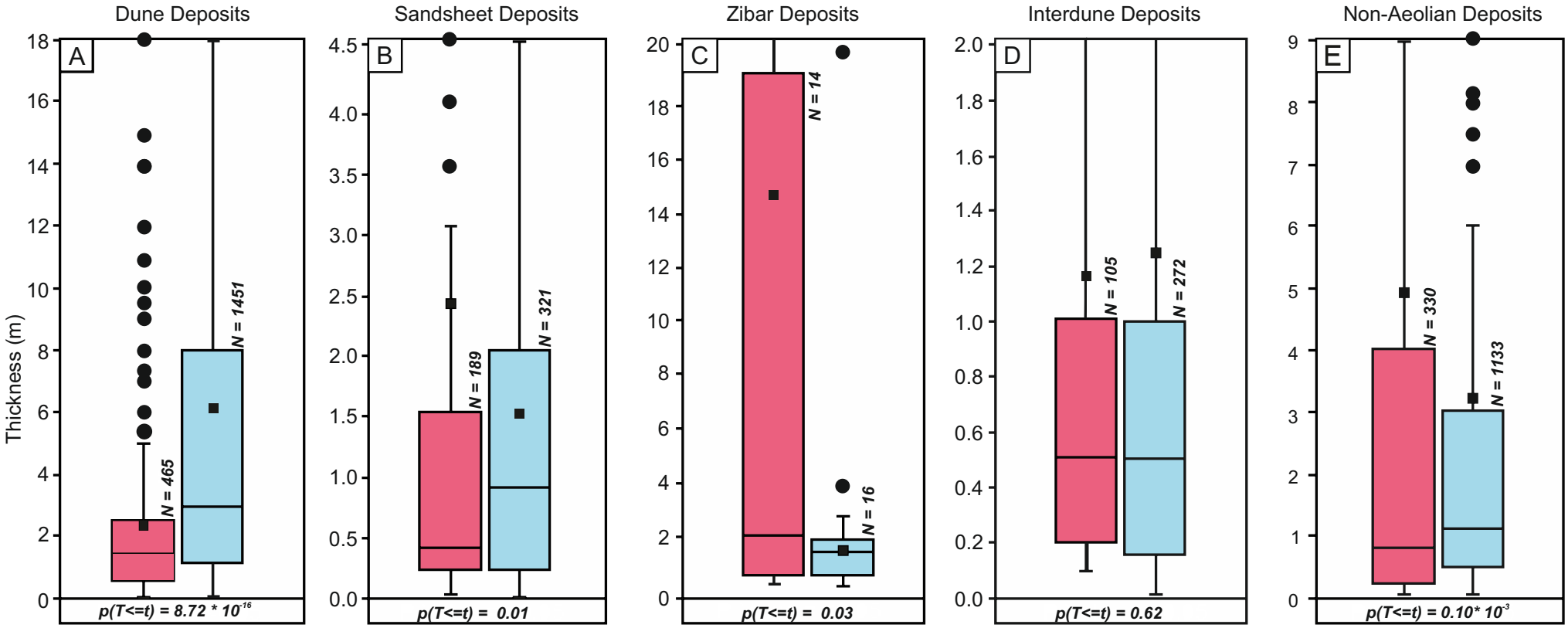

Figure 3: Thicknesses of various architectural elements in the Precambrian and Phanerozoic.

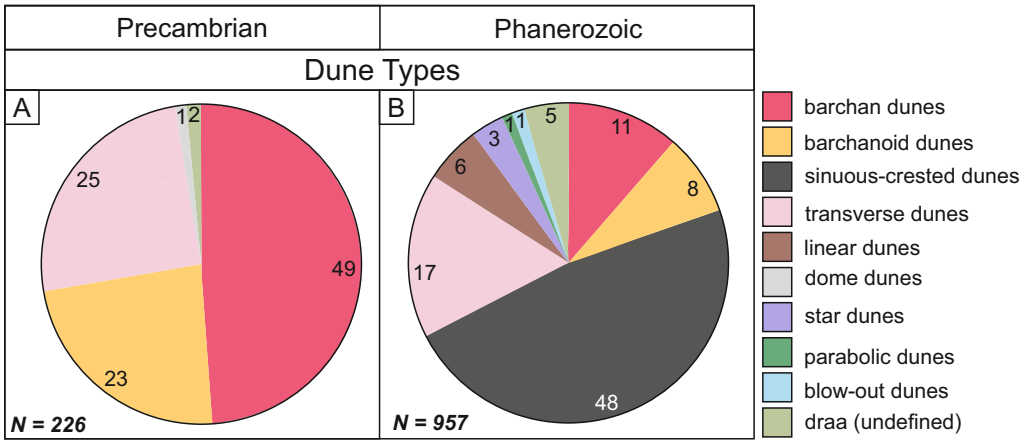

Figure 4: percentages of recorded dune types in the Precambrian and the Phanerozoic. Dune types making up <1% of recorded dune types are not shown.

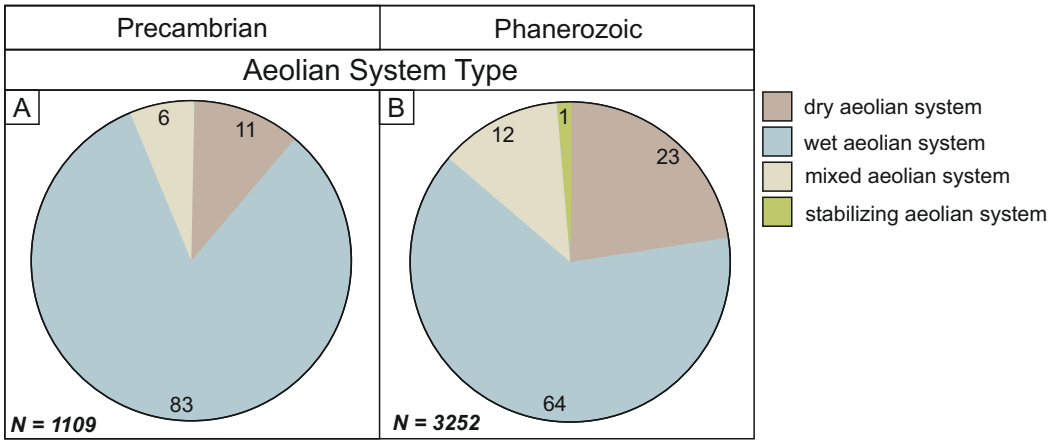

Figure 5: percentages of architectural elements deposited in dry, wet, mixed and stabilizing aeolian systems during the Precambrian and the Phanerozoic.

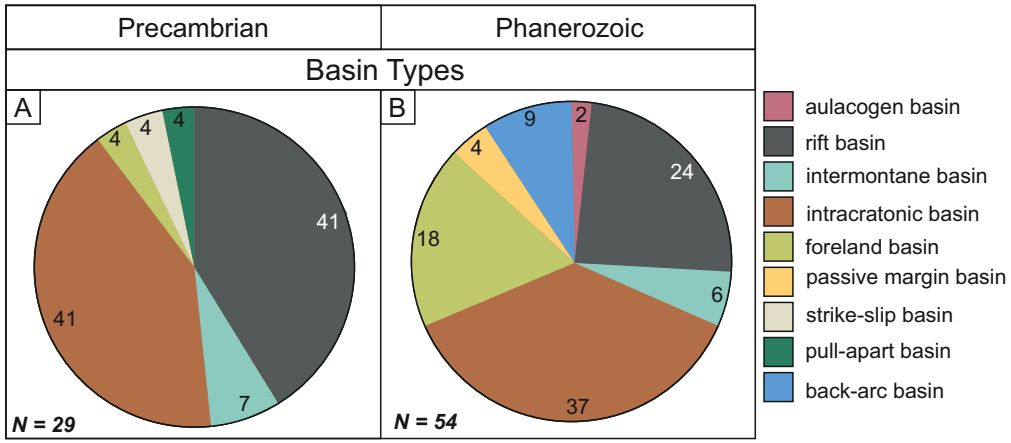

Figure 6: percentages of case studies included in this investigation deposited in different tectonic basin settings in Precambrian and the Phanerozoic.

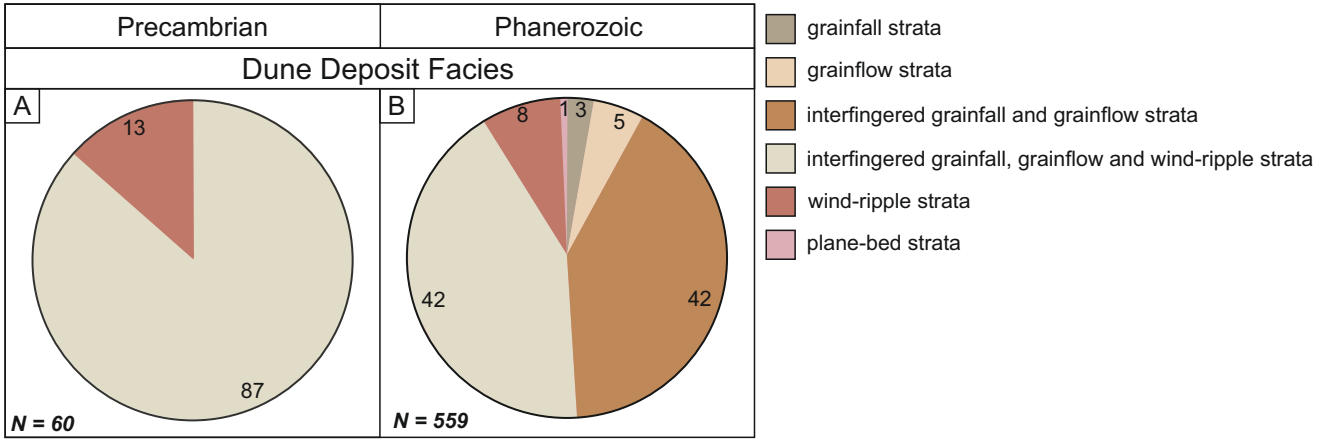

Figure 7: percentages of facies types found within Precambrian and Phanerozoic dune sets.

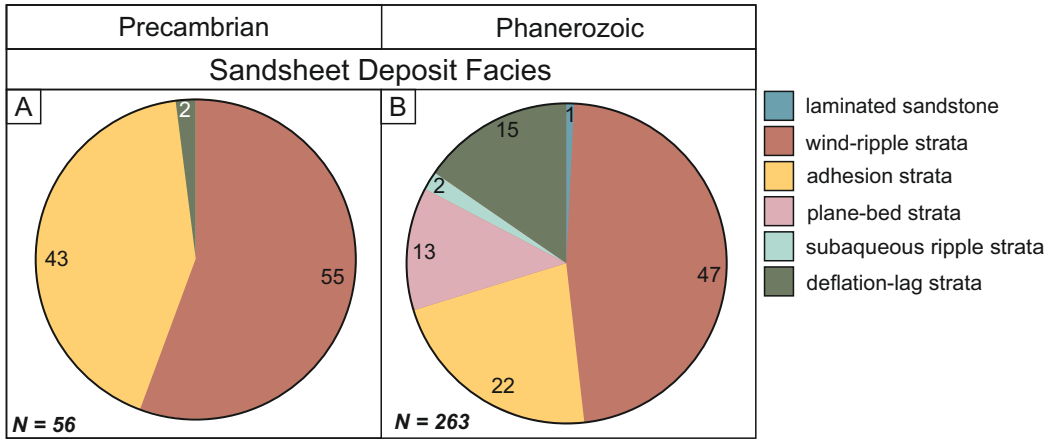

Figure 8: percentages of facies types found within Precambrian and Phanerozoic sandsheets.

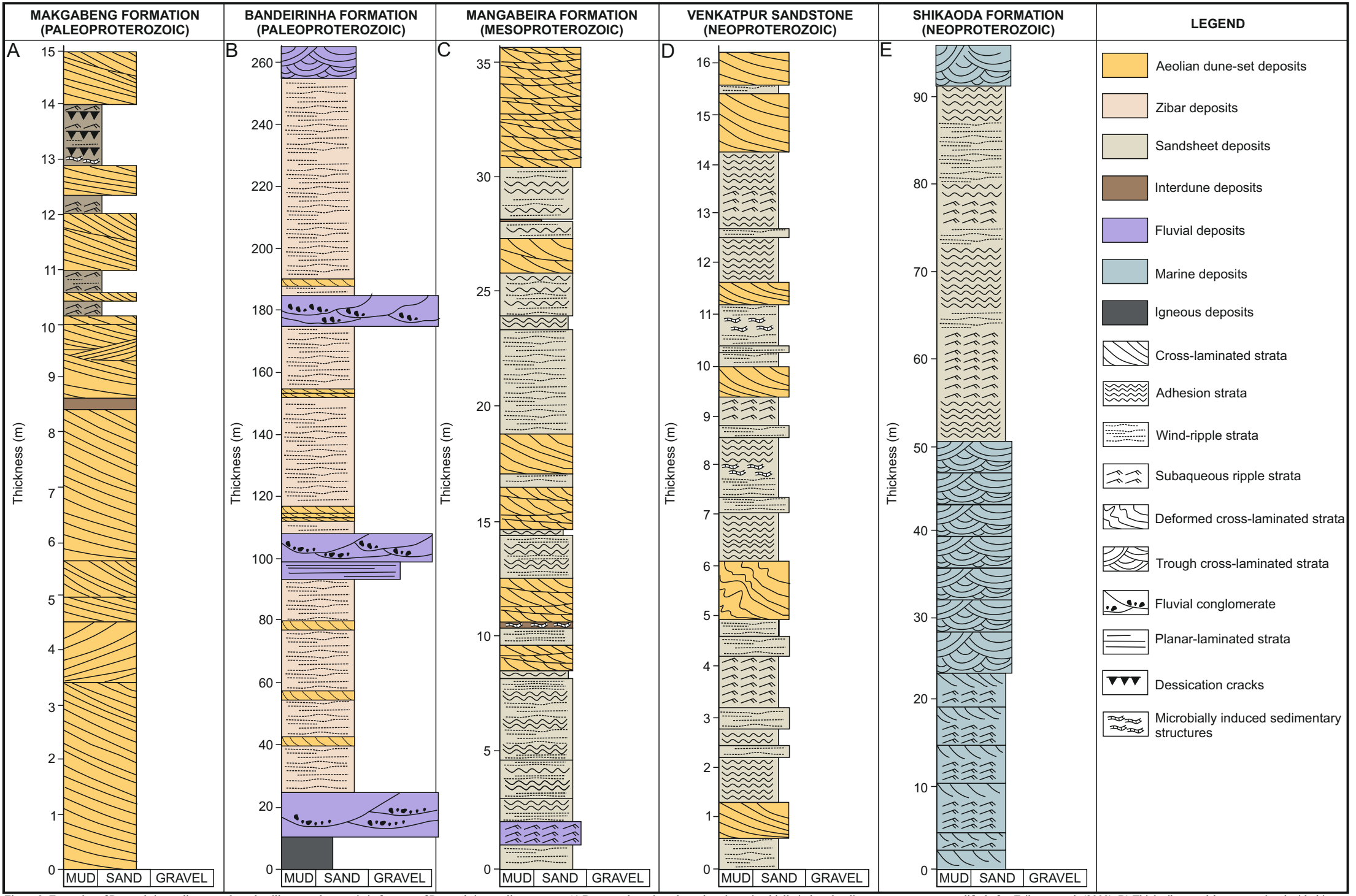

Figure 9: Examples of Precambrian sedimentary logs that illustrate characteristic features of Precambrian aeolian systems. A) Damp and wet interdunes housing microbially induced sedimentary structures; modified after Eriksson et al. (2000). B) Thick zibar sandsheets associated with thin aeolian dune sets and interdigitating fluvial channels; modified after Simplicio and Basilici (2015). C) Thick sandsheet deposits associated with the extensive development of adhesion facies; modified after Bállico et al. (2017). D) Microbially induced sedimentary structures associated with the development of microbial mats in a damp sandsheet environment; modified after Basilici et al. (2021). E) Sandsheet deposits in close association with marine deposits. Facies within sandsheets, including subaqueous ripples and adhesion strata indicate the frequent incursion of aqueous agents into aeolian sandsheet environments; modified after Chakraborty and Chakraborty (2001).

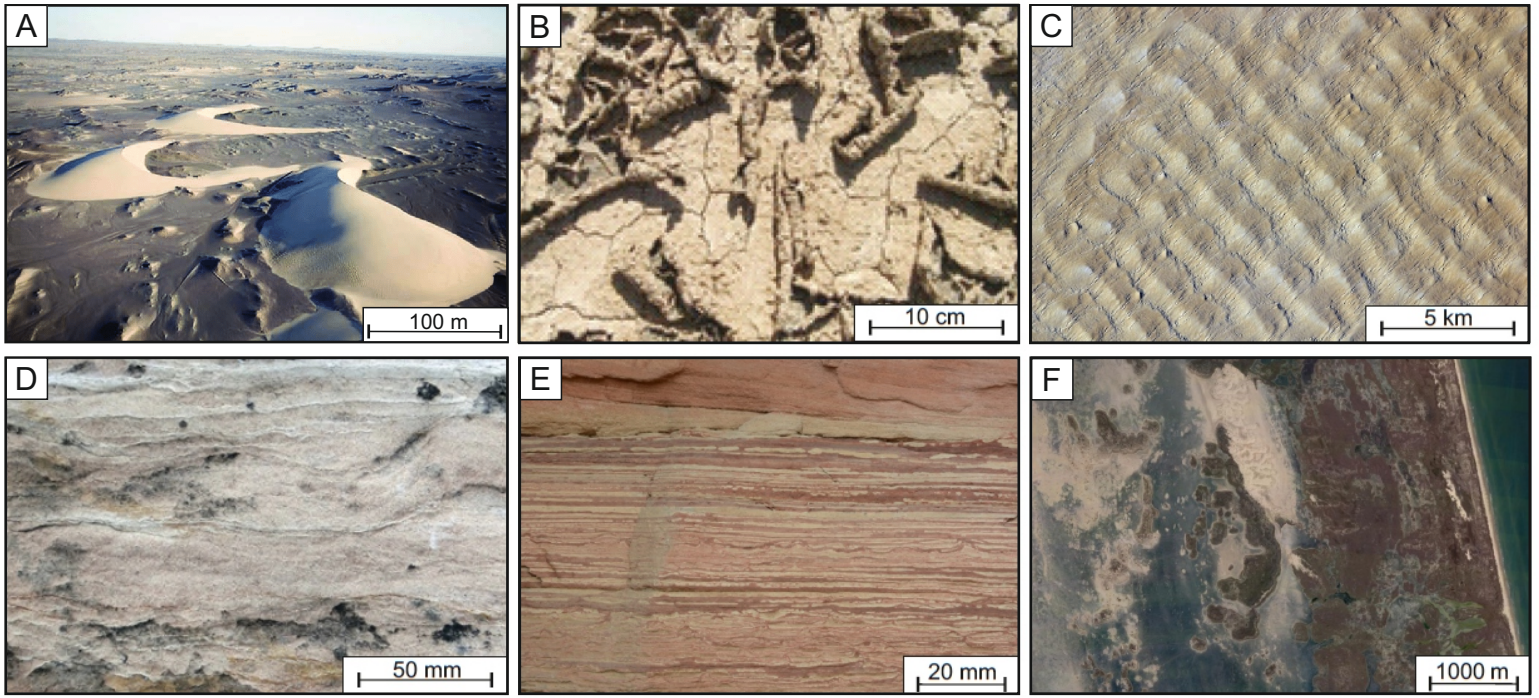

Figure 10. A) Barchan dunes developed on gravel surfaces in the northeastern part of the Kumtagh Sand Sea. Modified after Dong et al., 2012. B) Modern example of a muddy roll-up structure from the Sonoron Desert. The cigar-shaped structures are analogous to those found in the Paleoproterozoic Makgabeng Formation. Modified from Beraldi-Campesi and Garcia-Pichel (2010). C) Modern example of extensive zibar deposits from the Tenéré Desert, SE Niger. The zibars are rounded arcuate ridges smaller linear dunes are oriented at right angles to the zibar dunes and are a younger feature of the landscape. Image courtesy of the International Space Station Earth Observations experiment (Image ISS022-E-5258). D) Sandsheet deposits of the Managbeira Formation; sandsheets contain planar laminations and crinkly adhesion strata. Modified from Bállico et al., 2016. E) Biolaminated sandstone from the Neoproterozoic Venkatpur Sandstone. Planar laminations are interbedded with irregular laminations that are associated with disturbed planar beds that arise from the expansion, contraction, and destruction of microbial mat. Modified from Basilici et al. (2020). F) Modern example of coastal aeolian sandsheet, Padre Island, Texas, USA. Image courtesy of Google Earth.

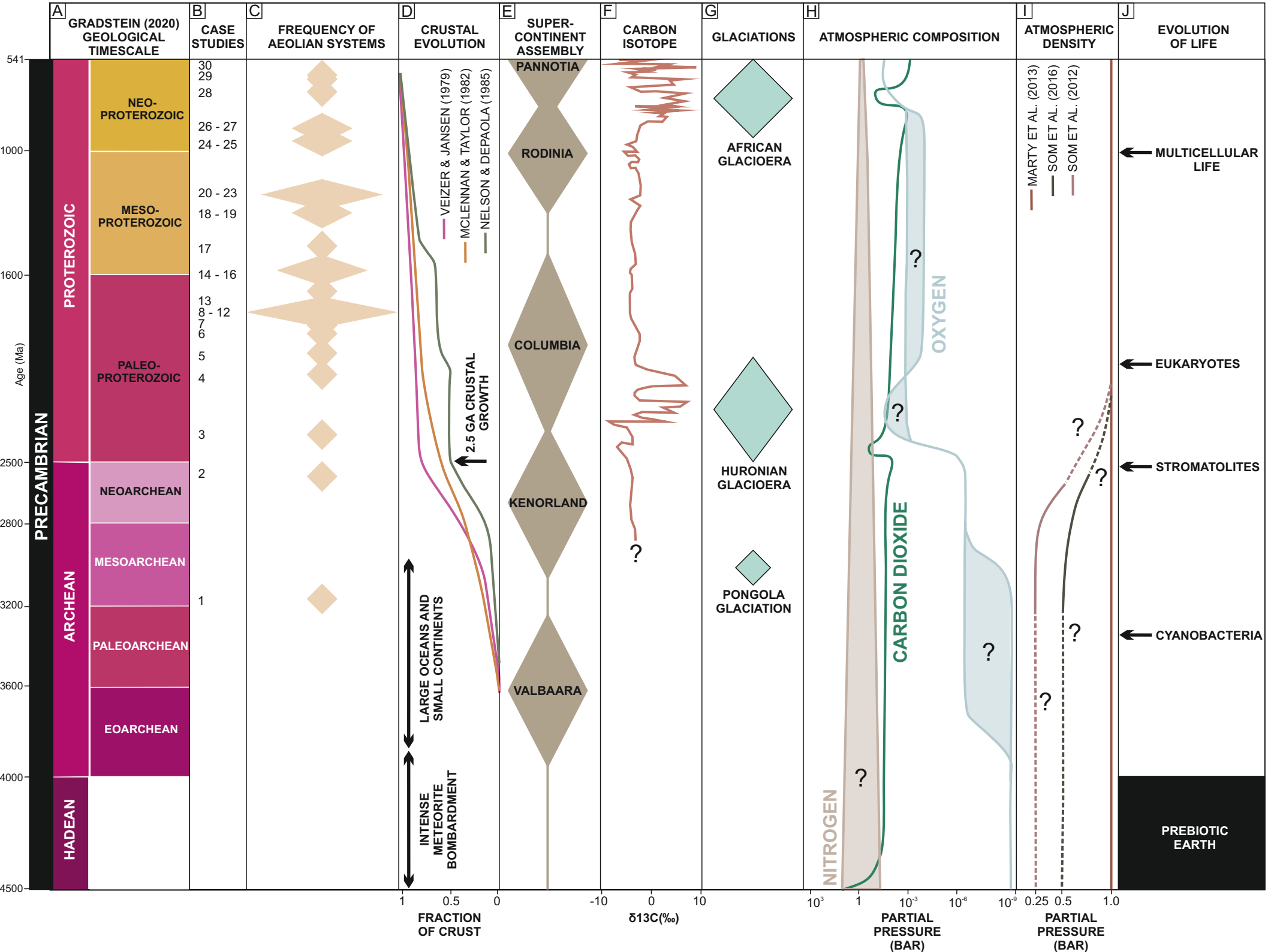
A
GRADSTEIN (2020) GEOLOGICAL TIMESCALE
B
CASE STUDIES
C
FREQUENCY OF AEOLIAN SYSTEMS
D
CRUSTAL EVOLUTION
E
SUPER-CONTINENT ASSEMBLY
F
CARBON ISOTOPE
G
GLACIATIONS
H
ATMOSPHERIC COMPOSITION
I
ATMOSPHERIC DENSITY
J
EVOLUTION OF LIFE
Age (Ma)
541
1000
1600
2500
2800
3200
3600
4000
4500
PRECAMBRIAN
PROTEROZOIC
ARCHEAN
HADEAN
NEO-PROTEROZOIC
MESO-PROTEROZOIC
PALEO-PROTEROZOIC
NEOARCHEAN
MESOARCHEAN
PALEOARCHEAN
EOARCHEAN
30
29
28
26 - 27
24 - 25
20 - 23
18 - 19
17
14 - 16
13
8 - 12
7
6
5
4
3
2
1
VEIZER & JANSEN (1979)
MCLENNAN & TAYLOR (1982)
NELSON & DEPAOLA (1985)
2.5 GA CRUSTAL GROWTH
LARGE OCEANS AND SMALL CONTINENTS
INTENSE METEORITE BOMBARDMENT
PANNOTIA
RODINIA
COLUMBIA
KENORLAND
VALBAARA
AFRICAN GLACIOERA
HURONIAN GLACIOERA
PONGOLA GLACIATION
NITROGEN
CARBON DIOXIDE
OXYGEN
MARTY ET AL. (2013)
SOM ET AL. (2016)
SOM ET AL. (2012)
MULTICELLULAR LIFE
EUKARYOTES
STROMATOLITES
CYANOBACTERIA
PREBIOTIC EARTH
1
0.5
0
FRACTION OF CRUST
-10
0
10
δ13C(‰)
10³
1
10⁻³
10⁻⁶
10⁻⁹
PARTIAL PRESSURE (BAR)
0.25
0.5
1.0
PARTIAL PRESSURE (BAR)

Figure 11: Schematic representation of the distribution of aeolian systems, alongside major changes in the Earth's geosphere, atmosphere and biosphere during the Precambrian. A) Geologic timescale after Gradstein et al. (2020). B) Distribution of case studies through geological time; the numbers of the case studies correspond with Figure 1 and Table 1. C) Schematic representation of recorded aeolian systems throughout Precambrian Earth history. D) Crustal growth models; modified after Simpson and Eriksson (1998). E) Schematic representation of supercontinents throughout Precambrian Earth history; modified after Bleeker (2004). F) Precambrian carbon isotope composition; modified after Prokoph et al. (2008) and Halverston et al. (2005). G) Schematic representation of glacioeras throughout Precambrian Earth history; modified after Parrish and Soreghan (2013). H) Precambrian atmospheric evolution; modified after Goldblatt (2018). I) Possible reconstructions of Precambrian atmospheric density based on Marty et al. (2013), Som et al. (2012) Som et al. (2016). J) Major events in the evolution of the Precambrian biosphere.

Figure S1: World map showing the geographic distribution of 59 Phanerozoic case studies analysed in this investigation. The numbers associated with the case studies correspond Table S1.

Case Study Name	Age (Ma)	Era	Location	Basin Setting	System Type	Data Source	Case Number
Lower Moodies Group (Swaziland Supergroup)	3200 - 3000	Mesoarchean	South Africa; Barberton Mountain Greenstone Belt.	Intramontane basin	Aeolian dune sets and sandsheets underlain by braided fluvial deposits.	Simpson et al. (2012)	1
Karutola Formation (Dongargarh Supergroup)	<2500	Neoarchean - Paleoproterozoic	India; Central Indian Craton.	Rift basin	Coastal aeolian sandsheet interfingered with shallow marine deposits	Chakraborty and Sensarma (2008)	2
Maguse Member (Kinga Formation; Hurwitz Group)	2450 - 2110	Paleoproterozoic	Canada; Hurwitz Basin.	Intracratonic sag basin	Aeolian dune sets, damp interdune and ponded wet interdune deposits.	Aspler and Chiarenzelli (1997)	3
Nora Formation (Deweras Group)	2100	Paleoproterozoic	Zimbabwe; Magondi Basin.	Rift basin	Aeolian dune sets interfingered with alluvial fan, braided stream and playa-lake deposits.	Master et al., (2010)	4
Gulcheru Quartzite (Cuddapah Supergroup)	2000	Paleoproterozoic	India; Cuddapah Basin	Rift Basin	Aeolian zibar deposits interfingered with ephemeral stream deposits.	Basu et al. (2014)	5
Makgabeng Formation (Waterberg Supergroup)	1850	Paleoproterozoic	South Africa; Waterberg Basin.	Transtensional basin.	Aeolian dune sets and dry, damp and wet interdune deposits interfingered with playa deposits.	Eriksson et al. (2000)	6
Kazan Formation, (Baker Lake Group)	1825 - 1811	Paleoproterozoic	Canada; Greater Baker Lake Basin.	Rift basin	Aeolian dune sets, sandsheets and wet interdunes interfingered with fluvial, lacustrine and playa deposits.	Hadlari et al. (2006)	7
Whitworth Formation (Haslingden Group)	1800 - 1740	Paleoproterozoic	Australia; Mount Isa Province.	Rift basin	Aeolian dune-sets and interdune deposits interfingered with fluvial and marine deposits.	Simpson and Eriksson (1993)	8
Lower Quilalar Formation (Haslingden, Group)	1800 - 1740	Paleoproterozoic	Australia; Mount Isa Province.	Rift basin	Aeolian dune sets interfingered with marine deposits.	Jackson et al. (1990)	9
Kunwak Formation, (Baker Lake Group)	1785	Paleoproterozoic	Canada; Greater Baker Lake Basin.	Rift basin	Aeolian dune sets interfingered with alluvial deposits.	Rainbird et al. (2003)	10
Amarook Formation (Wharton Group)	1785 - 1758	Paleoproterozoic	Canada; Greater Baker Lake Basin.	Intracratonic sag basin	Aeolian dune sets interfingered with lacustrine, alluvial, and braided fluvial deposits.	Rainbird et al. (2003)	11
Thelon Formation (Barrensland Group)	1720	Paleoproterozoic	Canada; Greater Baker Lake Basin.	Intracratonic sag basin	Aeolian dune sets interfingered with ephemeral stream deposits.	Jackson et al. (1984)	12
Bandeirinha Formation (Espinhaço Supergroup)	1700	Paleoproterozoic	Brazil; São Francisco Craton.	Intracratonic basin	Aeolian sandsheet and zibar deposits interfingered with minor ephemeral fluvial channel deposits.	Simplicio and Basilici (2015)	13
Hornby Bay Group	1600	Mesoproterozoic	Canada; Coopermine Homocline.	Intramontane basin	Aeolian dune sets interfingered with alluvial and ephemeral wadi deposits.	Ross (1984)	14
Dala Sandstone	1600	Mesoproterozoic	Sweden; Sveconorwegian Basin.	Intracratonic basin	Aeolian dune sets and interdunes.	Pulvertaft (1985)	15
Mangabeira Formation (Espinhaço Supergroup)	1600 - 1500	Mesoproterozoic	Brazil; São Francisco Craton.	Intracratonic basin	Aeolian dune-sets, interdune and sandsheet deposits interfingered with minor fluvial deposits.	Bállico et al. (2017)	16
Majût Member (Eriksfjord Formation)	1600 - 1300	Mesoproterozoic	Greenland; Gardar Basin.	Rift basin	Aeolian dune sets and sandsheets interfingered with fluvial deposits.	Tirsgaard and Øxnevad (1998)	17
Egalapenta Member (Srisailam Formation, Cuddapah Supergroup)	1327	Mesoproterozoic	India; Cuddapah Basin.	Rift basin	Aeolian sandsheet, zibar, and interzibar deposits.	Biswas (2005); Dasgupta et al. (2005)	18
Mussartût Member (Eriksfjord Formation)	1300	Mesoproterozoic	Greenland; Gardar Basin.	Rift basin	Aeolian dune sets interfingered with fluvial and alluvial deposits. In some cases, dune topographies are preserved by	Clemmensen (1988)	19

					lava flows.		
Stoer Group	1200	Mesoproterozoic	Scotland; Stoer Basin.	Rift basin	Aeolian dune sets, sandsheets and ponded interdunes interfingered with fluvial channel deposits.	Ielpi et al. (2016)	20
Hazel Formation	1200 - 1100	Mesoproterozoic	USA; Texas; Southwestern Basin and Range region.	Transpressive strike/slip basin	Aeolian dune sets interfingered with alluvial fan deposits.	Soegaard and Callahan (1994)	21
Copper Harbor Formation	1200 - 1000	Mesoproterozoic	USA; Michigan; Lake Superior Basin.	Rift basin	Aeolian dunes interfingered with fluvial and alluvial deposits.	Taylor and Middleton (1990)	22
Galho do Miguel Formation	1200 - 1000	Mesoproterozoic	Brazil; São Francisco Craton.	Intracratonic basin	Aeolian dune sets (simple and compound) and dry and wet interdune deposits.	Mesquita et al. (2021); Basilici et al. (2020)	23
Wildhorse Meadows Quartzite (Big Bear Group)	1100 - 750	Neoproterozoic	USA; California; Southern Great Basin.	Rift basin	Aeolian dune sets; possibly interfingered with tidal deposits.	Stewart (2005)	24
Pindyin Sandstone	1000 – 750	Neoproterozoic	Australia; Officer Basin.	Intracratonic basin	Aeolian dune sets interfingered with fluvial deposits. Aeolian deposits are overlain by tidal and sabkha deposits.	Zang (1995)	25
Mancheral Quartzite (Sullavai Group)	871	Neoproterozoic	India; Cuddapah Basin.	Rift basin	Aeolian dune sets and interdunes interfingered with fluvial and alluvial deposits.	Chakraborty and Chaudhuri (1993)	26
Venkatpur Sandstone (Sullavai Group)	871	Neoproterozoic	India; Cuddapah Basin.	Rift basin	Aeolian dune sets, sandsheets and zibars interfingered with marine deposits.	Chakraborty (1991); Basilici et al. (2020)	27
Lancer Member (Browne Formation)	720 - 635	Neoproterozoic	Australia; Officer Basin.	Intracratonic basin	Aeolian dunes and interdunes interfingered with	Haines et al. (2004)	28
Bakoye 3 Formation (Bakoye Group)	600	Neoproterozoic	Mali; Taoudeni Basin.	Intracratonic basin	Niveo-aeolian dune sets that are frequently reworked.	Deynoux et al. (1989)	29
Shikaoda Formation (Vindhyan Supergroup	>550	Neoproterozoic	India; Vindhyan Basin	Intracratonic basin	Aeolian sandsheet underlain by shallow marine deposits.	Chakraborty and Chakraborty (2001)	30

Table 1: List of all the case studies included in this investigation and associated information. Every Precambrian aeolian system included in the summaries provided by Simpson and Eriksson (1998) and Rodriguez-Lopez et al. (2014) have been included in this investigation, except in circumstances where the accompanying data was not of sufficient quality to warrant inclusion.

Aeolian Lithofacies	Description	Associated Architectural Elements	Precambrian Examples
Wind-Ripple Strata	The migration of wind-ripples generates a characteristic inverse grading (coarsening upwards within laminae; Hunter, 1977, 1981). This inverse grading enables easy visual recognition of this uniquely aeolian lithofacies.	Dune-sets, sandsheets, zibar-sandsheets, dry interdunes	Wind-ripple strata are commonly observed in Precambrian aeolian successions. Examples include: the Paleoproterozoic Nora Formation (Master et al., 2010) and the Mesoproterozoic Dala Sandstone (Pulvertaft, 1985).
Grainflow Strata	Grainflow strata form via the gravitational collapse of dry, loose sand on the lee slopes of aeolian dune (Hunter, 1977); grainflow avalanches form strata inclined at ca. 18 - 36˚ within cross-bedded foreset deposits.	Dune-sets	Grainflow strata are commonly recognised in Precambrian aeolian successions. Examples include the Paleoproterozoic Whitworth Formation (Eriksson and Simpson, 1998) and the Neoproterozoic Venkatpur Sandstone (Chakraborty, 1991).
Grainfall Strata	Grainfall strata form where sediment falls from suspension when a saltating cloud of grains moves over a dune brink and loses velocity and sediment carrying capacity (Hunter, 1977). Grainfall strata are commonly composed of very fine-grained sand that drape wind-ripple and grainflow strata on dune lee-slopes.	Dune-sets	The recognition of grainfall and plane bed deposits in dune sets has been challenging in the Precambrian record with only few examples described (Chakraborty, 1991; Eriksson and Simpson, 1998)
Plane-Bed Strata	Aeolian plane beds form in circumstances when ripple-forming processes of are inhibited; these conditions are typically associated with very strong winds. Plane-bed strata from parallel-laminated sets (Clemmensen and Abrahamsen, 1983).	Dry interdune, sandsheet, zibar-sandsheet	The recognition of grainfall and plane bed deposits in dune sets has been challenging in the Precambrian record with only few examples described (Chakraborty, 1991; Eriksson and Simpson, 1998)
Adhesion Strata	Adhesion strata form when wind blows across a damp surface. Adhesion strata include adhesion ripples, warts and plane beds (Kocurek and Fielder, 1982).	Wet interdune, damp interdune, sandsheets	Adhesion strata are commonly observed in Precambrian aeolian successions. Examples include the Paleoproterozoic Whitworth Formation (Eriksson and Simpson, 1998), the Neoproterozoic Mancheral Quartzite (Chakraborty and Chaudhuri, 1993), and the Neoproterozoic Venkatpur Sandstone (Chakraborty, 1991).
Microbially-Induced Sedimentary Structures (MISS)	MISS develop where cryptobiotic films and crusts develop on damp and wet sedimentary surfaces (e.g., Eriksson et al., 2000; Basilici et al., 2021)	Wet interdune, damp interdune, sandsheets (when associated with fluvial and marine incursions)	A variety of MISS are observed in Precambrian aeolian systems. Muddy roll-up structures are found in the Makgabeng Formation (Eriksson et al., 2000, 2007; Porada and Eriksson, 2009; Simpson et al., 2013; Heness et al., 2014); in the Venkatpur Sandstone MISS are predominantly composed of petee (cf. Gavish et al., 1985; Reineck et al., 1990; Gerdes et al., 1994), sand stromatolites (cf. domal sand build-ups; Bottjer and Hagadorn, 2007) and palimpsest ripples (cf. Bottjer and Hagadorn, 2007).

	All Dune Deposits		*Sandsheet*		*Zibar Sandsheet*	
	Precambrian	Phanerozoic	Precambrian	Phanerozoic	Precambrian	Phanerozoic
N	465	1451	189	321	14	16
Mean	2.3	6.2	2.4	1.5	20.4	1.7
Median	1.5	2.0	0.5	0.9	2.3	1.6
SD	2.9	9.3	5.5	2.2	32.1	1.0
p(T<=t)	$8.72 * 10^{-16}$		0.01		0.03	
	Interdune		*Non-Aeolian*			
	Precambrian	Phanerozoic	Precambrian	Phanerozoic		
N	105	272	330	1133		
Mean	1.2	1.2	4.9	3.3		
Median	0.5	0.5	0.8	1.1		
SD	2.3	2.2	11.0	7.4		
p(T<=t)	0.62		$0.10* 10^{-3}$			

Case Study Name	Age (Ma)	Age	Location	Basin Setting	System Type	Data Source(s)	Case Number
Hopeman Sandstone	259 - 254	Late Permian	Scotland, UK	Foreland basin	Large cross-bedded dune-sets interpreted to be the products of star dunes.	Clemmensen (1987)	31
Arran Red Beds	290 - 250	Permian	Isle of Arran, Scotland, UK	Intracratonic basin	Mixed aeolian – fluvial – alluvial system. Aeolian deposits comprise dune-set, and dry and damp interdune deposits.	Clemmensen and Abrahamsen (1983)	32
Sherwood Sandstone	252 - 242	Lower Triassic	UK (Onshore and Offshore England)	Continental rift basin	Aeolian dune-sets, sandsheets and wet and damp interdunes; aeolian deposits are often interbedded with fluvial deposits.	Cowan (1993); Meadows and Beach (1993)	33
Rotliegendes Sandstone including Rotliegend Group	299-252	Lower Permian	Germany, Poland, Denmark, Baltic Sea, Netherlands	Continental rift basin	Aeolian dune-sets and rare interdune deposits. Aeolian deposits are interbedded with fluvial and lacustrine deposits.	Ellis (1993); Newell (2001)	34
Boxtel Formation	< 1	Neogene	Netherlands	Continental rift basin	Niveo-aeolian sandsheets associated with fluvial and loam deposits.	Schokker and Koster (2004)	35
Sables de Fontainbleau Formation	38 - 34	Palaeogene	France	Intracratonic basin	Coastal aeolian dune-sets with preserved topography.	Cojan and Thiry (1992)	36
Escorihuela Formation	< 5	Middle–Upper Pliocene to Lower Pleistocene	NE Spain	Continental rift basin	Aeolian dunes-sets, sandsheet deposits, and damp and ponded wet interdunes.	Liesa et al. (2016)	37
Etjo Formation	140 - 135	Early Cretaceous	Namibia	Intracratonic basin	Exceptionally large dune-sets in predominantly dry aeolian system. In	Mountney and Howell (2000)	38

					places, Etendeka flood basalts preserve dune palaetopography.		
Entrada Sandstone	166 - 163	Middle Jurassic	Arizona, USA	Foreland basin	Large dune-sets in predominantly wet aeolian system. Aeolian deposits are associated with sabkha deposits. Dune-sets infill palaeotopography in places.	Kocurek and Day (2018)	39
Tumblagooda Formation	430 - 420	Late Silurian	Australia	Intracratonic basin	Aeolian sandsheets and small dune-sets. Aeolian deposits are found interbedded with fluvial deposits.	Trewin (1993)	40
Entrada Sandstone	166 - 163	Middle Jurassic	New Mexico, USA	Foreland basin	Aeolian dune palaeotopography buried beneath subaqueous strata.	Benan and Kocurek (2000)	41
São Sebastião Formation	200	Lower Cretaceous	Brazil	Continental rift basin	Aeolian dune-sets and dry sandsheets interbedded with channelized ephemeral fluvial deposits.	Formola et al. (2019)	42
Sergi Formation	148 - 144	Late Jurassic	Brazil	Intracratonic basin	Mixed fluvial, aeolian and lacustrine deposits. Packages of aeolian dune-sets reach up to 10 m in thickness.	Scherer et al. (2007)	43
Caldeirao Formation	298 - 272	Early Permian	Brazil	Intracratonic basin	Aeolian dune-sets and dry, damp and wet interdune deposits.	Jones et al. (2015)	44
Guara Formation	163 - 145	Late Jurassic	Brazil	Intracratonic basin	Dune sets – interpreted to be the products of crescentic dunes – and sandsheets interbedded with distal fluvial flood	Scherer and Lavina (2005)	45

					flows and channel-fill elements.		
Piramboia Formation	260 - 257	Early Jurassic	Brazil	Intracratonic basin	Aeolian sandsheet deposits overlain by dune-set and interdune strata.	Dias and Scherer (2008)	46
Cedar Mesa Sandstone	286 - 245	Early Permian	Colorado, USA	Foreland basin	Deposits representing erg centre and lateral erg margin deposits. The former is a predominantly dry aeolian system; the latter is predominantly wet aeolian system, associated with wet and damp interdunes and fluvial deposits.	Mountney and Jagger (2004)	47
Cedar Mesa Sandstone	286 - 245	Early Permian	Utah, USA	Foreland basin	Predominantly dry, though occasionally water table-influenced aeolian systems. Aeolian dune-sets, sandsheets interbedded with palaeosol and ephemeral lake deposits.	Mountney (2006)	48
Rio Negro Formation	10 - 4	Neogene	Argentina	Intracratonic basin	Dune-sets and dry and wet interdunes interbedded with paleosols	Zavala and Frieje (2001)	49
Chugwater Formation	250 - 245	Lower Triassic	Wyoming, USA	Intracratonic basin	Aeolian dune-set, sandsheet, and wet interdune deposits; aeolian deposits are interbedded with sabkha deposits.	Irmen and Vondra (2000)	50
Arikaree Formation	23 - 16	Neogene	Wyoming, USA	Intracratonic basin	Large cross-bedded dune-sets.	Bart (1977)	51

Ingleside Formation	299 - 280	Early Permian	Colorado, Wyoming, USA	Intracratonic basin	Dry aeolian dune-sets truncated by deflationary supersurfaces.	Pike and Sweet (2018)	52
Lower Cutler beds	300?	Late Carboniferous–Early Permian	Utah, USA	Foreland basin	Aeolian dune-sets, sandsheets and interdunes interbedded with fluvial, lacustrine and marine deposits.	Jordan and Mountney (2010); Wakefield and Mountney (2013)	53
Cedar Mesa Sandstone	286 - 245	Early Permian	Utah, USA	Foreland basin	Twelve separate aeolian erg sequences, each bounded by regionally extensive deflationary supersurfaces. Erg-centre is predominantly dry; though occasionally wet table-influenced aeolian systems. Erg-margin shows fluvial-aeolian interaction.	Loope (1985)	54
Navajo Sandstone	201 - 191	Early Jurassic	Utah-Arizona border, USA	Foreland basin	Large cross-bedded dune-sets in mainly dry aeolian system; in places dune-sets can be associated with damp and wet interdune and sabkha deposits. Large-scale soft-sediment deformation structures associated with rapid de-watering are also present.	Loope and Rowe (2003)	55
Entrada Sandstone	166 - 163	Middle Jurassic	Utah, USA	Foreland basin	Coastal aeolian system associated with dune-	Crabaugh and Kocurek (1993)	56

					sets and damp and wet interdune deposits.		
Wolfville Formation	227 - 210	Upper Triassic	Nova Scotia, Canada	Continental rift basin	Small scale dune-sets interbedded with caliche deposits, alluvial-fan conglomerates, braided-river sandstones and gypsiferous playa mudstones.	Leleu and Hartley (2018)	57
Page Sandstone	170 - 166	Middle Jurassic	Utah, USA	Foreland basin	Coastal aeolian dune-field system. Aeolian dunes and interdunes associated with channel- and lens-shaped ephemeral fluvial deposits.	Jones and Blakey (1997)	58
Unayzah A	265 - 247	Late Permian	Saudi Arabia	Continental rift basin	Aeolian dune-sets and damp and wet interdune deposits interbedded with sandy palaeosols, and ephemeral lake deposits.	Melvin et al. (2010)	59
Unayzah (middle member)	265 - 247	Late Permian	Saudi Arabia	Continental rift basin	Aeolian dune-sets and damp and wet interdune deposits interbedded with sandy palaeosols, and ephemeral lake deposits.	Melvin et al. (2010)	60
Nepean Formation	485 - 477	Ordovivian	Canada	Continental rift basin	Aeolian dune-sets and damp interdunes; in places aeolian deposits are locally eroded by ephemeral fluvial systems.	MacNaughton et al. (2002)	61
Rodjeberg Formation	388 - 383	Late Middle Devonian	Greenland	Foreland basin	Aeolian dune-sets and sandsheets interbedded with fluvial deposits.	Olsen and Larsen (1993)	62

Snehvide Formation	388 - 383	Late Middle Devonian	Greenland	Foreland basin	Small aeolian dune-sets located in the interchannel areas of terminal fan deposits.	Olsen and Larsen (1993)	63
Sofia Sund Formation	387 - 372	Middle Devonian	Greenland	Foreland basin	Aeolian dune-sets and sandsheets interbedded with fluvial deposits.	Olsen and Larsen (1993)	64
Galesville Member	501 - 492	Cambrian	Wisconsin, USA	Intracratonic basin	Thin (<0.3 m) cross-bedded aeolian dune-set and sandsheet deposits that laterally grade into braided fluvial deposits.	Dott et al. (1986)	65
Kilmurry Formation	393 - 382	Middle Devonian	Ireland	Continental rift basin	Large compound dune-sets overlying alluvial fan conglomerate deposits.	Morrisey et al. (2012)	66
Pewamo Formation	315 - 299	Late Carboniferous	Michigan, USA	Intracratonic basin	Aeolian dune-sets, sandsheets, and ponded ephemeral wet interdune lakes.	Benison et al. (2011)	67
St. Peter Sandstone	467 - 458	Middle Ordovician	Wisconsin, USA	Intracratonic basin	Coastal aeolian system coeval with shallow marine environments. Large-scale cross-bedded dune-sets, sandsheets and damp interdunes.	Dott et al. (1986)	68
Wonewoc Formation	501 - 492	Upper Cambrian	Wisconsin, USA	Intracratonic basin	Coastal aeolian system. Large-scale cross-bedded dune-sets interbedded with damp and wet interdune deposits. Wet interdunes may be associated with fluvial or marine incursions into interdune corridors.	Dott et al. (1986)	69

Phu Tok	126 - 93	Cretaceous	Thailand	Continental rift basin	Aeolian dune-sets and damp and wet interdunes. Wet interdunes associated with fluvial incursions into interdune corridors.	Hasegawa et al. (2010)	70
Sari	39 - 28	Paleogene	Tajikistan	Foreland basin	Aeolian dune-set and aeolian loess interbedded with fluvial and lacustrine deposits.	Wang et al. (2016)	71
Peshtova	39 - 28	Paleogene	Tajikistan	Foreland basin	Aeolian dune-set and aeolian loess interbedded with fluvial and lacustrine deposits.	Wang et al. (2016)	72
Lop Nor	< 7	Neogene-Quaternary	China	Continental rift basin	Lacustrine deposits interbedded with aeolian and fluvial deposits.	Liu et al. (2014)	73
Tianchihe	164 - 145	Late Jurassic	China	Intracratonic basin	Aeolian dune-sets and sandsheets interbedded with ephemeral fluvial channel and fluvial floodplain deposits.	Xu et al. (2019)	74
Santai	150 - 137	Late Jurassic/Lower Cretaceous	China	Continental rift basin	Aeolian dune-sets associated with abundant non-avian theropods footprints.	Xu et al. (2021)	75
Tangbian	84 - 72	Late Cretaceous	China	Back-arc basin	Aeolian dune-sets and interdunes. Aeolian deposits locally reworked by fluvial systems associated with monsoonal conditions.	Jiao et al. (2020)	76
Tangbian	84 - 72	Late Cretaceous	China	Back-arc basin	Aeolian dune-set, sandsheet, and wet, damp and dry interdune deposits.	Cao et al. (2020)	77

Tangbian	84 - 72	Late Cretaceous	China	Back-arc basin	Aeolian dune-sets and interdunes. Some intervals are associated with extensive soft sediment deformation triggered by monsoonal rains and seismic activity.	Rodriguez-Lopez and Wu (2020)	78
Matoushan	125 - 90	Mid-Cretaceous	China	Foreland basin	Aeolian dune-sets associated with soft sediment deformation; deformation associated with theropod tracks.	Rodriguez-Lopez and Wu (2020)	79
Nanxin	113 - 90	Mid Cretaceous	China	Continental rift basin	Aeolian dune-sets and interdunes interbedded with playa deposits.	Li et al. (2018)	80
Hutousi	90 - 84	Late Cretaceous	China	Continental rift basin	Aeolian dune-sets and interdunes interbedded with playa deposits.	Li et al. (2018)	81
Jiaguan	127 - 84	Mid-Cretaceous	China	Intracratonic basin	Aeolian dune-sets interbedded with damp and wet interdunes.	Hasegawa et al. (2010)	82
Page Sandstone	170 - 166	Middle Jurassic	Arizona, USA	Foreland basin	Coastal aeolian dune-field system. A series of -stacked, largely dry aeolian erg sequences, each separated by a regionally extensive supersurface characterized by polygonal cracks.	Kocurek et al. (1991)	83
Agrio Formation	130 - 129	Early Cretaceous	Argentina	Back-arc basin	Aeolian dune-sets and sandsheets in wet aeolian system; aeolian deposits are found frequently interbedded with fluvial deposits.	Viega et al. (2002)	84

Huitrin Formation	129 - 125	Early Cretaceous	Argentina	Back-arc basin	Aeolian dune-sets interpreted to be formed by linear and transverse dunes. In places, rapid fluvial flooding preserves dune palaeotopography.	Strömback et al. (2005)	85
Tsondab Sandstone	23 - 3	Neogene	Namibia	Passive margin basin	Dune-set deposits and massive sandstones interbedded with paleosols.	Kocurek et al. (1999)	86
Tamala Limestone	3	Neogene	Perth, Australia	Passive margin basin	Predominantly marine carbonates associated with minor aeolian dune-set deposits and palaeosol deposits.	Semeniuk and Glassford (1988)	87

Table S1: List of the Phanerozoic case studies included in this investigation. The case study number corresponds with the global map shown in Figure S2.